PEA PROTEIN MIXTURES AS STRUCTURING AGENT IN EDIBLE SOFT MATERIALS

LAKSHMINARASIMHAN SRIDHARAN

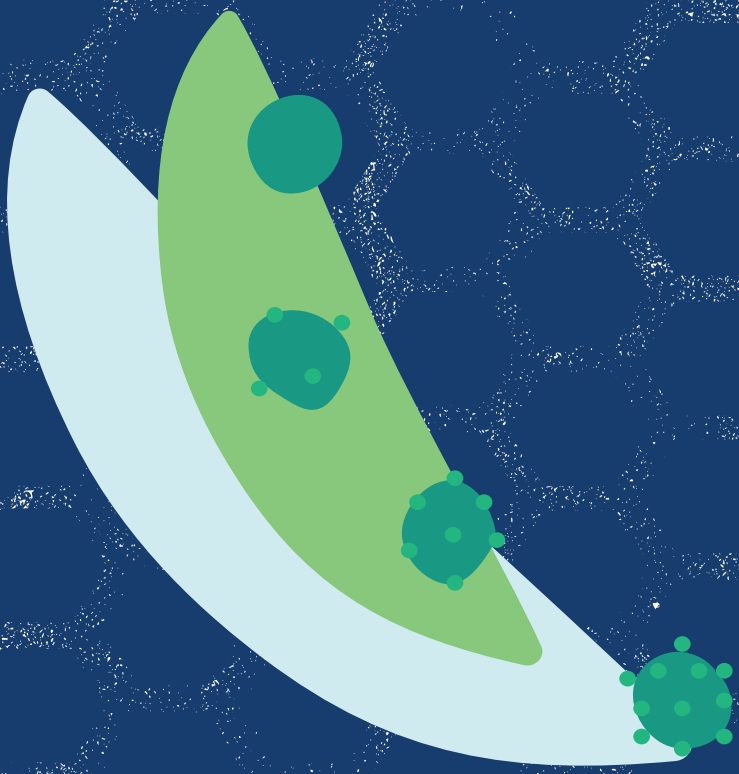

Propositions

1. Protein purification is unnecessary to use pea proteins as functional ingredients.
   (this thesis)

2. Insoluble plant protein particles can act as both emulsifiers and rheology modifiers.
   (this thesis)

3. Open access publishing in its current form incentivizes researchers who can afford to pay.

4. A publication-driven research environment has led to an overwhelming amount of scientific information but also to a lack of continuity in advancing our knowledge.

5. A wilful shift in people's consumption pattern is necessary to reduce the environmental impact of our food system.

6. Radical disagreements within our society expose our inability to have meaningful dialogue.

Propositions belonging to the thesis, entitled
Pea protein mixtures as structuring agent in edible soft materials
Lakshminarasimhan Sridharan
Wageningen, 17 December 2021

Pea protein mixtures as structuring agent in edible soft materials

Lakshminarasimhan Sridharan

Thesis committee

Promotor

Prof. Dr Johannes H Bitter

Professor of Biobased Chemistry and Technology

Wageningen University & Research

Co-promotors

Dr Costantinos V Nikiforidis

Associate Professor, Biobased Chemistry and Technology

Wageningen University & Research

Dr Marcel BJ Meinders

Senior Researcher, Wageningen Food & Biobased Research

Wageningen University & Research

Other Members

Prof. Dr Markus Stieger, Wageningen University & Research

Prof. Dr Patrick Anderson, Eindhoven University of Technology

Dr Elke Scholten, Wageningen University & Research

Dr Christophe Schmitt, Nestle R&D centre, Lausanne, Switzerland

This research was conducted under the auspices of graduate school VLAG (Advanced Studies in Food Technology, Agrobiotechnology, Nutrition and Health Sciences)

Pea protein mixtures as structuring agent in edible soft materials

Lakshminarasimhan Sridharan

Thesis

Submitted in fulfilment of the requirements for the degree of doctor
at Wageningen University
by the authority of the Rector Magnificus,
Prof. Dr A.P.J Mol,
in the presence of the
Thesis Committee appointed by the Academic Board
to be defended in public
on Friday 17 December 2021
at 11 a.m. in the Aula.

Lakshminarasimhan Sridharan
Pea protein mixtures as structuring agent in edible soft materials
176 pages

PhD thesis, Wageningen University, Wageningen, The Netherlands (2021)
With references, with summary in English

ISBN: 978-94-6395-748-9
DOI: https://doi.org/10.18174/554789

Table of contents

Chapter-1: General introduction	7
Chapter-2: Pea flour as stabilizer of oil-in-water emulsions	19
Chapter-3: Emulsifying properties of pea proteins at pH 3	39
Chapter-4: 3D printing jammed emulsions stabilized by pea proteins	63
Chapter-5: Effect of pea protein purification on the interfacial and emulsion properties	85
Chapter-6: Heat-set gelation of emulsions stabilized by pea flour	107
Chapter-7: General discussion	129
References	145
Summary	165
Acknowledgments	171
About the author	173
List of publications	174
Overview of completed training activities	175

Chapter-1: General introduction

1.1 Transition in the global food landscape

Food production generates about 30% of human-activity-related global greenhouse gas emissions and contributes to detrimental environmental impact [1,2]. Food production also occupies large amounts of land, with about 32% of all ice-free land is currently being used for agriculture and animal farming [2,3]. These statistics dictate the scale of food production for human consumption on our planet. With an expected population increase of 3 billion (to a total of 10 billion) in the next 30 years, the demand for food and its associated environmental impact will increase rapidly [2,4,5].

To reduce the environmental impact of food production, there is a need to modify food production systems [6]. When examining greenhouse gas emissions within food production, the main source of emissions is primary agricultural production, which includes the cultivation of crops and animal farming for meat and dairy production [7]. Specifically, animal farming for dairy and meat production is considered to emit higher amounts of greenhouse gases than plant-sourced foods [1,7]. For instance, to produce 100 grams of proteins from beef, 20-50 $kgCO_2$ equivalent emissions are paid compared to only 0.3-0.4 $kgCO_2$ equivalent for the same amount from peas [7]. Similarly, to produce 100-gram protein from beef, 164 m^2 land is required, while only 22 m^2 is needed for peas [7]. Therefore, it is clear that to reduce the negative impact of food production, there is a need to switch from an animal-centric food system involving high amounts of dairy and meat sources to a more plant-based food system.

Despite its negative impact, ingredients derived from animal sources, such as proteins from dairy and egg, are widely used to stabilize fat droplets in water, air bubbles in water, and entrap water to form an aqueous gel. Such functional behavior of proteins leads to the formation of emulsions, foams, and protein gels, which are basic structures in foods [8–10]. The basic structures are built hierarchically to give every food its characteristic texture. For example, whey proteins and casein proteins derived from milk are used to stabilize air pockets and fat droplets in ice-creams which aid in creating distinct structure and creaminess in ice-creams [11–13]. Therefore, when looking at the transition from animal-based foods to plant-based foods with lower environmental impact, understanding the ability of plant-based proteins to create basic structures in foods is essential.

1.2 Food structuring

The structuring of foods is a challenging process to understand since foods are made up of complex microscopic architecture [14]. Every food product is built up of essential constituents such as proteins, fats, carbohydrate polymers, minerals, etc. Among these constituents, proteins play a crucial role in creating food structures and delivering their macroscopic properties [15]. Proteins can associate and modify into complex entities ranging from individual proteins in the nanoscale to protein particles in the sub-micron to micron-scale [14,15]. Proteins also often interact with non-protein constituents such as fats and other bio-polymers to create a gel or an emulsion [15]. For instance, in milk, fat globules stabilized by proteins and phospholipids (1-20 μm) give milk their characteristic color and the familiar mouth feels. Similarly, proteins can coagulate and form a gel-like material that lies at the base of dairy-based cheeses [14]. Therefore, the oil droplet stabilization role of proteins (emulsifying property) and gelling behavior of proteins are essential functional properties.

Besides proteins, carbohydrates such as starch (amylose, amylopectin), pectins, xanthan, and guar gums are important structuring agents [16]. Starch gelatinization can lead to starch gels that can play an important role in structuring food products. Gums such as xanthan are considered additives that can help in increasing the viscosity of food products. These carbohydrate polymers are often used as texture modifiers in foods in combination with proteins and fat [17–19]. Therefore, plant mixtures are an excellent source of structuring agents such as proteins and starch.

Currently, a large proportion of functional proteins in foods are sourced from dairy. Dairy proteins are also derived from animals and are therefore associated with negative environmental impacts. Therefore, dairy proteins need to be replaced with plant proteins as a functional structuring agent in foods. However, plant proteins have complex molecular structures and physicochemical properties compared with dairy proteins. Plant proteins usually exist as hexameric or trimeric proteins with multiple chains of amino acids within each monomer [20]. In comparison, dairy proteins such as lactoglobulins exist in a monomeric or dimeric form [21]. Due to these fundamental differences, one-to-one replacement of dairy proteins with plant proteins to obtain similar functionality is not possible. Plant proteins may function differently compared with dairy when replacing them as emulsifiers or gelling agents in foods. Therefore, to use plant proteins as structuring

agents in place of dairy proteins and still obtain the original microstructure, a fundamental understanding of the molecular properties of plant proteins and their effects on their structuring ability needs to be thoroughly understood.

1.3 Extracting proteins from plant sources

Plant proteins can be employed as structuring agents in foods; however, they need to be extracted from their native seed matrix before using plant proteins. This separation process adds additional steps and energy requirements when considering the overall transition towards plant proteins. Therefore, a thorough examination of the rationale behind the protein extraction process from plant sources is necessary.

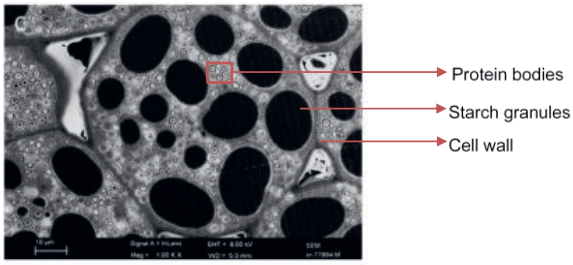

Figure 1.1: Electron micrograph showing the structure of pea seed cells with starch granules, protein bodies enclosed within the cell wall.

Proteins are stored together with other molecules such as fat ad starch within the cell matrix of the plant seed. **Figure 1.1** shows an SEM micrograph of the structural architecture of pea seed cells. Proteins are typically stored within the cell walls of the plant seed in specific entities known as protein bodies. The cell is bound by a cell wall comprised of fibers that provide a rigid boundary around the components. Therefore, to access the proteins from this complex architecture, mechanical forces are required. Traditionally plant proteins are extracted through an aqueous mechanical process.

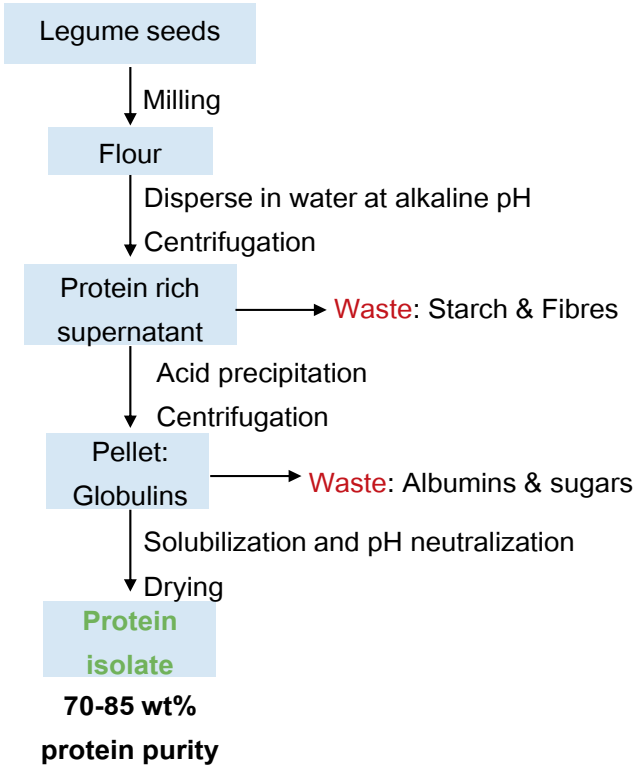

Figure 1.2: Process diagram for alkaline aqueous extraction method to produce legume protein isolate [22,23].

Figure 1.2 shows the conventional alkaline extraction process used to extract proteins from legume sources. The extraction process starts with a mechanical breakdown of the seeds, which ruptures the cells, and the protein bodies are accessible. Then to separate the proteins from non-protein components, a wet alkaline extraction process is used. The milled seeds are dispersed in water between pH 8-9.5 for several hours [22,23]. Then, they are centrifuged to remove any insoluble material. The protein-rich liquid (supernatant) is subject to an acid treatment at the iso-electric point of pH 4.5-5.0 [24]. The proteins become insoluble and are separated by centrifugation. The obtained insoluble protein is resolubilized and dried to obtain what is known as protein isolate. These pea protein isolates typically contain between 75-85 wt% protein, about 2 wt% starch, and small amounts of oil and minerals [25].

This protein extraction process focuses on high protein purity (>70 wt%) and consumes 30 MJ/kg energy, and 80-100 grams of water per gram protein extracted [26]. Therefore, modifications to the conventional wet extraction are proposed to improve its resource use [27]. One way to reduce the energy consumption of the extraction process is to use fewer and less energy-intensive steps-a, a so-called mild extraction process [27]. For instance, one way to mildly extract proteins from peas is to apply milling simply and air classification to physically separate proteins from non-protein components. Such a mild separation route would avoid water use and reduce the number of steps to create a protein extract. Such a process consumes only about 15 MJ/kg material processed compared with the conventional wet alkaline extraction process, which consumes 30 MJ energy/kg material processed [26].

While milder or minimal purification is energetically beneficial, it also creates fractions that contain large amounts of non-protein components [27,28]. Conventional wet processing can produce protein isolates with a purity of about 75-90 wt%, while mild processing or no processing yields proteins mixtures with 20-60 wt% purity. Therefore, when mild separation or minimal purification is employed, protein fractions containing large non-protein molecules such as starch, sugars, and fats are obtained. Therefore, to apply these mixtures as functional ingredients, it is essential to understand the functionality of these protein mixtures as structuring agents in food systems. Some studies have looked into using plant protein mixtures as structuring agents [28–30]. For example, the presence of sunflower phenols together with sunflower proteins has been shown to enhance the emulsification properties of sunflower protein mixtures [31]. Similarly, starch increases viscosity in certain protein stabilized emulsions, which can be beneficial in soft-solid food applications [28].

Minimally processed protein mixtures containing non-protein molecules such as starch could function as structuring agents with the proteins. However, a thorough understanding of the structuring ability of these protein mixtures is essential for them to be used in foods. Specifically, the composition and any synergistic or antagonistic effects of non-protein components need to be understood. Legume sources such as peas are attractive to study protein mixtures due to their wide availability and simple composition of 20-30wt% protein and about 40-60 wt% starch. Therefore, in this thesis, the structuring ability of protein mixtures is investigated using yellow peas as a model legume protein source.

1.4 Yellow peas

Yellow peas (Pisum sativum) are a leguminous crop grown in about 100 countries worldwide [32]. They are the third-largest leguminous crop produced globally with around 16 million tons/year, behind soy (36 million tons/year) and beans (22 million tons/year) [33]. Pea seeds are carbohydrate-rich sources with 40-55 wt% starch and 12-20 wt% fibers. They are also a good source of proteins with about 18-30 wt% protein along with minor amounts of oil and mineral content [25,34]. The composition of peas is given here as ranges since the composition varies depending on season and geographical location [34]. Peas grow well in dry and frosty conditions and are cultivated and consumed as part of traditional diets in many parts of the world to provide energy and essential macronutrients. Peas are also sought after as a techno-functional plant source to derive functional proteins and carbohydrates [35].

1.4.1 Pea proteins

Peas contain about 18-30 wt% of proteins. The proteins are stored inside the pea seed matrix in specific organelles known as protein bodies [36]. Pea proteins can be classified into the globulin fractions, accounting for about 80% of the total proteins, and the albumin fraction, which is the remaining 20% [35,37].

Albumins in peas are mainly PA1, PA2, which account for 20% of total protein content [38]. These albumin proteins are about 10-25 KDa in size, much smaller than their globulin counterparts. The albumin fractions are considered less interfacially active than globulins at the oil-water interface and, therefore, less well studied as emulsifying agents [39]. However, they are rich in sulfur-containing amino acids and are important dietary components in pea [38].

The globulin fractions in peas are larger molecules with molecular sizes above 150 KDa. The globulin fractions can be further sub-divided into Vicilin (7S) and Legumin (11S) fractions. Both these globular proteins are built up with a complex quaternary structure [37]. Legumin is a Hexameric protein with a total molecular weight of 350-400 KDa [37,40]. The structure of Legumin is shown in **Figure 1.3a**. Each Legumin hexamer is made of two identical trimers, held together by a double S-S bond. Each monomeric sub-unit of Legumin

is about 50 KDa in molecular weight. Each monomer can be subdivided into an α subunit (35 KDa) and β sub-unit of 20 KDa [37].

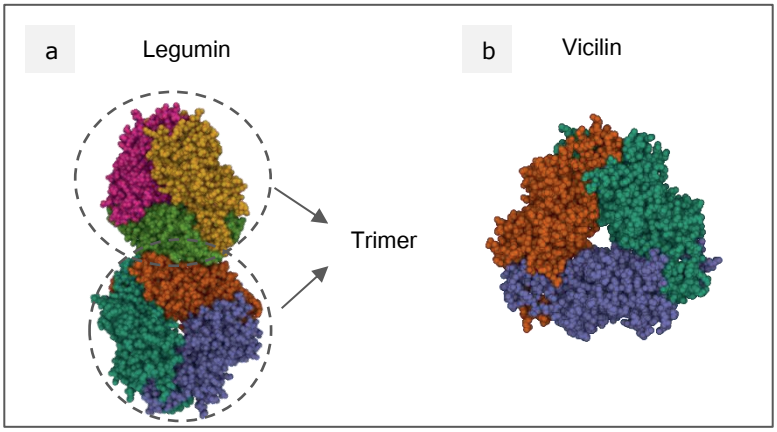

Figure 1.3: Molecular structure of pea globulins with contrasting colors indicating different polymeric chains (a) Hexameric form of Legumin showing two trimers bound together- the trimers each are circled for ease of distinguishing, (b) Trimeric form of Vicilin-like molecule. The structures were imported from protein databank UniProt [41].

Vicilin is a trimeric globular protein with a molecular weight of about 180-200 KDa. The structure of Vicilin is shown in **Figure 1.3b.** Vicilin monomers are about 60 KDa in molecular weight, and an S-S bond does not bind them. Each subunit can be subdivided into polypeptide chains of 35 KDa, 20 KDa, and 16 KDa [35,37,40]. These polymeric forms of Legumin and Vicilin are pH and salt content dependent [24,42,43]. The proteins at neutral or slightly alkaline pH values are known to retain their native quaternary form closely [44,45]. Both Legumin and Vicilin are known to reduce to trimers (for Legumin) and monomers (Vicilin) at low pH values [45].

The globulin fractions also possess a pH-dependent functional behavior. It has been noted that for Legumin and Vicilin at low ionic strength, their solubility has a typical bell shape curve [24,44]. The solubility is around 70% at pH values of pH 7-8. However, as pH moves towards pH 5, the proteins start to aggregate due to a reduction in the total surface charge of the proteins. pH 4.5-5.0 is said to be the iso-electric point for pea globulins [44]. Therefore, the proteins aggregate due to hydrophobic interactions in the absence of electrostatic repulsion. Studies have also shown that pea globulins are generally less

soluble in acidic environments than alkaline conditions, attributed to depolymerization into their monomeric subunits and exposure to hydrophobic patches [45,46]. Due to pea proteins' pH-dependent molecular properties, their ability to stabilize emulsions and form gels can also be tuned by adjusting pH. This is a relatively simple approach to tune structures in food products when using proteins.

Pea globulins are known to be excellent emulsifiers [24,47]. They can form stable oil-in-water emulsions with monomodal droplet size distribution at neutral pH values. In acidic pH conditions, pea globulins are said to form protein particles through weak hydrophobic protein-protein interaction. These protein particles supposedly stabilize emulsions through a Pickering mechanism [46]. Pea globulins are also known as good gelling agents upon heating. They denature and interact upon heating to form cohesive and firm gels [24,25]. Pea globulins are an important research focus of this thesis due to their excellent emulsifying and gelling ability.

1.4.2 Pea starch

Peas are starch-rich seeds containing between 45-60 wt% starch granules by dry weight [34]. The starch granules are found within the pea seed cells with a size between 8-40 μm in size with a peak of around 25-30 μm [48]. In terms of molecular composition, pea starches have varying amounts of amylose and amylopectin content. Pea starches contain anywhere between 40-70 wt% amylose and the remaining as amylopectin polymers [34,48]. Most researchers have found pea starches to be higher in amylose than in amylopectin [49]. Regardless of diversity in molecular composition, pea starch is widely used as a gelling agent [50]. They can swell in an aqueous environment and uptake water upon heating above 65°C [51]. This leads to starch gelatinization and the formation of starch gels. These starch gels play an essential role, such as viscosity modification in many food products.

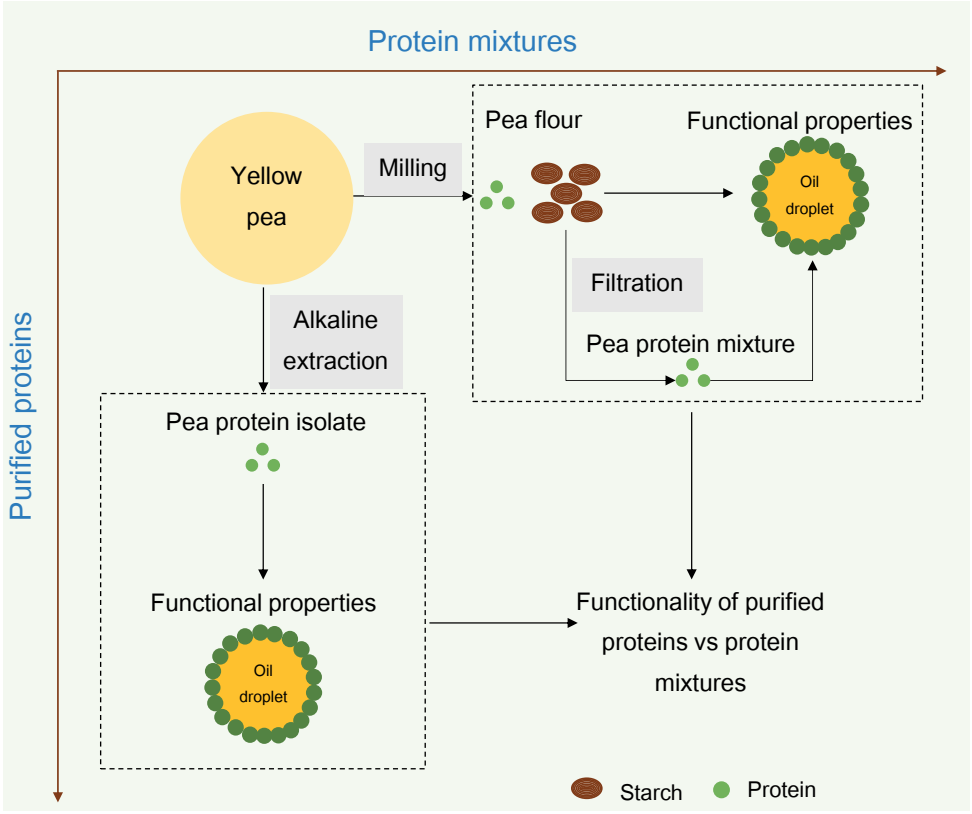

Figure 1.4: Overview of the primary aim and outline of the thesis.

1.5 Aim and scope of the thesis

Proteins and starch play an essential role in structuring food systems. Proteins can stabilize oil droplets, while starch can act as a viscosity modifier. Therefore, using a native pea mixture containing proteins and starch could be a beneficial approach to structure foods. However, understanding the structuring ability of these native mixtures in relation to their composition and interaction between components is essential. The interactions and structuring ability are also affected by environmental conditions such as pH and temperature. So, investigating the emulsifying (and gelling) behavior of pea protein mixtures as a function of pH will provide mechanistic insight into their functionality. Therefore, the **aim of this thesis** was to **create insights** into the **structuring ability of pea protein mixtures** in emulsion-based model food materials by linking the **molecular properties** of the ingredients **to the final material properties**. Specifically, the effect of

non-protein molecules in the interfacial stabilization and emulsion properties of pea protein mixtures were investigated.

The thesis can be divided into two broad sections, as shown in **Figure 1.4**. On the one hand, we investigate using an unpurified pea protein mixture as an emulsifying and structuring agent. The focus of this section is on proteins and starch, which are the major constituents in peas. We studied the emulsifying and emulsion properties in relation to the molecular properties of pea protein mixtures. The second section deals with gaining mechanistic insight into pea protein behavior at acidic pH values since this is lacking in scientific literature. In this section, we studied the properties of pea proteins and their effect on structuring functionality in emulsion systems. To gain mechanistic insights, purified pea protein isolate was used. The insights gained from investigating the purified proteins were then translated to the unpurified system. The knowledge obtained from the thesis provides design rules for structuring foods based on a mechanistic understanding of the behavior of pea proteins.

Chapter-2 deals with investigating the emulsifying ability of pea flour in oil-water systems. Native pea flour contains 20 wt% protein and 50 wt% starch, and it represents the most minimally processed native protein mixture obtainable from peas. Therefore, this chapter investigated the ability of native pea flour to reduce interfacial tension and form emulsions. Proteins were identified as a significant emulsifying agent within the mixture, while starch did not hinder the interfacial activity. The chapter lays the basis in this research, which shows that purification is not necessary to produce stable emulsions when using pea protein mixtures in a model emulsion system.

Chapters-3 and 4 deal with creating fundamental knowledge of structuring using pea proteins at acidic pH values. Pea proteins are known to self-assemble at pH 3 due to non-covalent weak physical interactions. This self-assembly nature of pea proteins was studied, and it was found that pea proteins at pH 3 exist as a mixture of protein molecules and self-assembled protein particles. The protein molecules stabilized the oil droplets while protein particles remained in bulk. In **Chapter-4**, the understanding of the stabilization mechanism was extended to understand the bulk material properties. In particular, the effect of free protein particles on the mechanical property of emulsion-gels was investigated. The presence of protein particles created droplet-droplet interaction, which resulted in emulsions with elasto-plastic 3D printable properties.

Chapter-5 builds upon the knowledge created by fundamental understanding obtained in chapters-3 & 4 from purified proteins and extends to pea protein mixtures. In chapter-3, we showed that in acidic pH, pea protein particles do not take part in interfacial stabilization, while the particles aid in creating more viscous emulsions. In Chapter-5, the pea protein mixture's interfacial and emulsion properties were compared with purified pea protein isolate at acidic and neutral pH conditions. The effect of protein purification on interfacial stabilization is studied. Emulsions are also prepared with the two protein extracts, and their material properties are compared. The results showed that minimally processed pea protein mixtures could perform equally well than purified pea proteins as emulsifying agents. The chapter gives a direct comparison between protein mixture and alkaline extracted protein isolate.

Chapter-6 deals with heat-set gelation of emulsions stabilized with pea protein mixture with and without starch. In pea flour, proteins and starch are the primary ingredients. Therefore, they could be explored as potential gelling agents upon heating in the presence of oil droplets. The research follows the gelation dynamics and gel microstructure both with and without the starch present. The research showed that while starch had minimal effect on increasing the gel strength, it played an essential role in altering the microstructure of the emulsion gels. The study provides insights into using protein-starch mixtures to structure emulsions under heat treatment.

In **Chapter-7**, we discuss our main findings obtained in chapters 2-6 and put our research into perspective. We also discuss our perspective on future research directions for plant proteins and areas of immediate attention.

Chapter-2: Pea flour as stabilizer of oil-in-water emulsions

Published as:

Sridharan, S., Meinders, M. B., Bitter, J. H., & Nikiforidis, C. V. (2020). Pea flour as stabilizer of oil-in-water emulsions: Protein purification unnecessary. *Food Hydrocolloids*, *101*, 105533. https://doi.org/10.1016/j.foodhyd.2019.105533

Abstract

Plant proteins have recently gained considerable attention as stabilizers of food-grade oil-in-water emulsions. However, the separation of plant proteins from their native matrix can be cumbersome due to the molecular complexity of plants. This issue could be alleviated by avoiding the protein purification step. In this work, we show that native pea flour containing 50 wt% starch and 20 wt% protein has similar interfacial properties compared to concentrated pea protein systems (~55 wt% protein). The interfacial tension profile of pea flour was similar to that of concentrated pea protein, indicating that proteins are the primary stabilizing agents of the interface. The fabricated oil-in-water emulsions (10.0 wt% oil) made with pea flour (PF) or pea protein mixture (PPM) containing 0.2 and 0.3 wt% protein showed a similar monomodal droplet size distribution. Moreover, both emulsions stabilized by the PF and the PPM had similar rheological properties, showing that starch granules did not impact the physical properties. This work clearly showed that stable oil-in-water emulsions could be produced with pea flour and that pea protein purification is unnecessary.

2.1 Introduction

Oil-in-water emulsions are primarily used in food products to create texture and, in some cases, protect the encapsulated substances [52]. Proteins commonly stabilize the oil/water interface of the food-grade emulsions as they possess an amphiphilic character [53]. However, mainly animal protein sources are used, such as milk or eggs, causing environmental stress due to the high impact of livestock on CO_2 production [7,27]. On the other hand, plant-based proteins, due to the lower CO_2 emission associated with the primary production, are considered more sustainable, thus, the effective replacement of animal proteins with plant proteins is an urgent matter.

Several plant-based proteins sourced from soy, yellow pea, lentil, and rapeseed have been considered suitable animal protein alternatives for use as emulsifiers [42,54,55]. Plant proteins co-exist with lipids, carbohydrates, and low molecular weight molecules, like saponins and phenols [28,56]. Therefore, plant protein extraction requires complex purification methods involving oil extraction using organic solvents and protein solubilization at highly alkaline pH values [57,58]. Besides, large amounts of water and chemicals are needed for protein extraction, and non-protein molecules in the plant matrix can interact with the protein and affect their physicochemical properties [59]. Furthermore, the protein purification steps require energy and cause mass losses [60,61]. For instance, it has been proven that conventional wet purification of pea protein consumes 30 MJ per kg of pea flour processed and generates waste amounting to about 30 wt% of the initial material [26].

Therefore, a logical approach to reduce energy consumption during protein purification and avoid losses would be to decrease the number of purification steps [26,62]. Such a processing method results in protein-concentrated systems mixed with other plant-derived molecules such as starch, fibers, and oil. When such mixtures are used to stabilize emulsions, the non-protein molecules may influence the emulsion properties.

For studying such a mixed system, yellow peas (Pisum *sativum* L.) were chosen as a suitable protein source. This is because their composition is relatively simple, containing proteins (25 wt%), starch (50 wt%), fibers (15 wt%), and they are cultivated in broad types of climate [34]. A few studies have already looked into using crude protein mixtures derived from peas [63–65]. However, the interfacial and emulsifying property of the unpurified pea

flour (PF) system has not been investigated yet. Therefore, we aimed to investigate pea flour's interfacial properties and emulsifying ability and compare it with pea protein mixture's (PPM) performance. We provide a comprehensive insight into the interfacial and physical properties of the formed emulsions, and the non-necessity of pea flour purification is demonstrated.

2.2 Materials and Methods

2.2.1 Materials

Yellow peas (Pisum *sativum* L.) were purchased from Alimex® B.V (Sint Kruis, The Netherlands). Rapeseed oil was obtained from Danone Nutricia Research (Utrecht, the Netherlands). Sodium hydroxide (NaOH), hydrochloric acid (HCl), Nile Blue, Rhodamine B®, and Whatmann® qualitative filter paper 5951/2 and Florisil® (activated magnesium silicate) were all purchased from Sigma-Aldrich (Zwijndrecht, The Netherlands. NuPage® precast SDS-PAGE gels and PageRuler™ prestained protein markers and NuPage SDS-PAGE reagents were obtained from Fischer Scientific® (Landsmeer, The Netherlands). Total starch assay kit (Alpha-amylase/amyloglucosidase method) and Total dietary fiber kits were obtained from Megazyme (Bray, Ireland).

2.2.2 Methods

2.2.2.1 Yellow pea flour preparation

Yellow peas were kept at -20°C and milled using a rotor mill (Retsch® GmbH, Haan, Germany). Milling was performed with temperature control using cold water flow to keep the overall temperature below 40°C. The milled flour was then sieved to obtain flour particles below 45 µm using a horizontal mechanical sieve shaker (Retsch® GmbH, Haan, Germany).

2.2.2.2 Compositional Analysis

The ash content in the samples was determined by drying a known mass (1 g) of sample in a calcination oven (P 330, Nabertherm GmbH, Lilienthal Germany) at 550˚C for 24 hrs, and the wt% of ash was calculated as follows.

$$\text{Ash} = \frac{\text{final sample mass}}{\text{initial dry sample mass}} * 100\ (\text{wt\%}) \qquad \text{Equation 2.1}$$

The final sample weight is the amount of sample left after the calcination oven, and the initial dry weight is the moisture-free sample mass before calcination oven treatment.

The amount of protein in PF and PPM was determined using a Dumas nitrogen analyzer (FlashEA 1112 series, Thermo Scientific, Interscience, Breda, The Netherlands). The measurement principle is that the sample is burnt at 900˚C, and nitrogen is detected against a standard curve made with D-Methionine. A conversion factor of 6.25 was used to convert nitrogen content into protein content [58].

$$\text{Amount of protein} = \frac{\text{nitrogen content} * 6.25}{\text{total dry mass of sample}} * 100\ (\text{wt\%}) \qquad \text{Equation 2.2}$$

Where nitrogen content is the result of the Dumas method, the Total dry mass of sample is the weight of dry sample added, and 6.25 is the nitrogen conversion factor.

The starch content of pea flour was measured using the Total Starch Glucosidase/α-Amylase assay kit (Megazyme International Ltd., Bray, Ireland) using the AOAC Official Method 996.11 [66]. While the starch in PPM dispersion was measured after filtering the starch using the method for dispersed starch content by enzymatic assay of Megazyme total starch assay kit (Megazyme International Ltd., Bray, Ireland). The total dietary fiber content of yellow pea flour was measured using the total dietary fiber assay kit (Megazyme International Ltd., Bray, Ireland) following the AOAC Method 991.43 [66].

The oil content in pea flour was determined using an automated Soxhlet extractor (Buchi, Hendrik-Ido-Ambacht, The Netherlands). A known amount of sample (1 gr) was weighed in cellulose thimble of known weight. The thimbles were fitted in the apparatus oil was extracted using Hexane for 4 hrs. Finally, the solvent was evaporated entirely, and the amount of oil was calculated gravimetrically by measuring the weight before and after extraction. All analyses were done in triplicate, and the mean value was reported.

$$\text{Amount of oil} = \frac{\text{final sample weight}}{\text{initial dry sample weight}} * 100\ (\text{wt\%}) \qquad \text{Equation 2.3}$$

Where final sample weight is the residue sample left in the thimble, and the initial dry sample weight is the amount of sample weighed into the thimble before extraction

2.2.2.3 Preparation of pea flour and pea protein mixture dispersions

A known amount of pea flour (<45 µm particles) was dispersed in ultra-pure water, and the pH was adjusted to pH 7 by adding a few drops of a NaOH (0.5 M) solution. The dispersion was gently mixed under magnetic stirring at room temperature for 3 hrs to allow hydration of the proteins in the mixture. This dispersion will be referred to as pea flour dispersion.

To obtain the PPM, the starch granules were removed by filtration using a filter paper with a cut-off of 4-7 µm (Whatman® 595 ½) using vacuum filtration. In brief, a known amount of pea flour was dispersed in ultra-pure water, and the pH was adjusted to 7. The dispersion was subject to vacuum filtration, and the filtrate was collected and used further, known here as PPM dispersion.

2.2.2.4 Interfacial properties

The oil/water interfacial tension of PF and PPM dispersion was measured using an automated drop tensiometer (ADT, Tracker, Teclis-instruments, Tassin, France). The rapeseed oil was treated with Florisil® overnight to remove any impurities present in the oil. Florisil and oil were mixed in the ratio (1:3) (w/w) and allowed to stir overnight. The slurry was centrifuged, and the clear oil was used for the experiments.

An oil droplet with a surface area of 30 mm^2 was formed at the tip of a stainless-steel needle immersed in the pea flour dispersion. The shape of the oil droplet was continuously monitored using a camera and transformed into interfacial tension (γ) by Wdrop® software from Teclis® (Tassin, France) [67]. All measurements were performed at 20˚C.

The interfacial tension reached a steady value after 3.5 hours, and the dilatational viscoelasticity was measured using an amplitude sweep test. The droplet was subjected to sinusoidal amplitude deformations where its area changed 2.5%, 5%, 10%, up to 30% of its original surface area. Each amplitude consisted of 5 cycles, 100 sec, followed by a rest period of 5 cycles (5 x 100 sec). The interfacial tension was recorded as a function of time together with the amplitude of deformation. The interfacial dilatational modulus (E_d)

$$E_d = \left| E_d^{'} + iE_d^{''} \right|$$ Equation 2.4

$E_d^{'}$ and $E_d^{''}$ are the storage and modulus obtained from the amplitude sweep tests.

2.2.2.5 Oil-in-water emulsion preparation

Pea flour dispersion and pea protein concentration dispersion of varying concentrations were used as an aqueous phase to make emulsions. The dispersions were initially sheared under a high-speed rotor-stator homogenizer (IKA®, Staufen, Germany) at 6000 rpm for 30 sec. Afterward, 10 wt% canola oil was slowly added to the dispersion and homogenized for 1 min at 10000 rpm. The coarse emulsion that was formed was further homogenized by passing 5 times through a high-pressure homogenizer at 250 bars (GEA®, Niro Soavi NS 1001 L, Parma, Italy). All emulsions were made in duplicates following the same procedure and were all stored for 3 hrs before further analysis. The composition of the pea flour emulsions is given in **Table 2.1**, while the composition of the PPM emulsions is given in **Table 2.2**. Protein concentration was standardized to the same amount for both PF and PPM emulsions.

Table 2.1*: Composition of pea flour emulsions made with various concentrations of protein*

Pea flour emulsion components			
Initial pea flour (g)	Water (g)	Oil (g)	Final protein concentration (wt %)
0.50	89.50	10.00	0.10
0.75	89.25	10.00	0.15
1.00	89.00	10.00	0.20
1.25	88.75	10.00	0.25
1.50	88.50	10.00	0.30

***Table 2.2**: Composition of pea protein mixture emulsion with different protein concentration*

Pea protein mixture emulsion components				
Initial pea flour (g)	Pea protein mixture (g)	Water (g)	Oil (g)	Final protein concentration (wt %)
1.10	0.35	88.90	10.00	0.20
1.65	0.52	88.35	10.00	0.30

2.2.2.6 Droplet size

Droplet diameter measurements were performed using a Malvern® Mastersizer 3000 (Malvern Instruments Ltd., Worchester, UK) equipped with a hydro dispenser. The droplet diameter was presented as volume mean diameter ($D_{4,3} = \frac{\sum_1^n n.D_I^4}{\sum_1^n n.D_i^3}$).

To measure the individual droplet size of the emulsions, the emulsions were centrifuged at 3000 g for 15 min to settle starch granules. The cream layer was carefully removed and mixed with 1 wt% SDS solution. The sample was immediately measured for droplet size using a refractive index of 1.47 of rapeseed oil. Every measurement was performed in triplicate.

2.2.2.7 Zeta potential

The surface charge of the emulsion droplets was measured using a Malvern® Nanosizer (Malvern Instruments Ltd., Worchester, UK). The emulsion samples were diluted 1:1000 (wt. ratio) in Milli-Q water. The diluted samples were then filled in a Malvern folded cuvette (DTS1061). The samples were placed in the instrument and equilibrated for 5 min before measurements were performed. The electrophoretic mobility of the droplets was measured at 20˚C and converted into surface potential ζ by the following equation

$$U_E = \frac{2\varepsilon\zeta(\kappa a)}{3\eta} \qquad \text{Equation 2.5}$$

Where U_E is the electrophoretic mobility, ε is the dielectric constant of the medium, η is the absolute viscosity of the medium. κα is known as the Henry function, where κ is the Debye

parameter which is a function of electric double layer and α is the radius of the particle/droplet.

2.2.2.8 Protein surface coverage of oil droplets

To quantitatively determine the protein concentration at the oil droplet interface, the prepared emulsions were centrifuged at 10000 g (30 min, 4°C), and the obtained phase-separated emulsions were kept at -20°C for 2 hrs. Subsequently, the cream layer was collected carefully from the frozen serum and dried in the oven at 60˚C for 48 hrs. The aqueous serum and the precipitate were collected and pooled, and the protein concentration in both cream and aqueous phases was measured using Dumas, as mentioned in section 0.

The protein surface load, Γ_s (in mg per m^2), was calculated as [68]:

$$\Gamma_s = \Gamma_T / S_T \qquad \text{Equation 2.6}$$

where Γ_T is the measured amount of protein at the interface and S_T is the total surface area, calculated by

$$S_T = \frac{6}{D_{(3,2)}} * V_{oil} \qquad \text{Equation 2.7}$$

V_{oil} the oil volume, and $D_{(3,2)}$ is the surface mean diameter obtained from laser diffraction experiments of the laser scattering analysis.

2.2.2.9 Qualitative analysis of proteins using electrophoresis (SDS-PAGE)

SDS-PAGE was conducted to qualitatively analyze the protein families present in the yellow pea flour and at the surface of the formed oil droplets. The samples were dissolved in NuPAGE® LDS sample buffer at a concentration of 1 mg/mL. Then, 200 µl NuPAGE® reducing agent was added to the sample. The samples were then heated at 90˚C for 15 min followed by centrifugation at 2000 rpm (425 g) for 1 min. Next, 20 µL clear samples were loaded into the wells of a NuPAGE® 4-12 wt% Bis-Tris precast gel. A protein standard (10 µL) (10 kDa – 200 kDa) was also loaded into the well, and the gel was fixed in the electrophoresis chamber. After filling it with MES Buffer, the electrophoresis was run at 200 V. Further, the gel was separated and washed with ultra-pure water and was gently shaken for 1 hr in Comaisse® blue stain. The gel was then destained with a solution

containing 20% ethanol, 50% acetone, 30% water for 1 hr. Finally, the gel was washed with ultra-pure water and stored.

2.2.2.10 Confocal laser scanning microscopy (CLSM)

The structure of emulsions was analyzed using a Nikon C2+ confocal laser scanning microscope fitted with a 40x oil objective and a camera. Coumarin-6® was used to stain the oil phase, and Rhodamine B® was used to stain the protein. The dyes were dissolved in propanol (Coumarin-6) and ultra-pure water (Rhodamine B) with a concentration of 0.1 mg/mL. 7 µL of each dye was added to 1 ml of the emulsion sample and gently mixed for 15 min. Subsequently, the samples were transferred onto a flat glass slide and imaged on the confocal microscope. Coumarin-6 was excited with a 405 nm laser, while Rhodamine was excited at 566 nm. The micrographs were captured using Nikon® image software and processed by ImageJ software.

2.2.2.11 Cryogenic Scanning Electron Microscopy (cryo-SEM)

Cryo-SEM imaging of the samples was performed to visualize better oil droplets' pea flour and interfacial structure and any possible interaction with starch granules. In short, the emulsion was first cryo-frozen using liquid ethane and then transferred to a cryo-planing setup. The planning was done in a cryo-microtome equipped with a diamond knife. The sample was then sublimated under a vacuum. The sample was transferred to a Jeol SEM chamber (Jeol B.V, Nieuw-Vennep, The Netherlands) cooled to -110°C using liquid nitrogen, sputter-coated with platinum under argon flow, and imaged.

2.2.2.12 Viscosity measurement

The rheological properties of the prepared emulsions were determined using shear sweep tests. Measurements were performed on an Anton-Paar® 301 (Anton Paar, Oosterhout, The Netherlands) rheometer equipped with a double gap geometry. Shear sweep tests were performed at 20ºC by increasing shear from 0.1/s to 1000/s measuring the apparent viscosity. The corresponding graph of shear rate vs. apparent viscosity was plotted in a log-log plot.

2.3 Results and Discussion

***Table 2.3**: Composition of pea flour and pea protein mixture on a dry basis.*

Sample	Protein (wt %)	Starch (wt%)	Oil (wt %)	Fibers (wt%)	Ash (wt %)
Pea flour	19.7±0.88	51.0±1.6	2.2±1.1	16.6±1.3	3.05±0.7
Pea protein mixture	57.2±1.2	6.0±0.43	N.D	N.D	N.D

The primary components in yellow peas are starch and protein [34,69]. Therefore, a major focus in this study is given on the effect of these two components on the interfacial and emulsion properties of yellow pea flour. Thus, besides the pea flour (PF), a pea protein mixture (PPM) was also produced by removing the starch by filtration. The compositions of the PF and the produced PPM are displayed in **Table 2.3**.

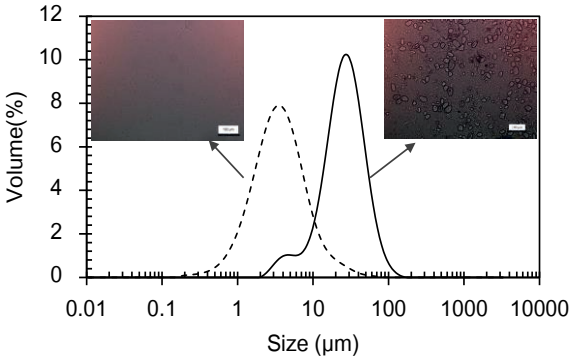

Figure 2.1: Size distribution of PF dispersion (solid line) and PPM dispersion (dashed line); insets showing corresponding light micrographs of the dispersion (pH 7, 20˚C, scale bar: 100 μm).

The PF contains starch granules, protein aggregates, and cell wall material of different sizes. The figure shows the size distribution of the PF and PPM dispersion in water and representative light micrographs. Two peaks can be observed in the size distribution curve for PF (**Figure 2.1**, solid line). A small one between 2 and 5 μm and a major one at around

30 µm. Starch granules are expected to have a diameter of around 30 µm, while protein aggregates are between 1 and 3 µm.

On the other hand, cell wall fragments are expected to have a broad size distribution from a few micrometers up to about 40 µm [36]. This is in line with the light micrographs shown in the inset, where starch granules and some cell wall fragments can be observed. Moreover, the particle size distribution of the protein mixture dispersion (**Figure 2.1**, dotted line) clearly shows the successful removal of starch since only a peak at 1-3 µm was observed. The removal of starch was also confirmed by the light micrograph image of protein mixture dispersion shown in the inset, where the large particles visualized in PF dispersion are not present.

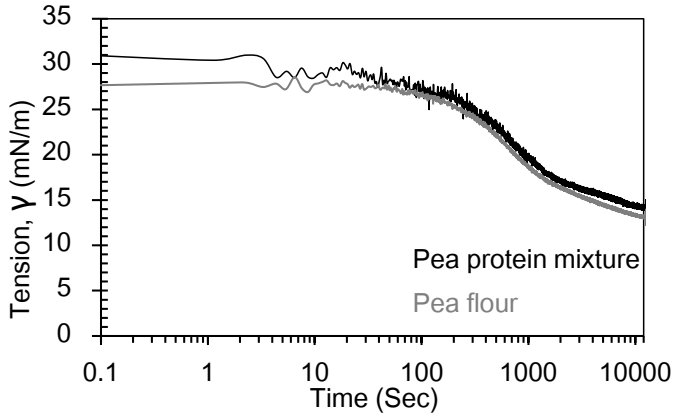

Figure 2.2: Dynamic interfacial tension measurement of PF (——) and PPM dispersion (——) standardized to 0.002 wt% protein (pH 7, 20˚C).

The interfacial activity of molecules can be studied by monitoring their ability to reduce the interfacial tension of oil/water interfaces [70]. **Figure 2.2** shows the interfacial tension reduction profile over time for PF and PPM. The interfacial stabilization of PF was similar to that of protein mixture dispersion. This shows that the interfacial behavior of the PF was similar to that of the PPM systems. Besides, three distinct phases can be observed in the interfacial tension graph for both systems, showing the typical behavior of amphiphilic proteins [42,71,72].

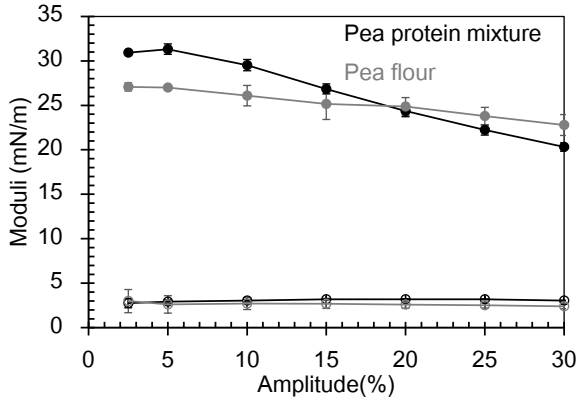

Figure 2.3: Dilatational elastic modulus (Ed': filled symbols) and viscous modulus (Ed": unfilled symbols) of PF dispersion (—) and dilatational PPM dispersions (━) standardized to 0.002 wt% protein, as a function of the amplitude of droplet deformation (pH 7, 20˚C).

Apart from reducing interfacial tension, the elastic and viscous nature of the interface formed by the PF and the protein mixture was studied by dilatational rheology. This analysis aimed to investigate the extent of interactions between adsorbed molecules and the nature of the formed interface [73]. In **Figure 2.3**, the dilatational elastic (E_d') and viscous (E_d'') moduli are plotted as a function of the amplitude of deformation. The elastic modulus was much higher for both the samples than the viscous modulus showing that the interface had a more elastic nature. The values for the elastic moduli are in the same order of magnitude as previously reported for pea proteins [29]. This indicates that the interface is stabilized by the proteins present in the PF. Moreover, the removal of starch does not change the elastic nature of the interface, which indicates that the presence of non-protein molecules does not influence the interfacial elastic network formed by proteins.

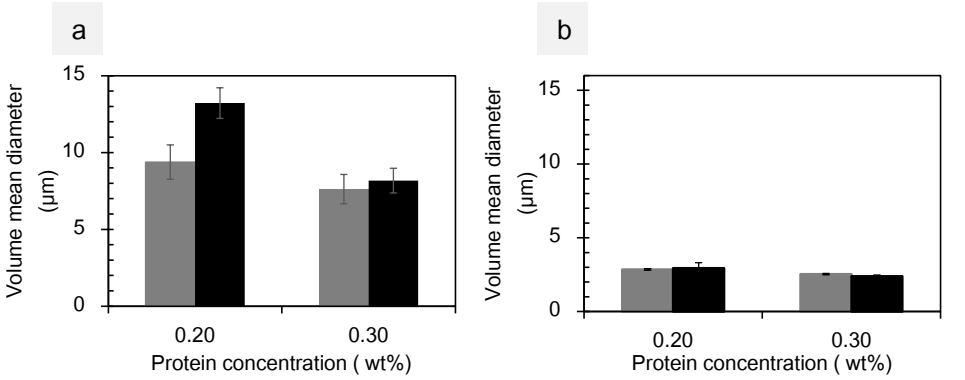

Figure 2.4: Mean droplet aggregate size of PF emulsion (gray); PPM emulsion (black) (a) and mean individual droplet size of PF emulsion (gray) and PPM emulsion (black) (b) at 0.2 wt% and 0.3 wt% protein concentration (pH 7, 20˚C).

Since it was concluded that the proteins present in the native matrix of the PF are interfacially active, the next step was to investigate their emulsifying ability. To clarify any possible effect of non-protein compounds on the emulsifying ability of pea proteins, emulsions with PF or PPM were prepared. For this purpose, two protein concentrations of 0.2 wt% and 0.3 wt% were chosen. These two protein concentrations were chosen because these concentrations are expected to have enough protein molecules to cover the interface [74]. Besides, higher protein content would lead to higher solid content and viscous emulsions. The prepared emulsions were compared with regard to individual oil droplet size distribution and stability against aggregation (**Figure 2.4**). The emulsions exhibited similar oil droplet and aggregate sizes, proving that starch, at this concentration, had a minor influence on emulsifying ability. Regardless of the presence of starch, the formation of aggregates can be attributed to hydrophobic forces, and the low electrostatic repulsion between the droplets since the surface charge was about -17±1.5 mV. The electrostatic potential was significantly lower than the -30 mV required for strong electrostatic repulsion [75]. Besides the weak electrostatic repulsion forces, it is possible that due to the presence of non-absorbed bio-polymers, depletion forces also arose, leading to extensive oil droplet flocculation [76].

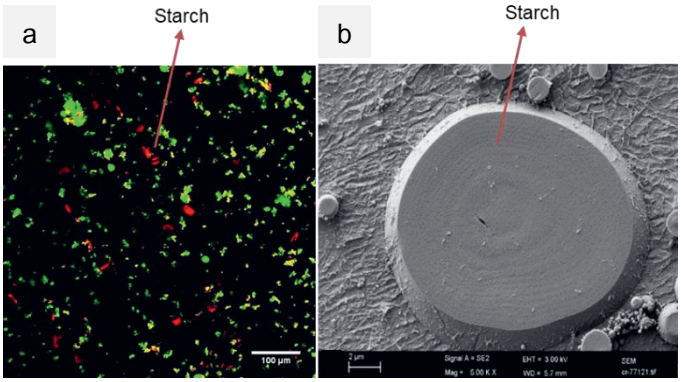

Figure 2.5: Confocal laser scanning (a) and scanning electron micrographs (b) of a PF emulsion (10.0 wt% oil, 1.0 wt% PF/0.2 wt% protein).

Confocal and electron microscopy were used to investigate the microstructure of the PF emulsions (**Figure 2.5**). The confocal micrograph (**Figure 2.5.a**) confirmed that starch granules do not associate with the oil droplets, and therefore do not contribute to the rheological properties of the system. Similarly, cryo-SEM analysis (**Figure 2.5.b**) showed that the starch granules retained their granular shape and didn't closely associate with the surrounding oil droplets.

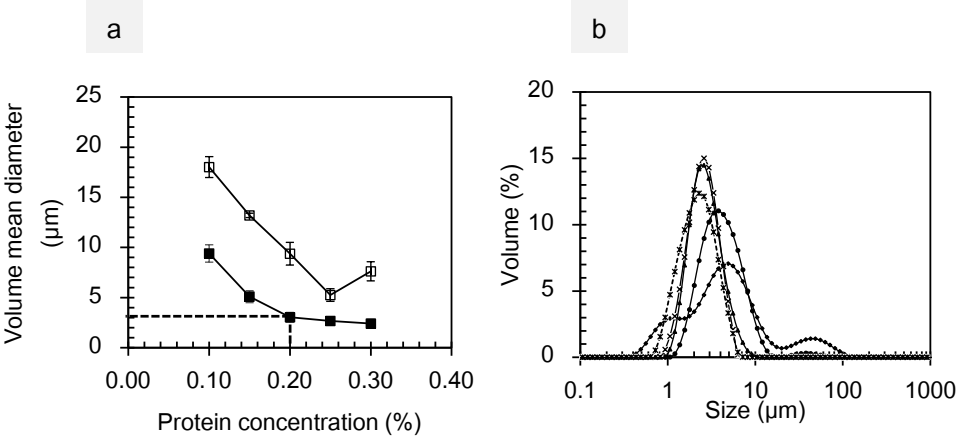

Figure 2.6: (a) Average particle size of individual oil droplets (■) and aggregates (□) as a function of protein concentration (wt%) and; (b) size distribution of individual oil droplets as a function of protein concentration; 0.10 (—◆—) 0.15 (—●—) 0.20 (—▲—) 0.25 (—✕—) and 0.30 (--✳--) wt% protein of PF emulsion (pH 7, 20˚C).

Since it was shown that PF showed similar emulsifying properties compared to protein mixture, PF emulsions were studied further. Therefore, the emulsifying performance of the PF, the average size of the individual oil droplets, and droplet aggregates were measured as a function of the protein concentration in the PF (0.1 wt%-0.3 wt %) (**Figure 2.6.a**). The emulsions with lower protein concentration (<0.2 wt%) had larger individual oil droplets, with an average diameter of around 10 µm. However, the average oil droplet size was decreased to around 2.5 µm with increasing protein concentration at 0.2 wt%. Above this protein concentration, the average size of the oil droplets was at the same regime. Besides the mean oil droplet size, the size distribution of the oil droplets is also an important parameter. The size distribution of the individual oil droplets with varying protein concentrations is shown in **Figure 2.6.b**. According to this graph, at lower protein concentrations (0.1 and 0.15 wt %), the size distribution was more comprehensive and multi-modal, while it was narrower and monomodal at higher protein concentrations (0.2-0.3 wt%). The changes of the oil droplet size with increasing protein content indicate that at lower protein concentrations, the amount of proteins present is insufficient to cover the created interface during emulsification. Under these conditions, the average droplet size is determined by the number of proteins and not by the energy input of the homogenization process, known as the protein-poor regime [77].

On the other hand, at higher protein content (≥0.2 wt%), which can be called the protein-rich regime, the protein concentration is sufficient. The droplet size is not dependent on the protein concentration. Therefore, 0.2 wt% was chosen as the critical protein concentration since this value lay between the protein-poor and protein-rich regime. This value lies within the wide range (0.1 - 1.0 wt%) of protein concentration used in previous studies to produce pea protein stabilized emulsions [29,74,78]. Higher protein concentrations (1.0 - 2.0 wt %) were not tested because the emulsions would be too thick due to the high solid content (5.0 - 10.0 wt% PF).

The protein surface load was analyzed to validate that 0.2 wt% protein was sufficient to stabilize a 10 wt% oil-in-water emulsion. From the 0.2 wt% protein present in the emulsion (0.02 g protein/mL of oil), about 0.12 wt% (0.012 ±0.002 g protein/mL of oil) was associated with the oil, while about 0.07 wt% was resting in the continuous phase (0.064 ±0.002 g protein total). This translates to a surface load of 5.9 ±0.6 mg/m^2. The previously reported value for complete droplet surface coverage for pea and lentil protein was between 4.6 –

5.5 mg/m^2 [55]. Therefore, the 5.9 mg/m^2 that was adsorbed in this case is expected to be sufficient to cover the entire interface formed and prevent the coalescence of oil droplets.

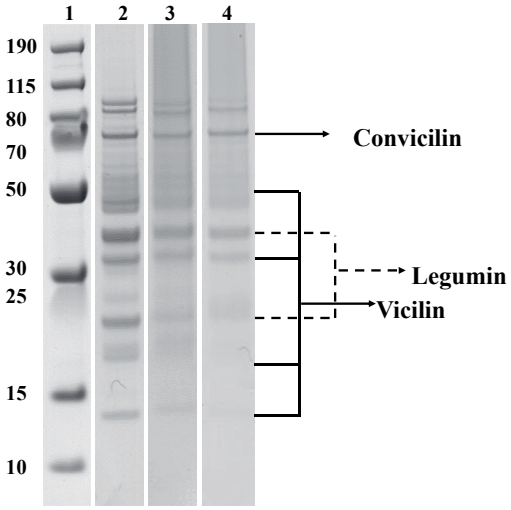

Figure 2.7: Gel electropherogram of a protein marker (lane 1); PF (lane 2); emulsion oil droplets (lane 3); emulsion continuous phase (lane 4) of 0.2 wt% protein PF emulsion.

Apart from the quantitative analysis of the number of proteins on the interface, the qualitative analysis of the proteins absorbed is also essential. Therefore, SDS-PAGE analysis was performed, and the electropherogram is given in **Figure 2.7**. As can be seen from the figure, the proteins in the PF, the oil droplet interface, and the continuous phase of the emulsions were very similar. The globular protein fractions pea legumin (11S) and vicilin (7S) were both associated with the cream and aqueous layers. The similarity in the aqueous and cream phases indicated that the pea proteins (legumin, vicilin, convicilin) are all interfacially active and adsorbed in the oil-water interface.

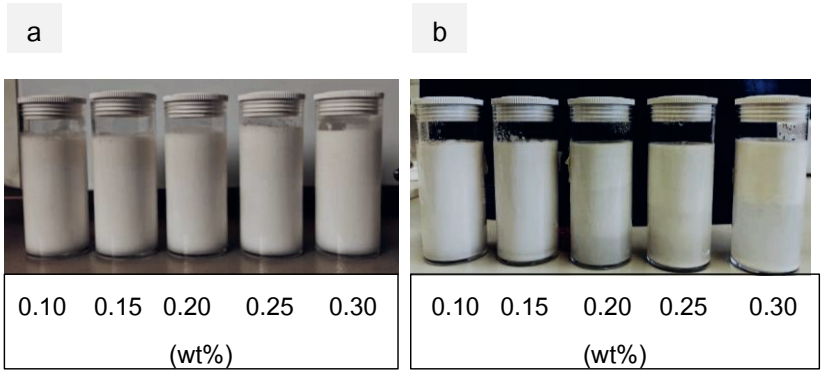

Figure 2.8: PF emulsions (10.0 wt% oil) made with increasing protein concentration (0.1- 0.3 wt%) (a) on day 0 and, (b) on day 7, when stored at 4˚C.

The macroscopic phase separation (creaming) of the oil droplets from the aqueous continuous phase is an essential physical stability parameter in emulsions. It is primarily dependent on the size of the oil droplets and their aggregates [79]. Therefore, the creaming behavior of the emulsions was visually monitored for 7 days (**Figure 2.8**). As shown in **Figure 2.8.b**, the emulsions made with lower protein concentration (0.1 - 0.15 wt%) showed no precise serum formation, whereas, at higher protein concentration, there was a more distinct cream layer boundary. This is contrary to the expected behavior based on the size of the droplets and aggregates (**Figure 2.6**). Since the emulsions with lower protein concentrations had larger droplets and aggregates, higher creaming rates should be expected [80]. However, the sizes of the aggregates measured during this analysis may not reflect the actual aggregate sizes in the emulsion. Weakly bound aggregates formed at higher protein concentration (>0.2 wt%) may separate during measurement. Nevertheless, the unexpected stability against creaming needs to be further investigated.

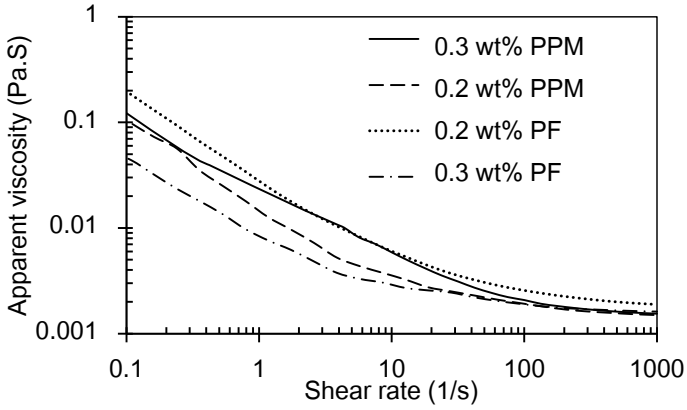

Figure 2.9: Apparent viscosity of oil-in-water emulsions (10.0 wt% oil) prepared with PF (·····) and PPM (– – –) standardized to 0.2 wt% protein; and PF (– · – ·) and PPM (——) standardized at 0.3 wt% protein.

Starch is a well-known thickening agent, which can increase viscosity when present in an aqueous solution. Therefore, the apparent viscosity of the emulsion systems as a function of shear rate was tested in **Figure 2.9**. Emulsions prepared with 0.2 wt% and 0.3 wt% protein in PF and protein mixture emulsion were used for this purpose. All four emulsions showed a decrease in viscosity as shear rates increased. This behavior is known as shear-thinning behavior, which is a characteristic behavior of emulsions that contain droplet aggregates that are weakly bonded [10]. At lower shear rates, the aggregates do not yet flow and exhibit higher viscosity rates. But, as the shear rate increases, the weak interactions between droplets can break, and the aggregates align in the shear direction, leading to viscosity reduction [79]. An important observation was that the emulsions stabilized by PF followed closely the flow behavior curve of the corresponding emulsion stabilized with PPM at the same protein content. The similar shear thinning behavior of both emulsions shows that starch granules had a limited effect on viscosity. Starch granules are in the bulk phase and do not associate with the oil droplet aggregates. This was also corroborated by the confocal micrographs shown in **Figure 2.5.a**. The slight differences observed at low shear rates can probably be attributed to the differences in the sizes of droplet aggregates.

2.4 Conclusions

The interfacial properties of the PF and PPM were very similar, indicating that the pea proteins are the main interfacially active components. Non-protein material, like starch, did not have any influence on the interfacial behavior of the mixture. Moreover, stable oil-in-water emulsions were produced using PF and PPM with the same protein content. The critical protein concentration required to produce stable emulsions was 0.2 wt% for emulsions with 10 wt% oil. In line with the interfacial study, emulsions produced with PF and PPM showed similar droplet size, aggregate size, and rheological behavior. It was shown that the emulsifying properties of the protein in the mixture were not affected by the presence of non-protein material. These results prove that native pea protein mixtures (such as PF) can produce stable emulsions, and the non-protein molecules do not hinder the techno-functionality. These insights can promote native pea protein mixtures as emulsifiers, leading to more straightforward process steps for food production.

Chapter-3: Emulsifying properties of pea proteins at pH 3

Published as:

Sridharan, S., Meinders, M. B., Bitter, J. H., & Nikiforidis, C. V. (2020). On the emulsifying properties of self-assembled pea protein particles. *Langmuir*, *36*(41), 12221-12229. https://dx.doi.org/10.1021/acs.langmuir.0c01955

Abstract

Pea proteins are promising oil-in-water emulsifying agents at both neutral and acidic conditions. In an acidic environment, pea proteins associate to form submicron-sized particles. Previous studies suggested that the emulsions at acidic pH were stabilized due to a Pickering mechanism. However, protein particles can be in equilibrium with protein molecules, which could play a significant role in the stabilization of emulsion droplets. Therefore, we revisited the emulsion stabilization mechanism of pea proteins at pH 3 and investigated whether the protein particles or the protein molecules are the primary emulsifying agent. The theoretical and experimental surface load of dispersed oil droplets was compared. It was found that protein particles can cover only 3.2% of the total oil droplet surface, insufficient to stabilize the droplets. In contrast, protein molecules can cover 47% of the total oil droplet surface. Moreover, by removing protein particles from the mixture and emulsifying with only protein molecules, the contribution of pea protein molecules to the emulsifying properties of pea proteins at pH 3 was evaluated. The results proved that the protein molecules were the primary stabilizers of the oil droplets at pH 3.

3.1 Introduction

Proteins are amphiphilic biopolymers that can stabilize oil-in-water emulsions by adsorbing onto the oil-water interface and decreasing the interfacial tension [8]. In food applications, dairy and egg proteins are mostly used as emulsifiers [81], however, due to environmental concerns, the demand for utilizing plant proteins has tremendously increased [7,62,82,83]. Therefore, several studies have already reported on the emulsifying properties of proteins obtained from plant sources such as soybeans, rapeseeds, and peas [7,35,52,84].

Among various plant protein sources, pea proteins have been widely studied in recent years. Peas mainly contain carbohydrates and proteins, which enables simpler extraction steps to obtain proteins compared to other oil-rich seeds such as soy and flaxseed proteins that require defatting [85–87].

Pea proteins extracted by alkaline extraction, mainly a mixture of trimeric 7S and hexameric 11S globular proteins, have been reported to stabilize oil-water emulsions [88]. The extracted proteins have their point of zero charge (PZC) at pH 4.5, whose emulsifying properties were shown to be different below and above the PZC [24,44]. Emulsification at acidic pH using pea proteins resulted in smaller oil droplets than at neutral pH [44,46,52]. Similar behavior has also been reported for other plant proteins such as soy.

The ability of soy and lentil proteins to stabilize smaller oil droplets in the acidic environment was attributed to the dissociation of proteins from their multimeric form into protein subunits (monomers) [89]. These protein monomers have an increased exposed hydrophobicity [90]. Due to this increased exposed protein hydrophobicity, adsorption of proteins to the droplet surface was promoted. Moreover, due to protein conformational changes at acidic pH, a visco-elastic interface is formed by weak protein-protein interaction [90].

The dissociation of multimeric proteins (hexameric and trimeric) into monomeric form (protein sub-units) is reported in the literature [45]. However, concerning emulsifying mechanism at acidic pH, pea proteins have been reported to self-assemble to form particles [46]. The protein particles are formed even though the proteins are positively charged could be attributed to the enhanced protein-protein physical interactions through hydrophobic and van der Waals forces [91]. These attractive forces may overcome the electrostatic repulsion leading to protein self-assembly. However, more research on the particle formation mechanism is necessary.

Therefore, the proposed mechanism for emulsification by pea proteins in an acidic environment is that the self-assembled protein particles adsorb on the oil/water surface and stabilize the oil droplets through a Pickering stabilization mechanism [35]. Pickering emulsions are associated with stable oil droplets stabilized by particles that are irreversibly adsorbed on the droplet surface [9,92]. The increased droplet stability of Pickering stabilization has attracted great interest in modifying pea proteins to act as Pickering particles in edible emulsion systems, such as by heating to form microgels [93]. However, a mechanistic study of emulsifying behavior of alkaline extracted, unmodified pea proteins at pH 3 has not yet been conducted.

The possible co-existence of proteins molecules (biopolymer) with protein particles (self-assembled) and their effect on droplet stabilization has not been investigated yet. As reported for proteins, and in general for biopolymer self-assemblies, there might be an equilibrium between the number of protein molecules and self-assembled protein particles [94]. In such cases, a considerable amount of protein molecules may still be present in the pea protein dispersion at pH 3. Due to the smaller size and faster diffusion of protein molecules than protein particles, they would be expected to play a significant role in reducing interfacial tension and stabilizing oil droplets. Therefore, the contribution of pea protein molecules to the interfacial properties of pea proteins at pH 3, containing self-assembled particles, needs to be evaluated carefully. A pH value of 3 was chosen to study the emulsifying behavior of pea proteins in acidic conditions relevant for foods while avoiding the possibility of acid hydrolysis.

In this research, we aimed to understand the emulsifying properties of pea proteins at pH 3.0. Specifically, we evaluate the possible contribution of protein molecules that could co-exist with self-assembled protein particles to droplet stabilization. Interfacial tension reduction and emulsifying properties of pea proteins were investigated. Further, we combined theoretical calculations with experimental techniques to gain critical insights into the emulsifying mechanism of pea proteins containing self-assembled protein particles.

3.2 Experimental section

3.2.1 Materials

Whole yellow field peas (Pisum sativum L) were obtained from Alimex BV® (Sint Kruis, The Netherlands). Sodium Hydroxide, Hydrochloric acid (analytical grade), Sodium Dodecyl

Sulphate (SDS) reagent, and fluorescent dyes Nile red and Fast Green® were all obtained from Sigma-Aldrich® (Zwijndrecht, The Netherlands). Whatmann® cellulose thimbles were obtained from VWR (Amsterdam, Netherlands).

3.2.2 Methods

3.2.2.1 Purification of pea proteins

Pea proteins were extracted from yellow peas by alkaline extraction and iso-electric point precipitation, commonly reported in literature [44,90]. In brief, pea seeds were dry milled into a coarse flour in a coffee blender (IKA®, Staufen, Germany). The flour was then soaked in water at 1:10 (w:w) solids to water ratio. The pH was adjusted to pH 8 with a 0.5 M NaOH solution under constant stirring. After 2 hrs of soaking, the slurry was blended in a kitchen blender at maximum speed for 2 minutes. The resultant slurry was centrifuged at 10000 g for 30 minutes to precipitate solids. Further, the protein-rich supernatant was separated, and the proteins were precipitated at a pH of 4.8 with a 0.5 M HCl solution. The solution was allowed to stand for 1 hour, and the precipitate was collected by centrifugation at 10000 g for 30 minutes. The residue was diluted (1:10 w/w) with ultra-pure water, neutralizing the pH (pH 7). The solution was further freeze-dried, and the obtained powder was termed simply pea protein. The protein powder was stored in the freezer (-18°C) for further use.

3.2.2.2 Composition analysis

The amount of protein in the extracted pea protein powder was determined using a Dumas nitrogen analyzer (FlashEA 1112 series, Thermo Scientific, Interscience, Breda, The Netherlands). The measurement is based on combusting the sample and analyzing the nitrogen released against a D-methionine standard. A conversion factor of 6.25 was used [58].

$$\text{Protein content (wt\%)} = \frac{\text{Nitrogen content} * 6.25}{\text{Initial sample dry mass}} * 100$$

Equation 3.1

The ash content in the samples was determined by drying a known mass (1 g) of sample in a calcination oven (P330, Nabertherm GmbH, Lilienthal, Germany) at 550°C for 24 hrs and the wt% of ash was calculated as follows.

$$\text{Ash (wt\%)} = \frac{\text{Final sample mass}}{\text{Initial dry sample mass}} * 100$$

Equation 3.2

The amount of oil present in extracted pea protein powder was determined by a solvent extraction process. A known amount of dry sample was added to cellulose thimbles. Empty round bottom flasks were weighed and filled with hexane. The thimbles were fitted into the extraction unit, and the round bottom flask with hexane was evaporated (60°C) and used to extract the oil for six hours. Afterward, the round-bottom flask containing oil and hexane was removed, and hexane was evaporated under a fume hood for six days. The solvent-free extract in the round-bottom flask was weighed. The amount of oil present was directly determined from the weight increase in the round-bottom flask after solvent evaporation.

$$\text{Oil content (wt\%)} = \frac{\text{Flask weight after extraction} - \text{Empty flask weight}}{\text{Sample weight}} * 100$$

Equation 3.3

3.2.2.3 Oil-in-water emulsion preparation

Oil-in-water emulsions were prepared using pea protein dispersions as an aqueous phase. 10.0 wt% rapeseed oil and 90.0 wt% of protein dispersions were used. The final protein content of the emulsion was standardized to 0.5 wt% by adjusting the protein content in the dispersion. The pH of the dispersion was changed to pH 3 using 0.5 M HCl. The dispersion was then stirred for 3 hours under magnetic stirring. The dispersion was then sheared for 15 secs at 6000 rpm in an IKA® (Ultra-Turrax, IKA®, Staufen, Germany) ultraturrax to ensure homogeneous dispersion of proteins. Further, rapeseed oil was added slowly, and the mixture was sheared for another 60 seconds at 10000 rpm to produce a coarse emulsion. The formed coarse emulsion was further homogenized by passing through a GEA® (Niro Soavi NS 1001 L, Parma, Italy) high-pressure homogenizer for five passes at a homogenization pressure of 250 bar. The obtained final emulsion was allowed to equilibrate 3 hours before any measurement was performed. The emulsions were called pea protein stabilized emulsions and were made in duplicates.

Emulsions were also prepared using protein molecule solution (supernatant after centrifugation). In brief, pea protein dispersions were prepared as explained above. Then the dispersion was ultra-centrifugated at 320,000 g for 45 minutes at 20ºC using a Beckman-Coulter L60 (Beckmann-Coulter Nederland B.V, Woerden, The Netherlands)

ultra-centrifuge in 40 mL tubes. The clear supernatants were carefully collected by pouring them onto a beaker. The collected solution was called protein molecules solution. Emulsions were prepared as described above with this solution.

3.2.2.4 Protein dispersion size and charge

The hydrodynamic size of the particles in the protein dispersion was measured at pH 3 using a Malvern® UltraSizer (Malvern, Worcestershire, United Kingdom). In brief, protein dispersions of 0.5 wt% were prepared as explained in the previous section and homogenized without the addition of oil. The homogenized protein dispersion was loaded into a disposable transparent cuvette, and the size was measured using a refractive index of 1.45, and a temperature of 20°C was set. Similarly, the protein molecules' solution size was measured under the same conditions.

The surface charge of proteins of the same dispersions was measured using a U-shaped cuvette in the Malvern Ultra sizer (Malvern®, Worcestershire, UK) at 20°C. All size and charge measurements were done after 120 seconds of equilibration and were performed in triplicates, and the average value was reported.

3.2.2.5 Droplet size measurement

The individual droplet size of the emulsions was measured using laser diffraction in Malvern® Mastersizer® 3000 (Malvern Instruments Ltd., Worchester, UK). The samples were dispensed using a hydro dispenser, and the droplet size was represented in volume mean diameter.

To measure individual droplet sizes, the emulsions were treated with 1 wt% SDS solution. The addition of SDS breaks droplet aggregation driven by protein interaction, so the size of individual oil droplets could be measured in this manner [95]. An equal volume of (1 mL) of emulsion and 1 wt% SDS solution was mixed, and the size was immediately measured using a refractive index of 1.47. Similarly, the droplet size distribution of the emulsions was determined after 7 days of storage at 4 ºC to assess the coalescence stability.

3.2.2.6 Measured protein surface coverage of oil droplets

The amount of protein covering the oil droplet surface was measured and reported in mg/m^2. The experimental surface coverage was measured according to our earlier work

[96]. In brief, the emulsion samples were centrifuged at 10000 g for 30 minutes at 4ºC. The cream layer was then collected by removing the serum layer from the centrifuge tube by puncturing a hole at the bottom of the tube. The cream was dispersed in ultra-pure water (1:10 (w:w) cream to water). The dispersion was centrifuged again at 3000 g for 15 minutes at 4ºC. The second washed cream layer was also collected, similar to the first centrifugation, and dried. As explained for protein content measurement, the amount of protein in the cream layer was measured using Dumas.

The protein surface load (Γs) was roughly estimated by using the equation below [68]

$$\Gamma_s = \frac{\Gamma_T}{S_T}$$ Equation 3.4

Where, Γ_T is the total measured protein content in the cream layer and S_T is the total surface area.

$$S_T = \frac{6}{D_{(3,2)}} * V_{oil}$$ Equation 3.5

Where V_{oil} is the volume of oil and $D_{(3,2)}$ is the surface mean diameter obtained from laser diffraction experiments.

3.2.2.7 Theoretical estimation of protein surface coverage of oil droplets

The measured surface load of the emulsions was compared with the theoretically estimated surface load. The theoretical surface load of protein molecules and protein particles can be calculated using **Equation 3.6** [97]. The reader is referred to the appendix section for more details on the mathematical considerations to derive the formula.

$$\Gamma = \frac{4}{3} * \rho_p * \varphi_{max} * r_p \quad (mg/m^2)$$ Equation 3.6

Where ρ_p is 1.37 g/cm^3, ϕ_{max} is 0.91 for circles packed on a flat surface with the assumption that the droplet surface is a 2-d entity and r_p the radius of protein/ particle

Two scenarios were considered for the theoretical estimation of the surface load. First, the interface was covered by protein particles, whose radius was based on the hydrodynamic

size obtained from size measurement. The second scenario was assuming that protein molecules solely covered the interface. The radius of the protein molecule was estimated based on its molecular weight according to the following equation [98].

$$r_p = 0.066 * M^{\frac{1}{3}} \text{ (nm)} \qquad \text{Equation 3.7}$$

Where M is the molecular weight of the protein in Daltons

The following assumptions were taken into consideration for calculating the theoretical surface load:

1. Equal amounts of Legumin (11S) and Vicilin (7S) proteins were present at the droplet surface. So, the average size between Legumin: 4.69 nm and Vicilin: 3.50 nm was used to calculate the theoretical radius of protein [98]
2. The density of both protein molecules and protein particles was assumed to be 1.37 g/cm^3
3. The proteins are circles on a 2-D droplet surface.

3.2.2.8 Interfacial tension and dilatational moduli

The interfacial tension reduction and dilatational rheology of oil-pea protein dispersion interface and oil-protein molecules solution interface were measured using an automated drop tensiometer (Tracker, Teclis-instruments, Tassin, France). 0.01 wt% pea protein and corresponding pea protein molecule solution (0.01 wt% protein dispersion after centrifuged) were prepared as explained in the emulsion preparation section.

Rapeseed oil was treated with Florisil® overnight to remove impurities was used as the oil phase. In brief, 1:3 (w/w) Florisil to oil were mixed overnight and centrifuged the next day to obtain contaminants-free oil, which was used in the interfacial study.

The rapeseed oil was loaded onto a 500 µL syringe fitted with a J-shaped needle in the drop tensiometer. The aqueous phase was filled into a clean, 7 mL optical glass cuvette. The needle was inserted into the aqueous phase, and a sessile drop of 15 mm^2 areas was made. The shape of the oil droplet was monitored continuously using a camera. This was converted into interfacial tension by the Wdrop® software from Teclis® Tassin, France).

The dynamic interfacial tension reduction profile was monitored continuously for 3.5 hours and plotted against time in a semi-log plot. The interfacial tension reduction was modeled using the curve fitting procedure using the equation below [99].

$$\gamma_t = \gamma_\infty + \gamma_1 e^{\frac{-t}{t_1}} + \gamma_1 e^{\frac{-t}{t_2}}$$

Equation 3.8

Where, γ_t is interfacial tension at a given time, γ_∞ is the final interfacial tension, γ_1 and γ_2 fit constants. While t is time in a sec, t_1 is time in secs, related to the lag phase, and t_2 is time in secs, related to the rearrangement phase.

After 3.5 hours, dilatational viscoelasticity was measured by changing the surface area of the droplet in a sinusoidal manner. The droplet was subjected to changes in surface area with amplitudes of 5%, 10% up to 30% deformation with respect to initial surface area (15 mm^2). Each amplitude was applied for 100 seconds with 5 cycles next to each other. This was followed by 500 seconds rest period before the next higher amplitude was applied. The interfacial tension change and change in the area were recorded during the oscillation, and the dilatational elastic ($E_d^{'}$) and viscous moduli ($E_d^{''}$) were obtained.

3.2.2.9 Light microscopy and Confocal Microscopy (CLSM)

Emulsions were visualized using light microscopy (Axioscope, Zeiss, Jena, Germany) using 100× magnification, 5 times dilution in ultra-pure water. The images were captured using an axiovert digital camera (Zeiss, Jena, Germany) and an axiovision imaging software (Zeiss, Jena, Germany).

The emulsions were imaged using a confocal laser scanning microscope (CLSM) with fluorescent dyes to visualize the microstructure. In brief, about 1 ml of the emulsion was mixed with 7µl of Nile red® and 7µl of Fast green FCF® in an eppendorf® tube. The tubes were sealed and allowed to mix for 15 minutes. Afterward, about 30 µl of the sample was deposited on a microscopy slide and mounted on the confocal table. A Leica® SP8® confocal microscope fitted with a 63x water immersion lens and white light laser was used to image the samples. Nile red stained the oil phase and was excited at 488 nm, and the emission was captured between 500-600 nm. Rhodamine B, which stained proteins, was

excited at 566 nm, and the emission was captured between 570-670 nm. The images were captured in a sequential manner using Leica® imaging software.

3.2.2.10 Transmission electron microscopy

The emulsions were imaged using TEM after fixating the sample on polymer resin. Briefly, the emulsions were mixed 1:1 (v/v) with 3wt% Agarose solution at 40°C. Then the mixture was allowed to solidify in the fridge at 4°C. The hardened tubes were cut into 1 mm*1 mm cubes. The cubes were then fixed with glutaraldehyde for 1 hour and washed three times with 0.1M phosphate buffer. The cubes were subsequently fixated with 1% osmium tetroxide and washed with ultra-pure water. Then dehydration protocol was started by ethanol washing. A series of 30 %, 50%, 70%, 80% up to 100% ethanol washing steps were performed, each lasting for 30 minutes. After the last ethanol wash, the samples were mixed with spurr embedding liquid in 3 steps 2:1,1:1 and 1:2 (ethanol: spurr), each step being 30 minutes long. After this, the samples were left in 100% spurr for 1 hour and refreshed with 100% spurr again, and left overnight. The following day, spurr was refreshed again for 1 hour, and then the sample was left to polymerize for 8 hours at 70°C. The spurr polymerized, and the samples were embedded in it. Next, the samples were sectioned using Leica EM rapid (Leica® Biosystems, Nussloch, Germany). Afterward, the samples were more precisely sectioned using Leica® ultramicrotome UC7 into 70 nm thin coupes. The coupes were collected with formvar film 150 mesh copper TEM grids. The grids containing the samples were loaded into Jeol® JEM1400 plus-120kV TEM (Jeol B.V, Nieuw-Vennep, The Netherlands) with an EM-11210SQCH specimen quick change holder. The samples were imaged at 120kV. The protein particles after homogenization were also viewed using the TEM. The protein particle dispersion was placed on a copper grid. The samples were stained with 2µl of Phospho-tungstic acid (PTA) for 15 seconds. Then the samples were dried using fiber-less filter paper pieces and washed once with water, and dried again. The dried copper grid was then transferred onto Jeol® JEM2100 TEM chamber and imaged.

3.3 Results and Discussion

The composition of the extracted pea proteins was 84 wt% protein, 6 wt% oil, and 3 wt% ash, similar to the already reported compositions of pea protein extracts [24,55]. The proteins were characterized for their surface charge density (zeta potential) and solubility as a function of pH (data not shown). The zeta potential and solubility curves showed were similar to what has been reported for pea proteins, with the zero charge point of pH 4.6 and minimum solubility between pH 4-5 [24,100].

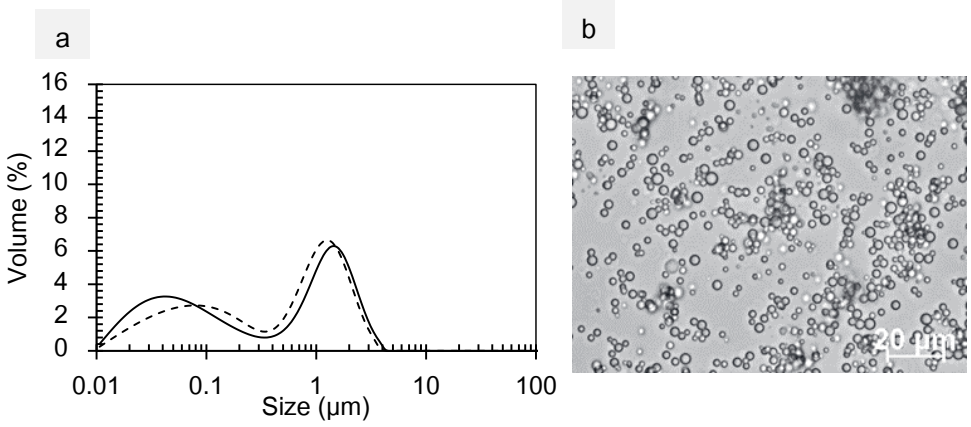

Figure 3.1:(a) Particle size distribution of 10.0 wt% oil-in-water emulsion freshly prepared (solid line) and after 7 days of storage at 4ºC (dashed line) stabilized using 0.5 wt% protein, pea protein extract; (b) Light micrograph of the emulsion shown (scale: 20 µm/diluted 5 times).

To further evaluate the emulsifying property of pea proteins, oil-in-water emulsions were prepared at pH 3.0. The particle size distribution of the resulting emulsion is shown in **Figure 3.1.a,** and the corresponding light micrograph of the emulsion is shown in **Figure 3.1.b**. The figure shows droplet size distribution for fresh emulsions and after storage for 7 days, and the light micrograph shows oil droplets in fresh emulsions. The size distribution curve shows a bimodal size distribution with a clear distinction between the two peaks. The hypothesis is that the oil droplets correspond to the curve in size range between 0.5 and 5 µm. The smaller sub-micron peak between 0.01 µm and 0. 7 µm could be related to protein particles [46].

After storage for 7 days, no significant change in the droplet size distribution was observed (**Figure 3.1.a,** dashed line), indicating that the amount of protein present at the droplet surface was sufficient to avoid droplet coalescence.

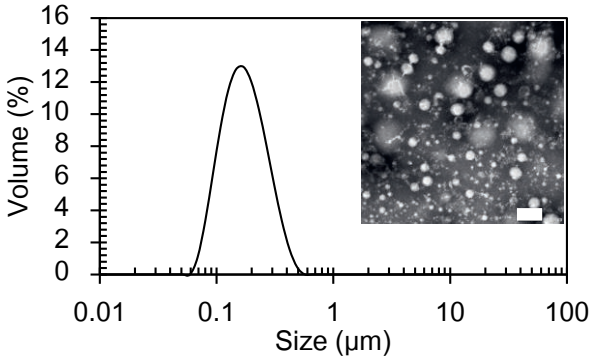

Figure 3.2: Size distribution self-assembled protein particles at pH 3, homogenized at 250 bar pressures, inset showing TEM image of protein particles (0.5 wt% protein).

The size distribution curve between 0.01 and 0.50 µm observed in **Figure 3.1** could correspond to the pea protein particles [46]. To investigate the cause of the submicron peak, the protein dispersion was homogenized at the same conditions as the emulsions without adding oil. The particle size of the homogenized dispersion is given in **Figure 3.2**. The figure shows a monomodal particle size distribution curve in the sub-micron range. The inset in **Figure 3.2** shows a representative transmission electron micrograph of the homogenized protein particle dispersion with spherical particles in light grey. The size distribution shows that particles in size range between 0.05 and 0.70 µm with a peak around 0.12 µm were observed. According to the literature, this peak could be attributed to self-assembled protein particles present in positively charged pea protein dispersion [46]. Moreover, spherical particles observed in the TEM correspond well with the size distribution and are most likely protein particles since the extracted protein powder used here contains about 85 wt% protein. Despite being below the iso-electric point, the presence of protein particles at pH 3 shows that the driving force for the formation of the protein particles could be a combination of physical forces such as hydrophobic and van der Waals that overcome the electrostatic repulsion.

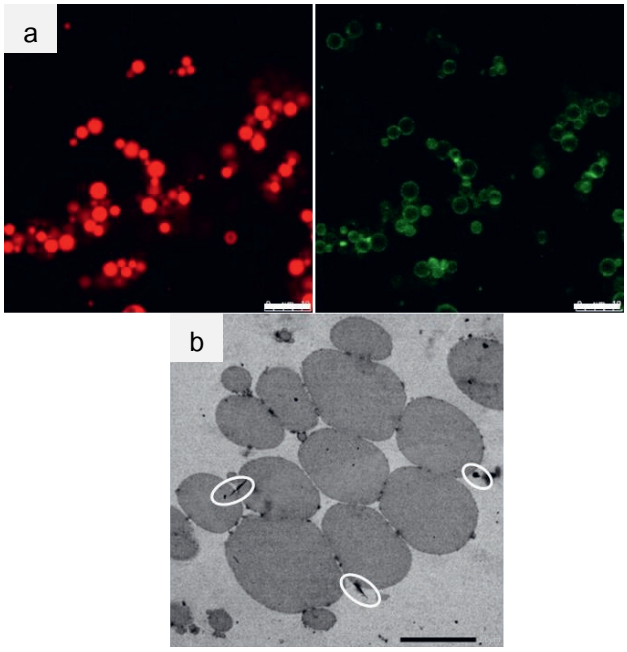

Figure 3.3: (a) Confocal micrograph showing oil droplets in red and protein surrounding the oil droplets in green (scale bar: 10 µm) and; (b) TEM micrograph of emulsion droplets with protein particles encircled (scale bar: 2 µm); of 10.0 wt% oil-in-water emulsion stabilized by 0.5 wt% pea proteins at pH 3.0.

The protein particles of size 0.05 µm and 0.70 µm (**Figure 3.2**) formed at pH 3.0 have been attributed as the droplet stabilizing agent in pea proteins through a Pickering stabilization mechanism [35,46,101]. Confocal and electron microscopy analysis was employed to investigate whether the protein particles were adsorbed on the oil droplet surface (**Figure 3.3**). The confocal micrograph (**Figure 3.3.a**) shows oil droplets (red) surrounded by proteins (green). The figure shows that the protein particles were only found in patches at the droplet surface and not seen as a homogeneous layer around the oil droplets. Besides, not all the oil droplets were covered by the protein particles. To gain a more detailed visualization of the droplet surface, transmission electron microscopy analysis was employed (**Figure 3.3.b**), which shows oil droplets in grey and proteins in black. The image shows a clear interface of oil droplets covered with denser regions, which are proteins. Besides, the protein particles are not covering the entire droplet surface, similar to the observation from the confocal micrograph.

It was not clear whether solely protein particles were stabilizing the oil droplet surface from the microscopy analysis. Therefore, more information on the state of the proteins adsorbed was required to understand the emulsifying mechanism. Therefore, the formed oil droplets' surface coverage (mass of protein per unit surface area) was calculated theoretically (using **Equation 3.6**) and compared with the experimentally measured surface coverage.

The positively charged pea proteins self-assemble to form particles, however since only physical forces such as van der Waals forces and hydrophobic forces drive the particle formation, an equilibrium between protein molecules and protein particles might exist [91,94]. Therefore, two scenarios were considered when calculating the theoretical surface load. The first one is based on a droplet surface stabilized by protein particles of 60 nm radius, obtained from the particle size analysis of homogenized pea protein dispersion, where the peak particle size is around 120 nm (peak value from **Figure 3.2)**. The second scenario is based on droplet surface stabilized by protein molecules of radius 4.1 nm, which was calculated from the molecular weight of the protein molecules according to **Equation 3.7**. The two theoretical scenarios were compared with the experimentally measured surface load, as shown in **Figure 3.4**. The figure shows theoretical surface load based on the two scenarios (top left) and experimentally measured surface load (top right). The bottom part of the figure compares the theoretical and experimental surface load for the two scenarios.

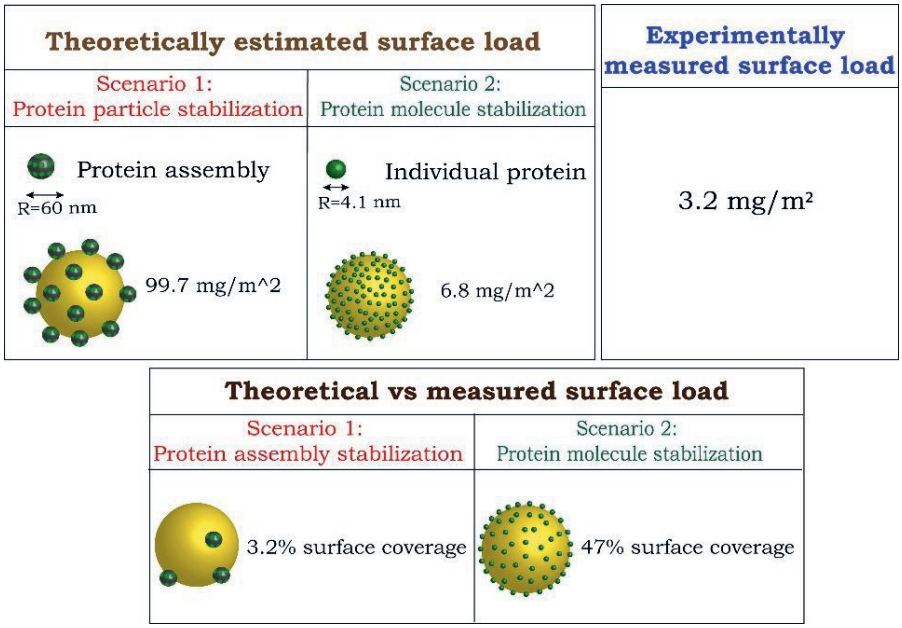

Figure 3.4: Comparison between measured surface load with theoretical surface load based on two scenarios (1) Protein particle stabilization (radius r_p=60 nm, obtained from **Figure 3.2**) and (2) protein molecules stabilization (radius r_p = 4.1 nm); of 10.0 wt% oil-in-water emulsion stabilized by pea proteins.

Considering the theoretical scenario that protein particles of 60 nm radius are adsorbed on the droplet surface, **Equation 3.6** suggests that 99.7 mg/m^2 of protein particles would be needed for complete surface coverage. In the theoretical scenario that protein molecules adsorbed on the surface, 6.82 mg/m^2 protein molecules would be needed for complete surface coverage. At the same time, the experimentally measured surface load of the emulsion oil droplets was only 3.2 mg/m^2 (**Equation 3.4**). Moreover, when comparing the measured and theoretical surface load for protein particle-stabilized surface, the surface coverage was 3.21% of the theoretical coverage. In the scenario where protein molecules stabilize the droplet surface, the fraction of surface covered was 46.94% of the theoretical coverage.

Studies have shown that model spherical particles can stabilize oil droplets by covering as little as 10-20% of the oil droplet surface [102]. However, in cases of protein particles such as soy glycinin, 40% or higher coverage was reported. Similarly, when whey protein nanogels were used, the surface coverage of 68% was critical [103,104]. Therefore, the

estimated surface coverage of 3.2% for Pickering stabilization for pea protein stabilized emulsion would not be sufficient to stabilize the oil droplets and avoid further coalescence [105,106]. Moreover, studies have shown that surface load for protein Pickering particles was between 20-25 mg/m^2, which is lower than what we have estimated theoretically but was much higher than the measured surface load in this research [103]. The comparison indicates that scenario two may occur: protein molecules are adsorbed on the droplet surface.

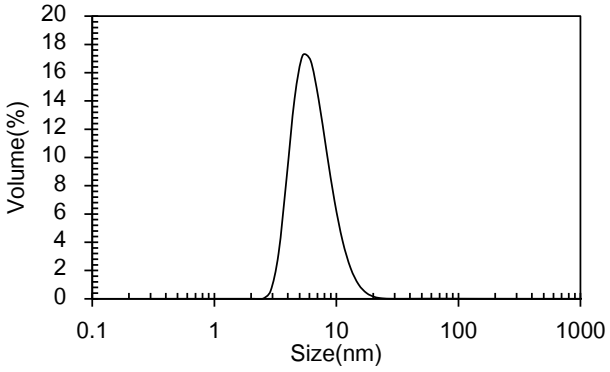

Figure 3.5: Particle size distribution of protein molecules solution obtained after centrifugation of 0.5 wt% pea protein dispersion at pH 3.0.

To confirm the hypothesis that protein molecules were also present in the pea proteins at pH 3, the protein dispersion was centrifugated using ultra-high rotation speed. The supernatant after ultra-centrifugation contained about 40 wt% of the proteins present in the initial dispersion (measured by Lowry method). Size distribution of the resultant supernatant shows a monomodal distribution between 3-20 nm (**Figure 3.5**). The figure clearly shows the presence of smaller proteins compared to the protein particles seen before homogenization. Moreover, the size distribution corresponds well with the theoretical protein molecule size of ~ 8.2 nm (4.1 nm radius). Moreover, the size distribution shown here corresponds well with what has been experimentally reported for pea protein molecules of legumin and vicilin (r_g ~4.5 nm) and protein assembly of 3-6 oligomers (r_g ~25 nm) [107–109].

The presence of protein molecules (3-20 nm) showed that the pea proteins co-existed as particles and as protein molecules in the pea protein dispersion at pH 3 with an equilibrium between them. Therefore, pea proteins at pH 3 can be described as protein particle-

molecule mixture. The fraction of protein particles and protein molecules in our case was 60:40 (wt: wt), respectively (measured by Lowry). The existence of protein molecules implies that a minimum protein concentration is required for self-assembly to occur. The concentration dependency for protein assembly indicates that the particle formation was diffusion-controlled and was driven by reversible physical forces [94].

Table 3.1: *Interfacial tension parameters of pea protein particle-molecule mixture and pea protein molecule solution measured using drop tensiometer for 12000 seconds at 20°C.*

Sample	Initial tension (mN/m)	Lag time (t1) (sec)	Rearrangement time (t2) (sec)	Final tension after 12000 sec (mN/m)
Protein particle-molecule mixture	24.7	154	3137	13.41
Protein molecule solution	23.2	121	2845	14.49

An essential requirement of the interfacially active molecules, like proteins, is their ability to adsorb onto the oil-water surface and reduce the interfacial tension. Therefore, pea protein particle-molecule mixture was compared with protein molecules solution for their interfacial tension reducing property. The shape of the tension reduction curve consisted of a lag phase and an adsorption phase which is characteristic for protein adsorption at the droplet surface [31]. During the lag phase, protein molecules do not sufficiently cover the droplet interface. There is no interaction between them at the interface, leading to a lack of interfacial tension reduction [65]. However, such a lag phase may not exist in a real emulsion system due to a much higher concentration of proteins. During the second phase (adsorption phase), proteins adsorb and rearrange at the droplet surface, which leads to a noticeable reduction in interfacial tension [30].

The tension curves were fit to an exponential equation (**Equation 3.8),** and the results are summarised in **Table 3.1.** The table shows that for both systems, the interfacial tension decreased over 3.5 hours from around 25 mN/m to around 14 mN/m. Moreover, the lag time (t1: ~150 sec) was much lower than the rearrangement time (t2: ~3000 sec) for both

systems. This indicated that, after the lag time, a gradual reduction in interfacial tension was associated with the interfacial rearrangement of proteins. The slow rearrangement has also been shown in literature for pea globulins at acidic conditions [110]. The slow decline has been attributed to the structural re-organization of pea globulins hexamers (and trimers) into their monomeric subunits. A similar tension reduction profile for both protein particle-molecule mixture and the protein molecule systems indicated that pea protein dispersion's interfacial tension reducing property mainly comes from the protein molecules and not from the protein particles.

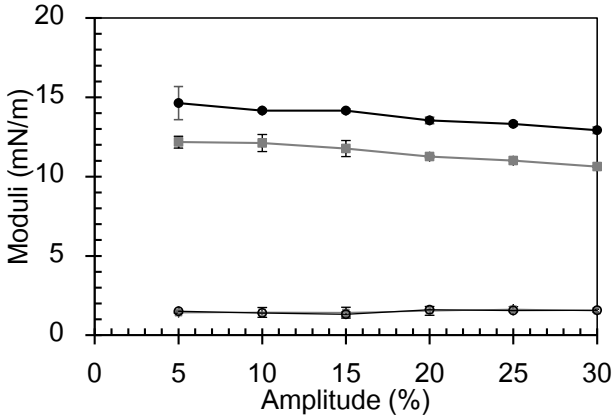

Figure 3.6: Dilatational elastic (filled) and viscous modulus (unfilled) of pea protein particle-molecule mixture (black) and pea protein molecules solution (grey) measured after 3.5 hrs of steady interfacial tension decrease as a function of the amplitude of deformation.

The visco-elastic properties of the film formed at the droplet surface give information on the interactions between the molecules adsorbed at the droplet surface. Therefore, interfacial dilatational experiments were performed. The resulting dilatational elastic (Ed') and viscous modulus (Ed'') of pea protein particle-molecule mixture and pea protein molecules are shown in **Figure 3.6**. The dilatational elastic modulus (E_d') was higher than the viscous modulus (E_d'') over the range of amplitude tested for both systems. The E_d' curves of the protein particle-molecule mixture and protein molecule solution follow each other closely. Therefore, it can be concluded that protein molecules in protein particle-molecule mixture mainly adhere to the droplet surface and form a cohesive network.

Moreover, the moduli curves did not show a large amplitude dependency over the tested range, indicating that the protein-protein interactions at the droplet surface lead to the

formation of a cohesive network that remained intact under the applied surface area changes. The protein network was probably formed by physical interactions, which overcame the electrostatic repulsion. The protein network can prevent the rupture of the droplet surface and subsequent destabilization of the droplet [111].

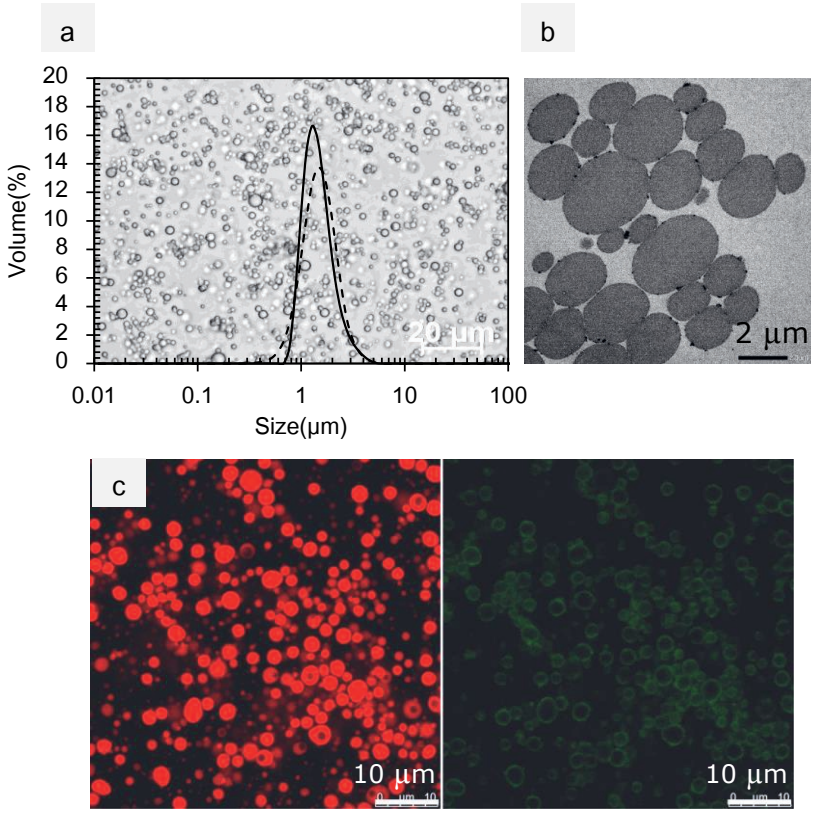

Figure 3.7: (a) Droplet size distribution of emulsion prepared with protein molecules solution day 0 (solid line) and day 7 (dashed line) and inset showing light micrograph of the emulsion at day 0 (scale: 20 μm/diluted 5 times); (b) TEM image of the emulsion stabilized with protein molecules (Scale 2 μm). and (c) Confocal micrograph of the emulsion prepared with protein molecules at day 0 (oil: Red/ protein: Green and scale: 10 μm).

Emulsions were prepared using the protein supernatant obtained after ultra-centrifugation to confirm further that protein molecules were the primary stabilizers of the oil droplets in the pea protein particle-molecule mixture. The same initial protein concentration was used for ultra-centrifugation compared to what was used to prepare pea protein emulsion (**Figure 3.1).** The droplet size distribution of the resulting emulsion is shown in **Figure 3.7.a**

for fresh emulsions (solid line) and after 7 days (dashed line). The distribution curve is monomodal with a size between 500nm to 5 µm. The inset in **Figure 3.7.a** shows a light micrograph of the formed emulsion in a fresh state. The droplet size distribution of the formed emulsion, was stable over storage for 7 days, indicating no coalescence (**Figure 3.7.a**.). Moreover, the droplet size distribution of the protein molecules stabilized emulsion corresponded well with the emulsions made with pea protein particle-molecule mixture (**Figure 3.1.a).** The light micrograph (**Figure 3.7, inset)** also showed that the droplets were spherical and showed a similar microstructure to pea protein particle-molecule emulsion (**Figure 3.1.b**).

To investigate the microstructure of the emulsion, confocal analysis (**Figure 3.7.c**) and TEM analysis (**Figure 3.7.b**) were employed. The confocal micrograph shows oil droplets (red) and proteins (in green). While the TEM micrograph (**Figure 3.7.b**) shows oil droplets in grey and darker patches of proteins. The confocal (**Figure 3.7.c**) showed that the formed oil droplets appeared with a homogeneous interface, and no dense protein areas could be observed. The homogeneous droplet interface without protein particles was also confirmed from the electron micrograph (**Figure 3.7.b)**. Besides, the electron micrograph clearly shows that the droplet surface of protein molecules stabilized emulsion was identical to that of the pea protein particle-molecule emulsion (**Figure 3.3.b)**. The similarity between the droplet surfaces of the two emulsions indicated that protein molecules in the pea protein particle-molecule mixture were responsible for the droplet surface stabilization. These findings clearly show that the protein particles do not play a significant role in the droplet surface stabilization of pea proteins at pH 3.0.

3.4 Conclusions

In this work, we investigated the interfacial and emulsifying properties of pea proteins at pH 3.0. We showed that pea proteins self-assembled to form particles of size between 0.05 µm and 0.7 µm. Most proteins were not present as particles since 40 wt% of the protein in the protein particle-molecule mixture existed as protein molecules. The size distribution of the protein molecules (**Figure 3.7**) was between 3-20 nm following the calculated size of pea globulins and with what has been reported in the literature for globular plant proteins at pH 3[90]. The protein particle-molecule mixture reduced interfacial tension and formed stable oil-in-water emulsions. The measured surface load of the emulsion was compared

with the theoretical surface load. The comparison showed that only 3.2% of the droplet surface would be covered when protein particles stabilize the surface.

On the other hand, when protein molecules stabilize the surface, 47% of the droplet surface would be covered. Therefore, protein molecules are more likely the primary stabilizing agent. To verify that protein molecules were responsible for stabilization, the emulsion was prepared with protein molecules. The resulting emulsion was stable against coalescence and showed a similar droplet size than the emulsion stabilized with the protein particle-molecule mixture. Therefore, we concluded that the emulsification mechanism in pea proteins at pH 3.0 is not based on protein particles but protein molecules. Besides, we show that protein molecules should not be neglected when studying the emulsifying properties of protein aggregates/particles.

Appendix

Theoretical surface load

The theoretical surface load of the proteins was calculated based on equations and then compared with measured surface load. For this purpose, simple mathematical representation of surface load was taken as starting point as follows:

$$\Gamma = \frac{M_p}{A_d} \quad (mg/m^2) \qquad \text{Equation A1}$$

Where, M_p is the mass of protein at interface (mg) and A_d is the total interfacial area (m^2)

$$M_P = N_p * m_p \quad (mg) \qquad \text{Equation A2}$$

Where, N_P is number of protein molecules (no unit) and m_p is the mass of one protein molecule (mg), which can be rewritten as $m_p = \rho_p*(4/3*\pi*r_p^3)$. Where, r_p is the radius of protein (m), and ρ_p is the density of protein (mg/m^3)

$$N_P = \frac{A_d * \varphi_{max}}{A_p} \quad (no\ unit) \qquad \text{Equation A3}$$

Where, A_d is surface area of droplets (m^2), ϕ_{max} is the maximum packing factor of circles and A_p is the area of protein molecules (m^2) which can be written as $A_p = \pi*r_p^2$

Substituting the expansions of **Equation A2** and **Equation A3** into **Equation A1**

$$\Gamma = \frac{1}{A_d} * \frac{A_d*\varphi_{max}}{\pi*r_p^2} * \rho_p * \frac{4}{3} * \pi * r_p^3 \quad (mg/m^2) \qquad \text{Equation A4}$$

Which can be simplified into,

$$\Gamma = \frac{4}{3} * \rho_p * \varphi_{max} * r_p \quad (mg/m^2) \qquad \text{Equation A5}$$

Equation A5 is given in the main text as Equation 3.7. It is used to calculate the theoretical surface load of the proteins at the droplet interface

Calculation size of individual pea proteins

The physical size of the protein molecule was calculated based on the equation below and the results are shown in table A1

$$r_p = 0.066 * M^{\frac{1}{3}}$$ Equation A6

*Table A1: Estimated size of pea legumin and vicilin from **Equation A6***

Protein	Molecular weight (Da)	Radius (nm)
Legumin (11S)	360000	4.70
Vicilin (7S)	150000	3.51

Chapter-4: 3D printing jammed emulsions stabilized by pea proteins

Published as:

Sridharan, S., Meinders, M. B., Sagis, L. M., Bitter, J. H., & Nikiforidis, C. V. (2021). Jammed Emulsions with Adhesive Pea Protein Particles for Elastoplastic Edible 3D Printed Materials. *Advanced Functional Materials*, 2101749. DOI: 10.1002/adfm.202101749

Abstract

3D printed materials are of great relevance to produce medicinal scaffolds and specialized foods. An approach to forming 3D printable materials is to use jammed oil droplets. Jammed oil droplets are highly viscous and can be extruded through the nozzle of a 3D printer, while after chemical crosslinking, they acquire a self-standing ability. However, the molecules currently used to stabilize and cross-link the oil droplets have questionable biocompatibility. Therefore, this study aims to produce a 3D printable jammed emulsion using pea proteins. This jammed oil-in-water emulsion is remarkably stable and viscoelastic enough to be extruded through the printer nozzle. Adhesive pea protein particles formed by pH adjustment act as physical cross-links between the oil droplets, forming a scaffold with elastoplastic rheological properties that flows above critical stress while, without any additional treatment, exhibits the required self-standing properties for 3D printing. By understanding the properties of pea proteins and their behavior in bulk and on interfaces, pea protein-based 3D printable material was created for the first time.

4.1 Introduction

Manufacturing materials using 3D printing is simple yet effective in creating intricate macroscopic structures [112,113]. 3D printing technique involves pushing the material through a nozzle and depositing it layer-by-layer to produce the required structure [113,114]. The challenge is to create a material that flows when stress is applied to pass through the nozzle while it behaves as solid at rest to hold the printed structure [115]. Materials with such rheological properties are known as plastic or yield stress materials.

The applications of 3D printing range from scaffolds for tissue cartilages and specialized functional foods [114,116–118]. Currently, food printing is mainly performed using carbohydrate polymer materials, with added cross-linking agents and other natural fillers such as vegetables or chocolates [119,120]. Besides 3D printing conventional foods with attractive designs, 3D printing is also widely studied to create specific food structures for specialized nutrition. For instance, 3D printing is investigated to produce foods for the elderly with mastication issues [121]. 3D printing can also be used to make foods with specific compositions in the context of personalized nutrition [122–124].

Unlike 3D printing traditional foods, specialized foods need to meet specific microstructure and nutrient requirements. This demands the creation of materials with precisely controlled composition and rheological properties. However, the number of edible biopolymers that can create food materials that possess the necessary plastic properties for 3D printing is minimal [125].

A route for creating edible 3D materials is the use of highly concentrated oil-in-water emulsions. The examples reported in the literature are concentrated oil in water emulsions with an oil volume fraction ϕ larger than 0.64. The oil droplets are stabilized through a Pickering mechanism by crystalline biobased particles such as chitin or cellulose nanocrystals [112,116,118,126]. The crystalline particles at the droplet interface and in the continuous phase create droplet-droplet interaction through weak physical attractive forces resulting in a soft elastic material, which can flow when subjected to sufficiently large shear stresses. However, chemical cross-linking and thermal treatments of the material are often necessary to provide self-standing property [116]. This step, together with the production of the crystalline particles used as stabilizers, often reduces the biocompatibility of the materials their potential use in foods.

Therefore, there is a need for printable emulsions where commonly accessible and edible polymers are used as stabilizing and crosslinking agents. An attractive edible biopolymer source that has not been used before to design emulsions that can be printable is plant-based proteins such as pea proteins.

Pea proteins have gained wide attention due to the lower environmental impact associated with them [7]. Moreover, pea proteins have excellent emulsifying properties and are widely available for use in edible applications [24,35,44,78]. Pea proteins assemble through physically attractive forces into adhesive protein particles at pH 3,[127] acting as natural crosslinking agents [116].

In this work, we investigated the oscillatory rheological properties of jammed emulsions stabilized by pea proteins and linked them to 3D printability. We established the role of the pea protein particles formed by pH-triggered self-assembly to create printable edible emulsions. Our research reveals that due to the adhesive properties of the pea protein particles, the droplets within the jammed emulsions are 'glued' together, enabling the formation of 3D printable edible materials. We present a simple pH-driven approach to create edible materials with 3D printable properties using pea proteins without the aid of additional cross-linking agents.

4.2 Experimental Section

4.2.1 Materials

Whole yellow field peas (Pisum sativum L) were obtained from Alimex BV® (Sint Kruis, The Netherlands). Sodium Hydroxide, Hydrochloric acid (analytical grade), Sodium Dodecyl Sulphate (SDS) reagent, and fluorescent dyes Nile red and Fast Green® were all obtained from Sigma-Aldrich® (Zwijndrecht, The Netherlands). Whatmann® cellulose thimbles were obtained from VWR (Amsterdam, Netherlands).

4.2.2 Methods

4.2.2.1 Purification of pea proteins

Pea proteins were extracted from yellow peas by alkaline extraction and iso-electric point precipitation, commonly reported in the literature [55,88]. In brief, pea seeds were dry milled into a coarse flour in a coffee blender (IKA®, Staufen, Germany). The flour was then soaked

in water at 1:10 (w:w) solids to water ratio. The pH was adjusted to pH 8 with a 0.5 M NaOH solution under constant stirring. After 2 hours of soaking, the slurry was blended in a kitchen blender at maximum speed for 2 minutes. The resultant slurry was centrifuged at 10000 g for 30 minutes to precipitate solids. Further, the protein-rich supernatant was separated, and the proteins were precipitated at a pH of 4.8 with a 0.5 M HCl solution. The solution was allowed to stand for 1 hour, and the precipitate was collected by centrifugation at 10000 g for 30 minutes. The precipitate was diluted (1:10 w/w) with ultra-pure water, and pH was neutralized (pH 7). The solution was further freeze-dried, and the obtained powder was termed simply pea protein. The protein powder was stored in the freezer (-18°C) for further use.

4.2.2.2 Oil-in-water emulsion preparation

Oil-in-water emulsions were prepared using pea protein dispersions as an aqueous phase. 70.0 wt% rapeseed oil and 30.0 wt% of protein dispersions were used. The final protein content of the emulsion was standardized to 1.4 wt% for 70wt% oil emulsion by adjusting the protein content in the dispersion. The pH of the protein dispersion was changed to pH 3 or 7 using 0.5 M HCl or 0.5 M NaOH, respectively. The protein dispersion was then stirred for 3 hours under magnetic stirring. The dispersion was then sheared for 15 secs at 6000 rpm in an IKA® (Ultra-Turrax, IKA®, Staufen, Germany) ultraturrax to ensure homogeneous dispersion of proteins. Further, rapeseed oil was added slowly, and the mixture was sheared for another 60 seconds at 10000 rpm to produce a coarse emulsion. The formed coarse emulsion was further homogenized by passing through a GEA® (Niro Soavi NS 1001 L, Parma, Italy) high-pressure homogenizer at a homogenization pressure of 650 bars. The obtained final emulsion was allowed to equilibrate 3 hours before any measurement was performed. The emulsions were called pea protein emulsions and were made in duplicates.

Emulsions were also prepared using pea protein solution (supernatant after removal of particles). In brief, pea protein dispersions were prepared as explained above. Then the dispersion was ultra-centrifugated at 320,000 g for 45 minutes at 20ºC using a Beckman-Coulter L60 (Beckmann-Coulter Nederland B.V, Woerden, The Netherlands) ultra-centrifuge in 40 mL glass tubes. The clear supernatants were carefully collected by pouring them onto a beaker. The collected solution was called protein molecules solution. Emulsions were prepared as described above with this solution.

4.2.2.3 Droplet size measurement

The individual droplet size of the emulsions was measured using laser diffraction in Bettersizer® (Bettersize Instruments Ltd., Hamburg, Germany). The samples were dispensed using a hydro dispenser, and the droplet size was represented in volume mean diameter. To measure individual droplet sizes, the emulsions were treated with a 1.0 wt% SDS solution. The addition of SDS breaks droplet aggregation driven by protein interaction, so the size of individual oil droplets could be measured in this manner [95]. An equal volume of (1 mL) of emulsion and 1.0 wt% SDS solution was mixed, and the size was immediately measured using a refractive index of 1.47.

4.2.2.4 Rheological measurement

The rheological properties of protein dispersion and emulsions at pH 7 and 3 were measured at 20°C using an Anton Paar 302 rheometer. The supplier software Rheocompass S1.25 was used to analyze and obtain raw data for all the measurements.

Emulsions were analyzed using oscillatory rheological measurements in a cone plate set up with a cone diameter of 50 mm and cone angle of 4° (gap truncation of 0.49 mm). Before measurements, emulsions were allowed to equilibrate at room temperature for at least 1 hour. The emulsions were then loaded onto the rheometer, and the upper plate was lowered to the required gap. The emulsion was allowed to equilibrate for 5 minutes before the measurement was started. First, emulsions were tested for their linear visco-elastic regime using a strain amplitude sweep at a constant frequency of 6.2 rad/s (~ 1 Hz). An amplitude where the modulus did not depend on strain value was chosen for further tests. Then a sequence of tests was performed, starting with a frequency sweep test using a constant strain determined from the strain sweep experiment.

A fresh emulsion sample was used to probe the large amplitude oscillatory shear rheology (LAOS) experiment. The emulsion sample was loaded in the same manner, and a strain sweep ranging from 0.1% strain up to 1000% strain at a constant frequency of 6.2 rad/s was performed. The raw waveforms collected during the sweep were analyzed using the MITlaos software, kindly provided as open-source (MITlaos V2.1, freeware distributed from MITlaos@mit.edu). Lissajous-Bowditch curves were plotted of stress versus strain and stress versus strain rate. The shapes of these Lissajous curves provide essential microstructural information about the materials.

To test the rheological behavior of the emulsion after 3D printing, the emulsions were first 3D printed in a cylindrical shape as described in the '3D printing emulsions' section below. To test the printed material, a 50 mm diameter plate-plate geometry was used. A serrated top plate was used to avoid any slip from the printed structure. A gap size of 2.5 mm was used. The 3D printed structures were carefully placed on the rheometer geometry, and a frequency sweep was performed similarly to the emulsions before 3D printing.

4.2.2.5 Confocal Microscopy (CLSM)

The emulsions were imaged using a confocal laser scanning microscope (CLSM) with fluorescent dyes to visualize the microstructure. In brief, about 1 ml of the emulsion was mixed with 7µl of Nile red® and 7µl of Fast green FCF® in an eppendorf® tube. The tubes were sealed and allowed to mix for 15 minutes. Afterward, about 30µl of the sample was deposited on a microscopy slide and mounted on the confocal table. A Leica® SP8® confocal microscope fitted with a 63x water immersion lens and white light laser was used to image the samples. Nile red stained the oil phase and was excited at 488 nm, and the emission was captured between 500-600 nm. Rhodamine B, which stained proteins, was excited at 566 nm, and the emission was captured between 570-670 nm. The images were captured in a sequential manner using Leica® imaging software.

4.2.2.6 3-D printing of emulsions

The emulsions were also 3-D printed using a byFlow® (Eindhoven, The Netherlands) commercial 3-D printer. A cube geometry design of length 30 mm, width 30 mm, and height 10 mm was fed to the printer. A honeycomb fill of 20% infill density was set. The emulsions were extruded through a nozzle of size 1200 µm. The printing was conducted at a speed of 10mm/s. In total, 13 layers were printed, one on top of each other. The reference design for the printed structure is shown in **Figure 4.1.a**.

To test the effect of 3D printing on the material, the rheology of the emulsions after 3D printing was also measured. Same printing settings as described above were used. The freshly prepared emulsions were 3D printed on a soft surface in a dense cylinder shape with a radius of 5 cm and a height of 2.5 mm. A 100% infill density in a rectilinear pattern was used. The reason for 3D printing a cylinder to measure rheology was to fit the material properly within a plate-plate geometry. Accurate filling (fitting) of the sample is essential to

measure the rheological property accurately. The reference image of the cylindrical structure to be printed is shown in **Figure 4.1.b**

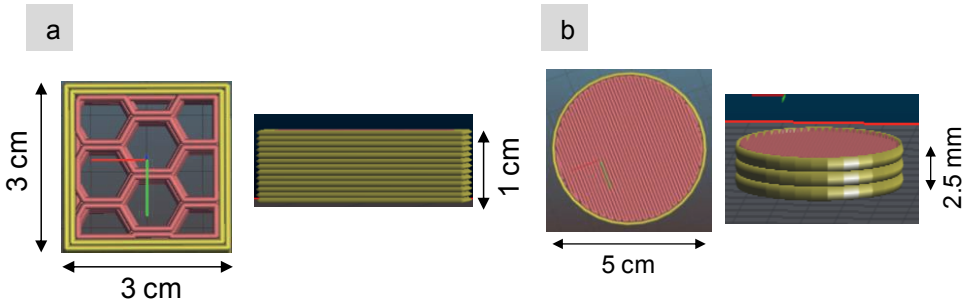

Figure 4.1: Model 3D printing structures generated and fed into the 3D printer (a) Honeycomb structure used to visually test the printability of the emulsions with dimensions (3 cm*3 cm*1 cm - l*w*h); (b) Cylindrical shape printed to test the rheology of the emulsion post-printing with dimensions (d: 5 cm and h: 2.5 mm).

4.3 Results and Discussions

4.3.1 Microstructure and rheological properties of jammed emulsions stabilized by pea protein molecules

We extracted pea proteins following a simple procedure to be relevant to edible and bio-compatible applications [22,24,127]. The obtained pea proteins exist predominantly as individual protein molecules with a ς-potential of about -25 mV at pH 7[43,127,128]. These protein molecules (pH 7) were used (1.4 wt%) to stabilize jammed oil-in-water emulsions containing 70 wt% oil (φ=0.72) [129].

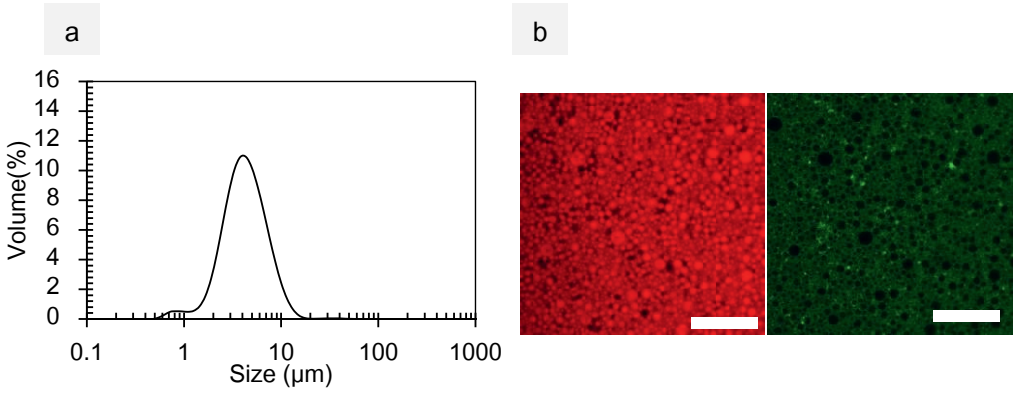

Figure 4.2: (a) Oil droplet size distribution of 70.0 wt% oil-in-water emulsions at pH 7 stabilized with 1.4 wt% pea proteins; (b) Confocal micrograph of emulsion stabilized with pea protein molecules; Oil in red (Nile red) and protein in green (Fast green), scale bar 50 µm.

The oil droplet size distribution of the emulsions is shown in **Figure 4.2.a**. The size distribution was monomodal, with droplets mostly between 1 and 10 µm. The distribution in droplet sizes and the deformable nature of the oil droplets enable their packing above the theoretical random close packing fraction (ϕ=0.64) in these emulsions. It shows that pea proteins can stabilize emulsions well above the oil droplet close packing (ϕ=0.64), indicating their excellent emulsifying ability. The microstructural properties of the jammed oil droplets were investigated using confocal microscopy (**Figure 4.2.b**.). The micrograph shows oil in red and proteins in green. The micrographs show that pea proteins can stabilize oil droplets in close contact with each other.

For the emulsions to be 3D printed, they should possess a strong yield stress behavior (plastic). Therefore, the rheological properties were investigated to characterize whether the formed jammed emulsion is suitable for 3D printing. The rheological shear elastic (G') and loss modulus (G'') of the emulsions as a function of frequency (0.1 rad/s – 100 rad/s) at constant strain (0.5%) and as a function of strain amplitude (0.1%-1000%) at a constant frequency of 6.28 rad/s are shown in **Figure 4.3.a & b.**

The frequency-dependent response provides insights into the dynamics of microstructural changes during shear (**Figure 4.3.a**). The G' of the pea protein stabilized emulsions was higher than G'' over the entire range of applied frequencies. The elastic nature of the emulsions results from the Laplace pressure of the jammed droplets. Moreover, the elastic

and loss moduli have a power-law dependence on frequency, suggesting that the material behaves like a viscoelastic soft solid [130,131].

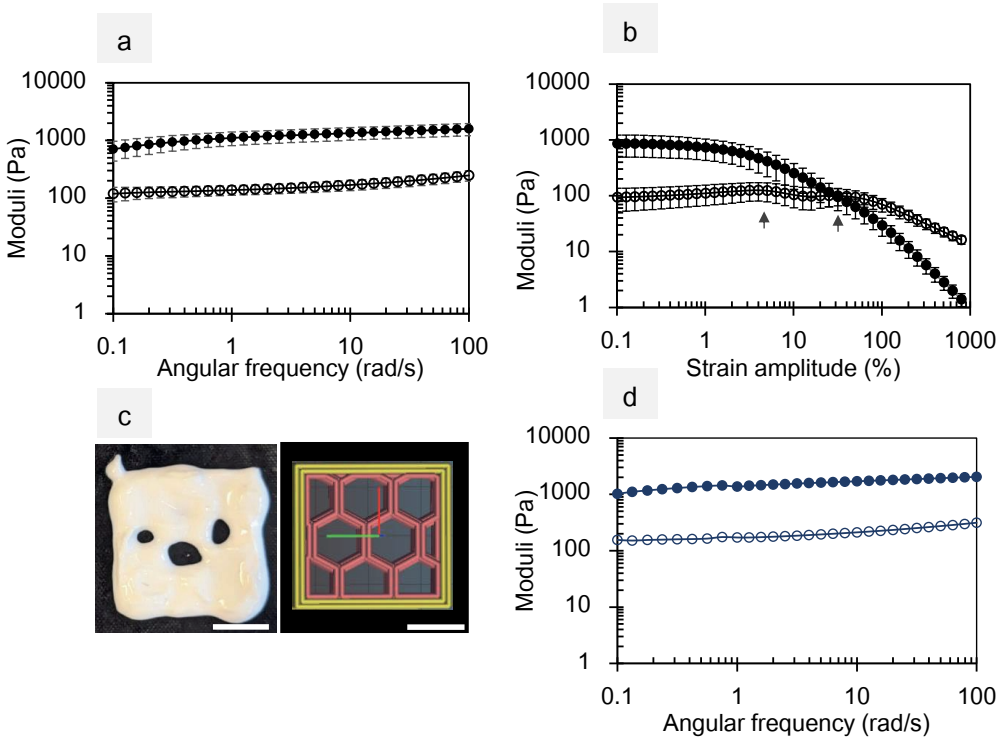

Figure 4.3: Elastic (G': Filled symbols) and Loss modulus (G": open symbols) of 70 wt% oil emulsion stabilized by pea protein molecules as a function of (a) increasing frequency at a constant strain of 0.5% and; (b) as a function of increasing strain at a constant frequency of 6.28 rad/s; (c) Photographs of pea protein stabilized emulsion upon 3-D printing at room temperature, top view with scale bar 1 cm and the envisioned honeycomb structure: 3cm*3cm*1cm (l*w*h); (d) Elastic (G': Filled symbols) and loss modulus (G'': Unfilled symbols) as a function of frequency for 3D printed emulsion (a flat, dense cylinder of diameter of 5 cm and height of 2.5 mm).

Figure 4.3.b shows the G' and G'' curves as a function of strain amplitude in a log-log plot. The rheological response of the emulsions as a function of strain provides information on structure breakdown and whether it possesses a plastic-like rheological response necessary for 3D printing. The elastic moduli (G') were higher than the loss moduli (G'') at low and intermediate strains (strain amplitude < 20%), indicating the emulsions behave predominantly as an elastic material.

The G' curve as a function of strain decreases gradually above 2% strain progressively until about 40% strain. From a strain amplitude of about 40%, G' is smaller than G'' and the system behaves more as a viscoelastic liquid. The gradual decrease in G' shows that the microstructure breakdown was smooth, probably due to the gradual loss of droplet-droplet contact as strain increases.

The loss moduli (G'') curves as a function of strain in **Figure 4.3.b** reveal additional information about the microstructure of the jammed emulsions. The G'' curve shows two strain values where G" first mildly increases, followed by a decrease, called a weak overshoot [132]. This is attributed to the typical behavior of highly concentrated emulsions and jammed systems [133–135]. The overshoot arises when sudden flow or rearrangement occurs within jammed emulsions. Initially, the jammed emulsions droplets are restricted to move under small strains due to the neighboring droplets. However, as strain increases, the droplets break their confinement momentarily and start to flow or rearrange.

The first overshoot occurs around 5% strain and the second around 40% strain, and these may be related to two different microstructural relaxation processes [136]. The first overshoot at low strain could be related to the disruption of droplet contact. Even though the droplet contacts are broken, they cannot yet move due to the high concentration of droplets and are trapped in a cage of surrounding droplets [137]. The second overshoot (G'') at a higher strain (~40%) is related to large droplet rearrangement or flow. At this higher strain, droplets escape their cage, and the emulsion starts to flow [136,138]. Therefore, the emulsions exhibited a typical rheological response of a jammed emulsion system, with only weak droplet-droplet interactions [139,140].

The jammed emulsion stabilized by pea protein molecules was tested for their 3D printability using extrusion-based 3D printing at room temperature. The emulsions were extruded with a continuous flow through the nozzle having a pore size of 1200 µm. However, after printing a honeycomb structure (l*w*h =3cm*3cm*1cm) with 13 layers, the emulsions could not self-support their structure (**Figure 4.3.c**). The emulsion structure collapsed within a few minutes, and the different layers merged. Even though the emulsions were jammed and have visco-elastic soft solid properties, the G' and G" were insufficient to retain the printed structure. This is likely due to insufficient droplet-droplet attractive forces.

For 3D printing, a nozzle with a large pore size of 1200 µm was used. Such a large nozzle dimension provides the ability to extrude our material easily and deposit it onto the surface. Moreover, droplet sizes in the emulsions are mostly below 10 µm, flow through the nozzle is not expected to destabilize the oil droplets. No oiling off was observed, indicating that the emulsion droplets did not destabilize.

To test the effect of 3D printing on the material property, a frequency sweep on the emulsions was performed after 3D printing. For this purpose, a cylindrical shape was printed instead of a honeycomb (see methods section). **Figure 4.3.d** shows frequency sweep after 3D printing. The figure shows that even after 3D printing, G' is higher than G'' following the same pattern as before 3D printing (**Figure 4.3.a**). This finding clearly shows that the material properties are unaffected by 3D printing.

4.3.2 Moving from soft jammed to plastic emulsion material using adhesive pea protein particles

To increase droplet-droplet interaction for 3D printing of emulsions, cross-linking and/or thermal treatments are commonly employed [114,116]. However, for edible applications, it is desirable to avoid such chemical cross-linking. Therefore we attempted to use the adhesive nature of pea protein particles to create stronger droplet-droplet interactions by changing the pH of the protein dispersion before emulsification.

Upon pH change to pH 3 in an aqueous phase, Pea proteins self-assemble into protein particles with sizes between 50-500 nm. This is despite that; they possess a surface charge of about +30 mV [46,127]. The protein particles are formed through attractive hydrophobic and van der Waals forces that overcome the electrostatic repulsion [127]. Under these conditions, the dispersed pea protein particles are in equilibrium with single protein molecules at a weight ratio of 60:40. As shown by emulsification and interfacial measurements, when a mixture of pea protein particles and molecules are used to stabilize oil droplets, the protein molecules are mainly adsorbed on the oil droplet interface. The protein molecules are sufficient to produce stable emulsion droplets of the same size when mixed with protein particles. These protein particles do not participate in interfacial stabilization but simply adhere to the primary protein layer on the oil/water interface or are present in bulk [127]. Due to the attractive nature of protein particles, they could “glue”

neighboring oil droplets when they are forced to be in contact, like in a jammed emulsion (see **Figure 4.8.b**).

To investigate the potential use of the pea protein particles for this purpose, we triggered the formation of particles by adjusting the pH of a protein dispersion to pH 3 before forming jammed emulsions (70 wt% oil, ϕ = 0.72). At this condition, pea protein molecules are expected to be adsorbed on the interface, while the protein particles are expected to be entrapped between the oil droplets.

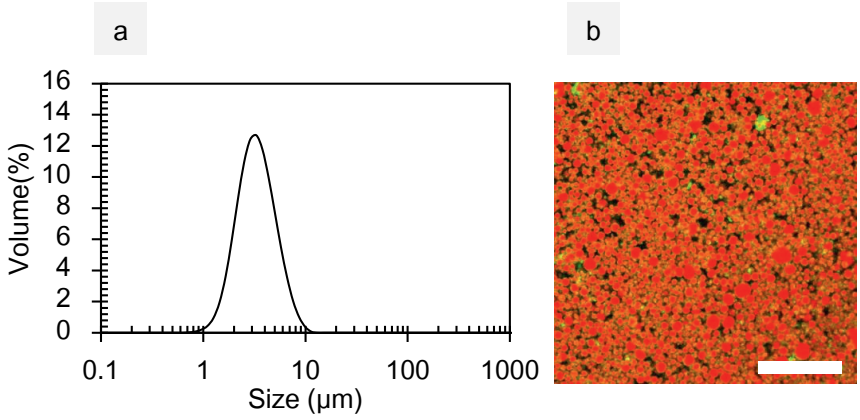

Figure 4.4: (a) Oil droplet size distribution of 70.0 wt% oil-in-water emulsions at pH 3 stabilized with 1.4 wt% pea proteins; (b) Confocal micrograph of emulsion stabilized with pea protein molecules; Oil in red (Nile red) and protein in green (Fast green), scale bar 50 μm.

Figure 4.4 shows the oil droplet size distribution for emulsions at pH 3 and the confocal micrograph of the emulsions. The droplet size of the formed emulsions was again monomodal, and droplets mainly were between 1-10 μm. Pea proteins form similar droplet sizes at both pH 7 and pH 3.

As observed with confocal microscopy, the microstructure of emulsions in the presence of protein particles (**Figure 4.4.b**) shows that the droplets are closely packed. Protein particles (green fluorescence) are visible between the packed oil droplets. These were not seen when only pea protein molecules were used to stabilize the emulsions.

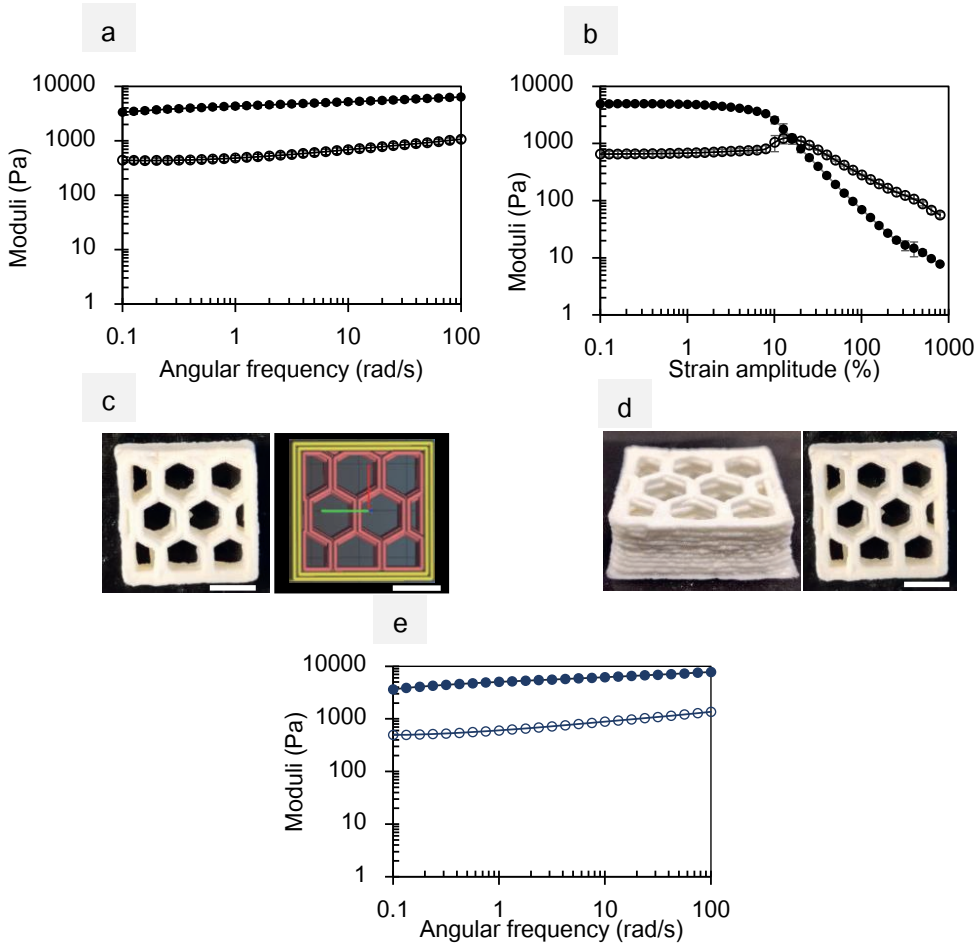

Figure 4.5 (a) Elastic (G': Filled symbols) and Loss modulus (G": Unfilled symbols) as a function of increasing frequency at a constant strain of 0.5% and (b) as a function of increasing strain at a constant frequency of 6.28 rad/s; (c) Photographs of 3D printed emulsions in the presence of protein particles at room temperature top view with scale bar: 1 cm with print dimensions of 3cm*3cm*1cm (l*w*h) and the designed honeycomb structure to be 3D printed and (d) 3D printed structure after 48 hours of storage at room temperature; (e) Elastic (G': Filled symbols) and loss modulus (G'': Unfilled symbols) as a function of frequency for 3D printed emulsion (a flat, dense cylinder of diameter of 5 cm and height of 2.5 mm).

Regarding the rheological properties of the jammed emulsions with pea protein particles, the elastic and loss modulus as a function of frequency is shown in **Figure 4.5.a**. The emulsions showed higher G' than G'' with both depending on frequency as a power law, showing that they behave as soft solids, similar to when only pea protein molecules were

used (**Figure 4.3.a**). However, the absolute values of the elastic and loss modulus of emulsions with pea protein particles were higher than the emulsion where only pea protein molecules were present. This points to a stronger droplet-droplet interaction when protein particles are present.

The elastic and loss moduli of the emulsions in the presence of protein particles as a function of strain are shown in **Figure 4.5.b**. At low strains, the G' curve is higher than G'', indicating a predominantly elastic behavior. Unlike emulsions with only pea protein molecules, there is no gradual decline, but a sharp decrease in G' occurs above 10% strain. At strain around 15%, the G' curve crosses the G'', indicating a predominantly viscous response for strain amplitudes larger than about 15%. The decrease in G' is related to the breakdown of the microstructure due to loss of contact between neighboring droplets. In these systems, the yielding of the structure is much more abrupt than in the jammed emulsions stabilized by protein molecules.

The loss moduli curve shows a single sharp overshoot while the G' drops, demonstrating a sharp loss of droplet-droplet contact and immediate flow or rearrangement [141,142]. The sharp structural change points to the presence of strong droplet-droplet interactions and network formation. In such systems, the process of bond breaking and cage disruption co-occur, leading to a single overshoot. Pea proteins associate with protein particles through physical forces such as van der Waals and hydrophobic forces that overcome the weak electrostatic forces at pH 3. The electrostatic forces are not strong enough to prevent the association of pea proteins at this condition [13]. Similarly, the droplet-droplet network could be mediated by protein particles through attractive hydrophobic and van der Waals forces.

The disruption in interaction leads to the material flow, which is desirable for pushing the emulsion through the nozzle for 3D printing. Besides, due to the higher stiffness at low strains, the material can be expected to retain its shape better upon depositing from the nozzle. Therefore, the emulsion may be a suitable candidate for 3D printing through a simple extrusion method.

The emulsions with pea protein particles were tested for their printability by extrusion-based additive manufacturing a honeycomb structure. The emulsions flowed through the nozzle (1200 μm pore size) continuously. The photographs of the printed structures are shown in **Figure 4.5.c**. The emulsions were able to retain the printed structure as seen from the

photographs. The shape of the extruded material was also clearly visible and resulted in a sharp printed structure. The cross-section (**Figure 4.5.c**) shows that the emulsion layers deposited by the 3D printer were distinct and self-supported.

The self-supporting structure retained its shape for over 48 hrs. (**Figure 4.5.d**) without the need for any post-printing treatment. There was no oiling off of the printed structure during this period, indicating that the emulsions were not destabilized.

The rheological behavior of the emulsions was also tested after 3D printing using a frequency sweep. The frequency sweep is shown in **Figure 4.5.e**. The figure shows that G' is higher than G'' following the same pattern as the emulsion before 3D printing (**Figure 4.5.a**). This similar behavior shows that 3D printing does not affect material properties.

We successfully designed a 3D printable material by using jammed emulsion in the presence of pea protein particles. The stability of the printed structure clearly shows that, without any additional treatments, like chemical cross-linking, adhesive pea protein particles can enhance the interactions between neighboring oil droplets through hydrophobic and van der Waals forces.

4.3.3 Pea protein particles stick jammed oil droplets together through physical forces

To get more direct insights into the role of the protein particles, we analyzed the non-linear shear rheology of the emulsions using Lissajous plots. The plots provide information about the microstructural breakdown and provide a rheological fingerprint of the material properties. For instance, for a material to be 3D printable, a plastic material response is required. For such a material, the Lissajous plots take on a rectangular shape (Fig. 5a). Therefore, to assess the 3D printability of materials, characterizing their Lissajous plots against standard curves would be a powerful approach.

Lissajous plots were plotted for jammed concentrated emulsions with and without pea protein particles **(Figure 4.6**). The figures show a loop plotted as total stress vs. total strain normalized by the maximum stress and strain, respectively. A dashed line inside the loop is also plotted, which corresponds to the elastic contribution to the total stress [143].

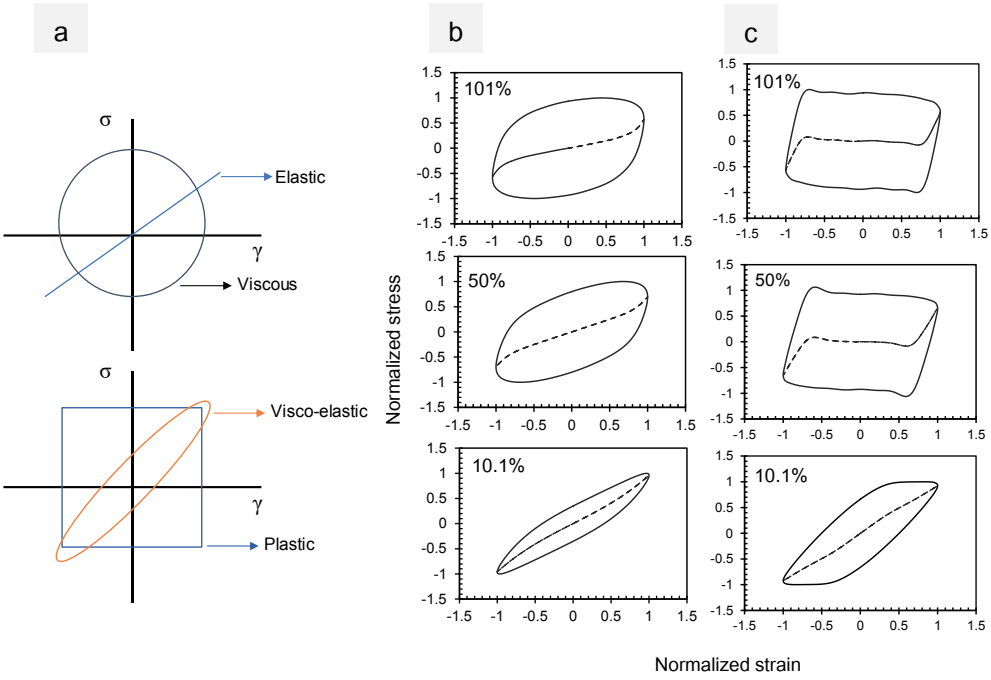

Figure 4.6: (a) Reference Lissajous curves showing the basic shapes of standard material responses for reference and (b) Lissajous curves of 70 wt% oil emulsions with pea protein molecules and (c) Lissajous curves of 70 wt% oil emulsions with pea protein particles; As a function of increasing strain amplitude (10.1%, 50%, 101%) at a constant frequency of 6.28 rad/s at 20°C with stress vs. strain normalized by maximum stress and maximum strain, respectively.

At low strains (10.1%), emulsions without protein particles show a tilted nearly elliptical shape closely resembling the reference curve in **Figure 4.6.a**. This shape points to a mildly nonlinear viscoelastic behavior was in-line with the G' and G'' measurement of the amplitude sweep [144]. The elastic contribution to the stress showed a nearly straight line, with a slight increase in slope near the maximum strain, which points to a weak strain hardening behavior. In contrast, at 10.1% strain, emulsions with protein particles show a more rhomboidal shape, with intra-cycle softening behavior near the maximum strain.

At 50% and 100% strain, emulsions without protein particles show wider loops in the form of a rounded rhomboid. The increase in loop area at these strains demonstrates that the viscous component becomes more apparent than the elastic component [144]. These plots' shape corresponds to emulsions that show progressive softening upon increased strain

while maintaining a small but finite slope in the elastic contribution. This is consistent with our earlier observation that there is no abrupt yielding in these systems and that for emulsions without protein particles, the droplet-droplet interactions are relatively weak.

Contrarily, at 50% and 100% strains, emulsions with protein particles show rectangular shapes with sharp corners. The sharp rectangular shape points to an abrupt yielding behavior [145]. A slight overshoot is visible at the rectangle corners in the total stress and the elastic contribution to the stress (dashed line). The overshoot can be associated with the stretching of attractive droplet-droplet bonds under applied strain [146]. Due to such stretching, the stress within the emulsion increased momentarily, and as the strain changed further, the bonds between the droplets were broken. Once the bonds were broken due to strain, the emulsion droplets started to flow, as shown by the flat stress response with increasing strain. The structure breakdown indicates that the emulsion droplets in the presence of protein particles interact with each other mediated by the protein particles. The adhesive protein particles through van der Waals and hydrophobic interactions make the droplets 'stick' to each other [146,147]. Therefore, pea protein stabilized emulsions with protein particles form a yielding, plastic-like material.

To confirm whether protein particles were solely responsible or if pH affected the material response, emulsions were prepared at pH 3 after removing the protein particles. The rheological and microstructural properties of the jammed emulsions stabilized by pea proteins after the removal of protein particles are shown in **Figure 4.7**.

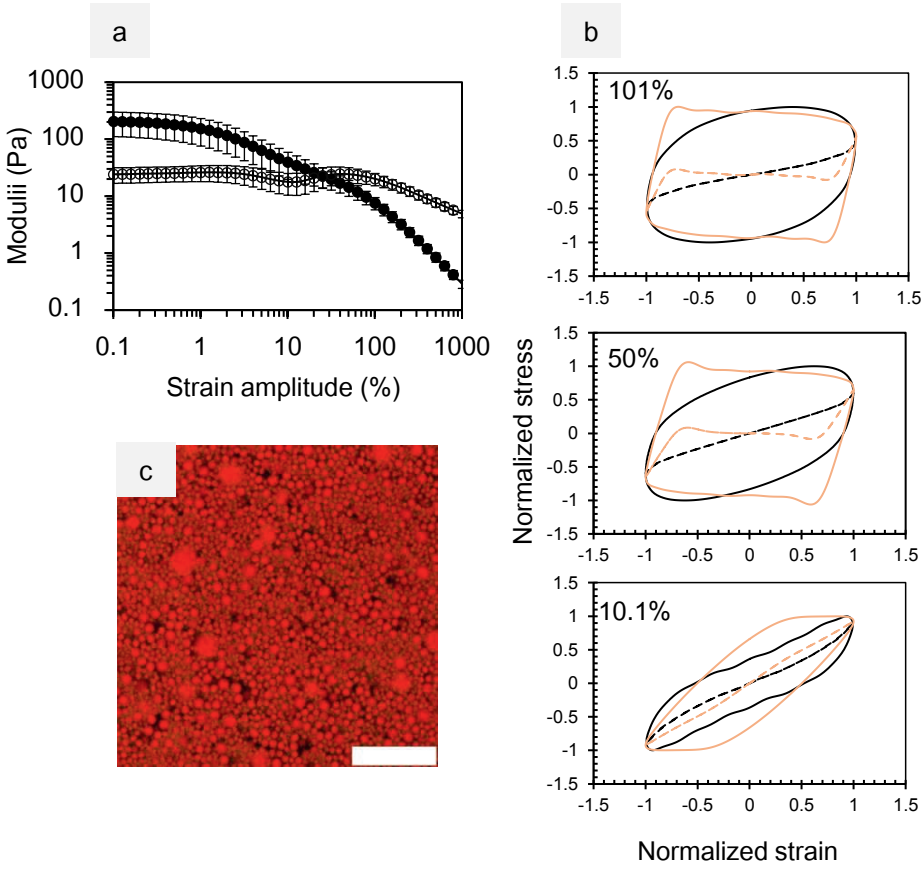

Figure 4.7: (a) Elastic (G'/ filled symbols) and loss modulus (G''/ unfilled symbols) of 70 wt% oil emulsions (black) made at pH 3 after removal of protein particles by centrifugation plotted as a function of strain amplitude and (b) Lissajous curves of 70 wt% emulsions after removal of protein particles (black), with stress vs. strain normalized by maximum stress and strain respectively. The Lissajous plots of 70 wt% emulsions at pH 3 with pea protein particles are given for reference (red). (c) Confocal micrograph of the emulsion showing the microstructure (scale bar: 50 μm).

The confocal micrograph of jammed emulsion at pH 3 after removing protein particles is shown in **Figure 4.7.c**. It shows that the protein molecules were still able to produce stable jammed oil droplets. However, the interstitial space seems to be void of proteins, which confirms the protein particles being successfully removed.

The strain sweep of the emulsion at pH 3 prepared without protein particles is shown in **Figure 4.7.a.** The graph shows G' (filled circle) and G'' (unfilled circle) as a function of strain

amplitude. The figure shows that G' values were slightly higher than G'' at strain values below 20%. Above 20%, the G'' was higher, and the emulsion showed predominantly viscous behavior. The emulsions without particles at pH 3 had lower moduli values than emulsions containing particles at the same pH value (**Figure 4.3.b**). This behavior of the jammed emulsion at pH 3 in the absence of protein particles was similar to the jammed emulsion formed at pH 7, showing an apparent effect of the protein particles on the rheological properties [136].

Figure 4.7.b shows Lissajous plots of jammed emulsion stabilized with pea proteins at pH 3, with (red) and without protein particles (black) as a function of different strain amplitudes. The shapes of the loops of the emulsions without protein particles at pH 3 are similar to that of jammed emulsions without protein particles at pH 7 (**Figure 4.6.b**).

The shapes of the loops clearly showed that the emulsions without protein particles at pH 3 have a different microstructure than the emulsions with protein particles at pH 3 (red loops). When particles were not present, at 10% strain, the emulsion displayed a nonlinear visco-elastic response with mild strain hardening near the maximum strain, similar to the pH 7 emulsions. Moreover, when protein particles were not present at 50% and 100% strains, the shapes of the curves were rounded rhomboids. In contrast, the presence of protein particles resulted in sharp rectangular responses (yielding, plastic-like). Also, the overshoot in stress at the corners when particles were present is not seen when particles were absent.

Even though the mass fraction of proteins in the emulsions is much less than oil droplets (~1:100), the particles are vital for creating plastic-like emulsions. The microstructure formation mechanism stems from the presence of protein particles between oil droplets, as shown in **Figure 4.8**. The protein particles themselves are formed by protein-protein attractive hydrophobic and van der Waals forces [127]. Therefore, the protein particles create adhesive droplet-droplet interaction by 'sticking' with interface-bound protein molecules through hydrophobic and van der Waals interactions. The droplet-droplet adhesion results in soft solid material with a plastic-like response [148]. Without protein particles, the oil droplets are simply jammed and do not form a printable material.

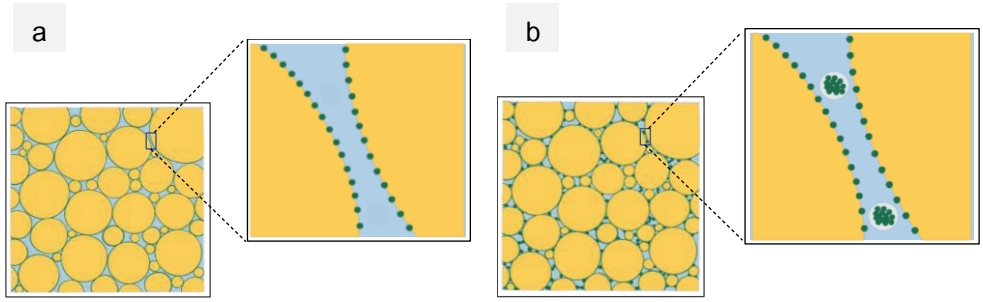

Figure 4.8: Graphical depiction of emulsion microstructure (a) without protein particles showing oil droplets in contact with each other and (b) with protein particles associating with the close-packed oil droplets creating droplet-droplet interaction through weak adhesive forces.

The ability to produce a 3D printable material using pea protein stabilized emulsions opens avenues for utilizing plant protein-based edible materials for specialized foods without the need for any additional cross-linking agent. For instance, pea protein-based emulsions could deliver hydrophobic molecules through encapsulation for special dietary needs and therapeutic foods [121,149]. By controlling the shape and fill density of the printed structure, encapsulation and release of molecules and the sensory attributes of the material can be modified [150]. Therefore, plant protein-based materials could play a vital role in specialized foods. Beyond food, we envision that the printable material could be used as a sacrificial template for producing tissue analogs, for instance, in structured cultured meat research.

We created a 3D printable material by simply changing the pH of jammed emulsions stabilized by pea proteins and extruding it at room temperature. However, using nozzles of micron-scale or elevated temperatures might affect the stability of emulsion droplets and, thereby, the stability of the printed material. Further studies on these aspects would be necessary.

4.4 Conclusions

3D printable materials should flow when applying an external force to get them through a nozzle and should self-stand after printing. In this research, we successfully designed such an edible 3-D printable material based on a jammed emulsion using the pH-dependent self-assembling property of pea proteins. The emulsions formed without protein particles (pH 7) were visco-elastic soft solids with weak droplet-droplet interactions. Whereas emulsions formed in the presence of protein particles (pH 3) behaved like elastoplastic material, with

relatively strong adhesive droplet-droplet interaction. The protein particles through hydrophobic and van der Waals forces ‘stick’ the droplets together. The printability of the two emulsions was tested using a 3D printer at room temperature. Emulsions without particles could not retain the printed structure, while the emulsions with protein particles were extruded and could retain the printed structures for over 48 hrs. Therefore, using the self-assembled adhesive protein particles in a jammed emulsion, we designed a 3D printable material. The use of self-assembled adhesive pea protein particles is an attractive method to form edible 3D printable materials since proteins form an integral part of edible systems. This is the first time a simple pH-driven technique is applied to create 3-D printable edible emulsions structures based on plant proteins. Our method also eliminates additional pre and/or post-treatments used to stabilize the printed structures [116]. Therefore, our research opens up possibilities to employ accessible molecules such as pea proteins (plant proteins) to design edible printed emulsion structures. We envision more plant proteins would be explored as biopolymers to produce printable materials for specialized foods and bio-compatible applications such as scaffolding.

Chapter-5: Effect of pea protein purification on the interfacial and emulsion properties

Submitted as:

Sridharan, S., Azzouani, A., Hommel, J., Meinders, M. B., Bitter, J. H., & Nikiforidis, C. V. (2021). Effect of pea protein purification on the interfacial and emulsion properties.

Abstract

Pea proteins are studied as emulsifying agents in food systems. Pea protein extraction methods consume energy and demand the use of water. To reduce this energy consumption, extensive purification should and could be avoided. However, a protein mixture with lower protein purity (~50 wt%) is obtained using less extensive purification. To use the less purified pea protein mixtures (PPM) as emulsifiers, the emulsifying functionality of PPM need to be investigated and compared with extensively purified pea protein isolates (PPI-85 wt% protein purity). Therefore, in this study, we investigated the interfacial properties of PPM and the properties of emulsions stabilized by PPM and compared them with PPI. Both PPM and PPI reduced interfacial tension and formed a protein layer around the oil droplet at both pH 7 and pH 3. Furthermore, emulsion properties were investigated by preparing 50 wt% oil-in-water emulsions at pH 7 and pH 3. At pH 7, emulsion properties were similar for PPM and PPI with a droplet size distribution between 1-10 µm, viscosity around 1 Pa.s, and gel strength of 1 Pa. At pH 3, the PPM emulsions formed slightly larger oil droplets (~ 5 µm) than PPI emulsions (~ 2 µm). PPM emulsions were more viscous (~40 Pa.s) than PPI emulsions (1 Pa.s), and PPM emulsions formed firmer gels (300 Pa) than PPI emulsions (2.5 Pa). The higher viscosity and gel strength in PPM emulsions at pH 3 are attributed to the low solubility of proteins in PPM (20%) compared with PPI (70%). The insoluble protein particles aid in increasing droplet-droplet interaction and increase in viscosity and gel strength. Overall, our study showed that PPM behaves well as an emulsifying agent when compared with PPI. Moreover, the increased viscosity and gel strength of PPM emulsion at pH 3 indicates that using PPM may be beneficial for soft solid-like food products.

5.1 Introduction

Emulsions are mixtures of two immiscible liquids, where one liquid phase known as the dispersed phase is distributed in the form of droplets throughout the other, the continuous liquid phase. The dispersed droplets are stabilized by interfacially active molecules known as emulsifiers. In food systems, emulsions stabilized with dairy and egg proteins are widely used [126,151] since they are the building blocks of various products, such as yogurt, spreads, mayonnaise, etc. [152].

In recent years, there is a shift in dietary patterns towards plant-based ingredients due to environmental, societal, and health reasons [7,82]. Therefore, there is also an increased interest in using plant proteins as functional emulsifying agents in foods. Several plant proteins from chickpea, rapeseed, sunflower, and pea have been studied as emulsifiers in food systems [153,154]. Among these plant proteins, peas have been investigated as a viable plant protein source since they contain about 20 wt% protein and are widely cultivated worldwide [24,155]. About 80% of pea proteins are globulins, namely legumin and vicilin, while 20% of the proteins are albumins, namely PA1, PA2 [37,38].

The globular pea proteins, legumin, and vicilin are extracted through alkaline aqueous extraction and acid precipitation or ultra-filtration. [24,35,100] These alkaline extracted pea proteins, known as pea protein isolates (PPI), contain 70-90 wt% proteins. PPI is a suitable emulsifier of oil-in-water emulsions and are the most common form of pea proteins used [35]. However, the alkaline extraction process comprises multiple energy-intensive steps such as centrifugation and drying to remove water. Each of these energy-intensive steps could consume between 2-7 MJ/kg materials processed [62]. Moreover, the process focuses on obtaining highly purified proteins and produces side streams such as starch and fibers considered low-value products [27]. Therefore, a simpler protein separation process by avoiding steps such as centrifugation has been explored to prevent intensive purification. Such processing routes consume only 1-2 MJ/kg (compared to 7 MJ/kg) material processed and produce protein mixtures containing 40-60 wt% protein and large amounts of non-protein components such as starch [26,27,62].

In our previous work, we investigated the effect of starch on emulsifying properties of native pea flour in a model oil-in-water emulsions at neutral pH by comparing it with PPM where the starch was removed using a simple filtration technique[96]. By comparing emulsions

stabilized with pea flour and PPM, we showed that at pH 7, native proteins are the primary emulsifying agent, and starch does not influence the emulsion properties. To replace commonly used PPI (75-90 wt% protein) with less purified pea protein systems, it is essential to directly compare the systems for their emulsifying properties. To compare PPI with less purified systems, PPM (~ 50 wt% protein) was chosen as the unpurified system. PPM contains only 5 wt% starch, similar to in PPI, which contains 3 wt% starch. The low amount of starch in both systems makes the comparison and interpretation of their functional properties more straight forward. Therefore, a direct comparison would reveal the effect of protein purification on the emulsifying properties. Specifically, a comparison of properties of emulsions stabilized by PPI and PPM at both neutral and acidic pH conditions relevant for food products is necessary.

In this work, we investigate the emulsifying properties of pea proteins at pH 7 and pH 3. PPM (55 wt% protein) and PPI (85 wt% protein) were studied for their interfacial properties and the rheological properties of emulsions stabilized by PPM and PPI. This research provides insight into the interfacial activity and emulsifying functionality of pea proteins in PPM compared with PPI. Overall, our study sheds light on using less purified PPM in place of extracted PPI as emulsifying functionality in food systems.

5.2 Materials and Methods

5.2.1 Materials

Yellow peas were purchased from Alimex® B.V (Sint Kruis, The Netherlands). Rapeseed oil was obtained from Danone Nutricia Research (Utrecht, the Netherlands). Sodium hydroxide (NaOH), hydrochloric acid (HCl), Nile blue dye, and Rhodamine B® and Whatmann® qualitative filter paper 595 ½ were all purchased from Sigma-Aldrich (Zwijndrecht, The Netherlands).

5.2.2 Methods

5.2.2.1 Pea protein mixture preparation

Yellow peas were milled, at 40°C, using a Retsch® (Retsch GmbH, Haan, Germany) Rotor mill fitted with a sieve cut-off of 80 µm. The milled protein flour (PF) was then sieved to obtain flour particles below 45 µm (for us the lowest achievable size) using a Retsch®

horizontal mechanical sieve shaker. To produce pea protein mixture (PPM), starch granules were removed by vacuum filtration using a Whatman® 595 ½ filter paper with a cut-off of 4-7 µm. In brief, a known amount of PF was dispersed in ultra-pure water and the pH was adjusted to 7. The filtrate i.e. pea the protein mixture (PPM) dispersion was collected and used further. The PPM fraction contained about 55 wt% protein and 6 wt% starch [96].

5.2.2.2 Alkaline extraction of Pea Proteins

Pea proteins were extracted from yellow peas by alkaline extraction and isoelectric point precipitation, commonly reported in the literature [58,88]. In brief, pea seeds were dry milled into coarse flour in a coffee blender (IKA, Staufen, Germany). The flour was then soaked in water at a 1:10 (w:w) solids to water ratio. The pH was adjusted to 8 with a 0.5 M NaOH solution under constant stirring. After 2 h of soaking, the slurry was blended in a kitchen blender HR2093 (Philips, The Netherlands) at maximum speed for 2 min. The resultant slurry was centrifuged using Sorvall Legend XFR (Thermo Fischer Scientific, Waltham, MA, USA) in 250 mL centrifuge tubes at 10000 g for 30 min to precipitate solids. Further, the protein-rich supernatant was separated, and the proteins were precipitated at pH 4.8 with a 0.5 M HCl solution. The solution was allowed to stand for 1 h, and the precipitate was collected by centrifugation at 10000 g using Sorvall Legend XFR (Thermo Fischer Scientific, Waltham, MA, USA) in 250 mL centrifuge tubes for 30 min. The precipitate was diluted (1:10 w/w) with ultrapure water, and the pH was neutralized (pH 7). The solution was further freeze-dried, and the obtained powder was termed pea protein isolate (PPI). The protein powder was stored in the freezer (−18 °C) for further.

5.2.2.3 Solubility and surface charge

The amount of protein soluble in water as a function of pH was determined using the Lowry method. In brief, 0.2 wt% protein dispersions (0.25 wt% solids for PPI and 0.4 wt% for PPM) were prepared in 50 mL ultra-pure water. The pH of the dispersions was set to 2,3,4,5,6,7 using 0.1M HCl or 0.1 M NaOH solutions. The dispersions were then left to stir at room temperature for 3 hours at 300 rpm using a magnetic stirrer.

The surface charge of proteins of the same dispersions was measured with a U-shaped cuvette in the Malvern Ultra Sizer (Malvern Instruments Ltd., Malvern, U.K.) at 20 °C. The

measurements were done after 120 s of equilibration inside the ultra sizer and were performed in triplicate, and the average value was reported.

For solubility measurements, the protein dispersions were centrifuged using a Sorvall Legend XFR (Thermo Fischer Scientific, Waltham, MA, USA) in 50 mL centrifuge tubes at 10000 g for 30 min at 20 ºC. The clear supernatant was collected, and the Lowry test was performed at 700 nm using VWR® UV-1600PC spectrophotometer (Amsterdam, The Netherlands). A standard curve for protein was created using BSA as a protein standard. The number of proteins in the ultra-centrifuged protein solution was also measured according to the same protocol.

5.2.2.4 Interfacial tension and dilatational rheology

The interfacial tension reduction and dilatational rheology of the oil–PPI and oil-PPM interface were measured with an automated drop tensiometer (Tracker, Teclis Instruments, Tassin, France). A 0.002 wt % pea protein dispersion was prepared for PPM and PPI. The pH was adjusted to pH 7 or pH 3 using 0.5 M NaOH or 0.5 M HCl, respectively.

Rapeseed oil was treated with Florisil overnight to remove impurities and was used as the oil phase. In brief, a 1:3 (w/w) ratio of Florisil to oil was mixed overnight and centrifuged the next day to obtain contaminant-free oil, which was used in the interfacial study.

The rapeseed oil was loaded onto a 500 µL syringe fitted with a J-shaped needle in the drop tensiometer. The aqueous phase was filled into a clean, 7 mL optical glass cuvette. The needle was inserted into the aqueous phase, and a sessile drop of 20 mm^2 areas was made. The shape of the oil droplet was monitored continuously with a camera. This was converted into interfacial tension by the Wdrop software from Teclis Instruments (Tassin, France). The dynamic interfacial tension reduction profile was monitored continuously for 3.5 hrs and plotted against time in a semi-log plot.

After 3.5 hrs of measurement of the interfacial tension, dilatational viscoelasticity was measured by changing the surface area of the droplet in a sinusoidal manner. The droplet was subjected to changes in surface area with amplitudes of 5 and 10% up to 30% deformation with respect to the initial surface area (20 mm^2). Each amplitude was applied for 100 s with five cycles next to each other. This was followed by 500 s of rest period before the next higher amplitude was applied. The interfacial tension change and change

in the area were recorded during the oscillation, and the dilatational elastic (Ed′) and viscous moduli (Ed″) were obtained.

5.2.2.5 Oil-in-water emulsion preparation

Emulsions were prepared with PPM and PPI dispersions. The protein concentrations in all the dispersions were standardized to 1.0 wt% (in the final emulsion with 50 wt% oil) by appropriately changing the dry matter content. The protein concentration was chosen based on our previous research, where we showed that an oil-to-protein ratio of 1:50 is sufficient to produce stable emulsions [96]. The protein content referred to in these emulsions are final protein concentrations (after adding oil).

First, the protein dispersions were sheared under a high-speed rotor-stator homogenizer (IKA®) at 6000 rpm for 30 s. Afterward, 50 wt% canola oil was slowly added to the dispersion and homogenized for 1 minute at 10000 rpm. This resulted in a coarse emulsion. The coarse emulsion was further homogenized by passing through a GEA® (Niro Soavi NS 1001 L, Parma Italy) high-pressure homogenizer five times with the homogenization pressure set of 450 bars. All emulsions were made in duplicates following the same procedure and were allowed to rest for 3 hrs before further analysis.

5.2.2.6 Particles size

Droplet diameter measurements were performed using a Bettersizer S3 Plus (3P INSTRUMENTS GmbH & Co. KG, Odelzhausen, Germany) equipped with a hydro dispenser. The droplet diameter was presented as volume mean diameter $D_{4,3}=\left(\frac{\sum_1^n nD_i^4}{\sum_1^n nD_i^3}\right)$.

5.2.2.7 Rheological properties

The rheological properties of PPI stabilized and PPM stabilized emulsions at pH 7 and 3 were measured at 20°C using an Anton Paar 302 rheometer. The supplier software Rheocompass S1.25 was used to analyze and obtain raw data for all the measurements.

Emulsions were analyzed using oscillatory rheological measurements in a cone plate set up with a cone diameter of 50 mm and cone angle of 4° (gap truncation of 0.49 mm). Before measurements, emulsions were allowed to equilibrate at room temperature for at least 1

hour. The emulsions were then loaded onto the rheometer, and the upper plate was lowered to the required gap. The emulsion was allowed to equilibrate for 5 minutes before the measurement was started. An oscillatory strain sweep ranging from 0.1% strain up to 1000% strain at a constant frequency of 6.2 rad/s was performed. The Elastic (G') and Loss modulus (G'') were recorded as a function of strain. Another fresh emulsion sample was loaded into the same geometry, and a steady shear viscosity was measured from 0.1/s to 100/s.

5.2.2.8 Confocal microscopy

The emulsions were imaged using a confocal laser scanning microscope (CLSM) and fluorescent dyes to visualize the microstructure. In brief, about 1 mL of the emulsion was mixed with 7 µL of Nile red and 7 µL of Fast green FCF in an Eppendorf tube. The tubes were sealed and allowed to mix for 15 min. Afterward, about 30 µL of the sample was deposited on a microscopy slide and mounted on the confocal table. A Leica SP8 confocal microscope fitted with a 63× water immersion lens and white light laser was used to image the samples. Nile red stained the oil phase and was excited at 488 nm, and the emission was captured between 500 and 600 nm. Rhodamine B, which stained proteins, was excited at 566 nm, and the emission was captured between 570 and 670 nm. The images were captured sequentially with Leica imaging software.

5.3 Results and Discussion

The study focuses on investigating the emulsion properties of pea protein mixtures (PPM) containing 55 wt% proteins, 5 wt% starch, 3 wt% oil, and 10 wt% sugars when compared with alkaline extracted pea protein isolate (PPI) containing 80 wt% proteins, 5 wt% oil, 3 wt% ash and 6 wt% sugars [96,127]. In our previous work, we have shown that in the unextracted PPM, proteins are the primary emulsifying agent [96], similar to when using extracted protein isolates. Therefore, when comparing these two mixtures, differences in the protein properties such as protein charge and solubility could affect their ability to adsorb and stabilize the oil-water interface.

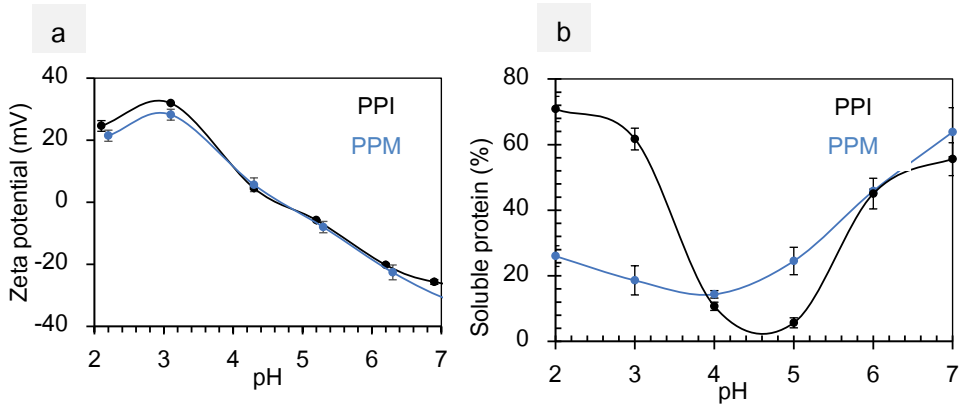

Figure 5.1: (a) Net surface charge and (b) Protein solubility, as a function of pH for 0.2 wt% protein concentration in PPM dispersion (blue) and PPI dispersion (black) measured at 20°C.

Figure 5.1 shows the net surface charge and percentage of soluble proteins as a function of pH in PPM and PPI standardized to 0.2 wt% protein. The surface charge (**Figure 5.1.a**) of both the samples is similar across the entire pH range and represents the net surface charge of proteins. At pH 2, the net surface charge is around +30 mV for both PPI and PPM dispersion, and the surface charge decreases as the pH goes to around 4. The surface charge reaches 0 at pH 4.8, which is known as the iso-electric point. Further increase in pH leads to an increase in net surface charge to about -30 mV at pH 7.

The solubility curve is shown as percentage soluble proteins compared to the initial amount of proteins added in the dispersion as a function of pH in **Figure 5.1.b**. The figure shows that PPI has a 'U'-shaped solubility curve with 60% solubility at pH 7. The solubility decreases to about 5% as the pH approaches pH 4-5. At these pH values, the proteins are close to their iso-electric point (pH 4.8), and due to lack of repulsive surface charges, the proteins aggregate which might explain the low solubility. Further, when pH decreases to pH 2, the solubility increases to about 70% since the proteins obtain a net surface charge of +30 mV at this pH value. In PPM dispersion, the solubility at pH 7 is 60 wt%, and it decreases to 20% as the pH is around the IEP. Upon decrease in pH to 2, the solubility remains constant at 20%, unlike in PPI, where at pH 2 the solubility rises to 60%. Therefore, in PPM, the proteins remain in aggregated, insoluble state further away from their iso-electric point where they have a net positive surface charge.

The solubility of proteins in PPM and PPI differ below their iso-electric point (pH 4.8). In PPI, even though the solubility at pH 3 is 60%, we have previously shown that the proteins in PPI also form soluble protein particles [127]. The proteins in PPI self-assemble due to hydrophobic and van der Waals forces into particles between 100 and 500 nm. Due to relatively small size, they do not precipitate during solubility measurement. In the case of PPM, the solubility at pH 3 is around 20%, much lower than PPI. The low solubility shows that majority of the proteins formed large protein particles, that precipitated during solubility measurement. It could be hypothesized that, similar to in PPI, the proteins in PPM could also self-assemble due to hydrophobic forces and van der Waals forces. However, in the case of PPM, the proteins could form larger particles in micron scale. These large particles may be insoluble due to their large size. The exact size of such protein particles is difficult to establish due to the co-existence of fibers, minor quantities of starch and other small molecules in PPM. Future investigation is necessary to understand the formation of insoluble protein particles in PPM. Therefore, at pH 3, PPM forms insoluble protein particles while PPI forms soluble protein particles.

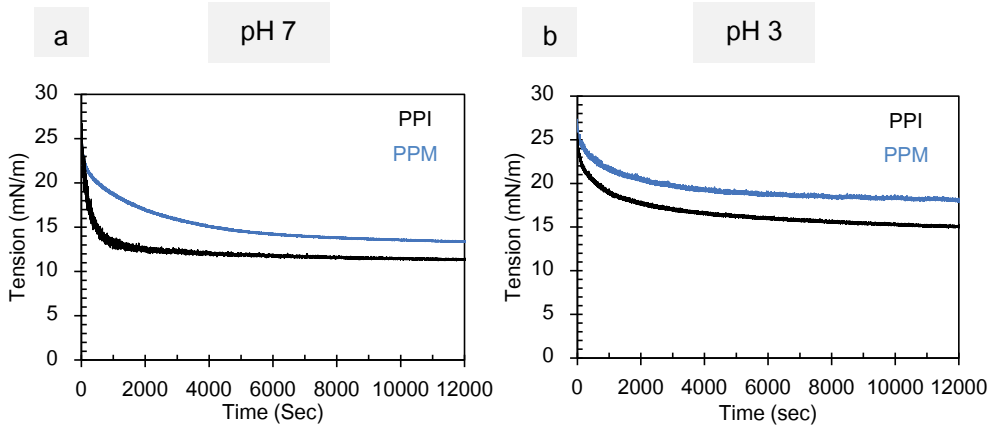

Figure 5.2: Interfacial tension as a function of time for 0.002 wt% protein in PPM dispersion (blue) and PPI (black) at (a) pH 7; (b) pH3. Measured at 20°C for 12000 sec.

The interfacial behavior of PPM and PPI were investigated using drop tensiometry. **Figure 5.2** shows the dynamic interfacial tension decrease as a function of time for PPM and PPI dispersions at the oil-water interface at pH 7 and 3.

Figure 5.2.a shows the tension decrease at pH 7. Initially, the interfacial tension (IFT) in both PPM and PPI samples starts around 25 mN/m. As time progresses, the IFT value decreases sharply up to about 2000 sec. Beyond 2000 sec., IFT decreases gradually. After 12000 sec., IFT is between 13-15 mN/m for both the samples. In the initial stages, the IFT for PPI dispersion decreases more steeply compared with the PPM dispersion. The faster decrease in PPI indicates that the PPI proteins can adsorb and form an interfacial layer faster than the proteins in PPM. However, above 2000 sec, the decrease in tension slowed down for both systems. After 12000 sec, PPI dispersion reduced the tension to about 13mN/m while the protein mixtures were reduced to about 15 mN/m.

Figure 5.2.b shows the decrease in IFT at pH 3. The pattern of IFT decrease at pH 3 is similar to at pH 7 for both samples. Initially, a rapid decrease in IFT is followed by a long period of slow decline. The IFT goes from 25 mN/m to about 16 mN/m for PPI and about 18 mN/m for PPM. Despite differences in solubility between PPI and PPM at pH 3, both proteins reduce IFT with a similar slow profile. This indicated that the proteins in both samples were equally surface-active regardless of their purification routes.

The IFT decreases slowly at pH 3 for both samples compared with pH 7. A slower decrease indicates that the proteins take longer to adsorb to the interface and rearrange [156,157]. At pH 3 higher IFT values were reached at the end of 12000 sec (17-19 mN/m) for both the systems compared with pH 7 (13-15 mN/m). This difference for PPM is likely caused due to presence of insoluble protein particles at pH 3, leading to fewer proteins available to adhere to the oil droplet interface. To verify this hypothesis, we compared the rate of decrease in IFT at pH 7 and 3 for PPM in the first 1000 sec. The rate of decrease is simply the slope of the IFT curve in the first 1000 seconds. Therefore, the rate of decrease of IFT for PPM at pH 7 is 0.0077 mN/m.sec while at pH 3 is 0.0048 mN/m.sec. The rates could be translated into percentage differences as PPM at pH 3 decreases IFT 38% slower than at pH 7. In comparison, the difference in protein solubility for PPM at the two pH values is about 45%. Therefore, the difference in protein solubility is proportional to the rate of decrease of IFT for PPM at the two pH values.

In PPI, at pH 3, the proteins also form protein particles much smaller in size (100-500 nm). Therefore, they do not precipitate during solubility measurement (centrifugation) and are termed soluble aggregates. Therefore, in PPI, the slow decline of IFT is likely caused by the presence of self-assembled protein particles. The particles are also unavailable to

interact with oil droplets, leading to higher final interfacial tension than PPI at pH 7. However, since the protein particle formation does not lead to lower solubility in PPI, a direct correlation as in PPM is not possible.

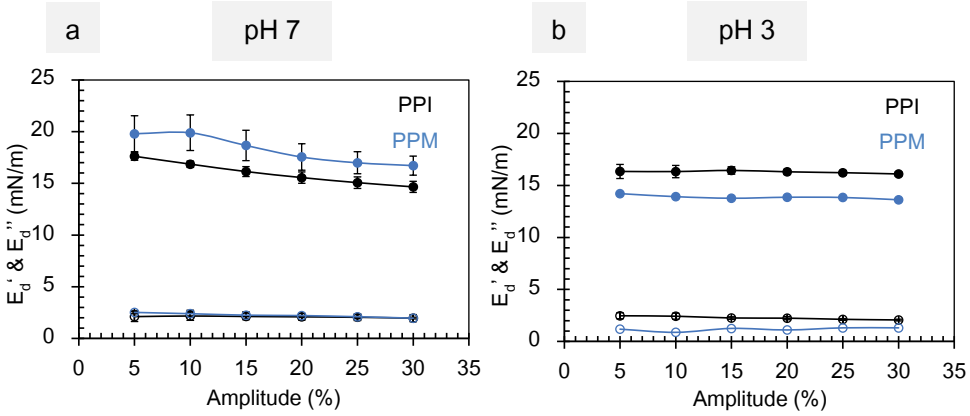

Figure 5.3: Dilatational elastic (filled) and viscous moduli (unfilled) as a function of strain amplitude of 0.002 wt% protein stabilized interface in PPM dispersion (blue) and PPI (black) at (a) pH 7 and (b) at pH 3.

Proteins upon adsorption to the oil-water interface stabilize the oil droplet by forming a visco-elastic layer around the droplet. The visco-elastic properties of the protein layer around the oil droplet were investigated using dilatational amplitude sweep measurements. **Figure 5.3** shows the interfacial dilatational elastic (E_d') and viscous (E_d'') as a function of dilatation amplitude for PPM and PPI dispersions at pH 7 and pH 3.

Figure 5.3.a shows the dilatational moduli as a function of amplitude at pH 7. For both, the samples E_d' was higher than E_d'', throughout the amplitudes tested. The higher E_d' indicated that the interface was visco-elastic with a dominant elastic nature. The E_d'' curves for both samples were a straight line and coincided with each other between 2-3 mN/m. The E_d' curves for both PPM and PPI decreased as a function of amplitude from ~20 mN/m at 5% to ~17 mN/m at 30% amplitude. Besides, the E_d' curve for PPM was higher than for PPI, indicating a slightly weaker elastic network in PPI compared to PPM. Overall, at pH 7, both PPI and PPM form an interfacial layer with similar stiffness (E_d') with a slight decrease as a function of amplitude. **Figure 5.3.b** shows the dilatational moduli curves as a function of amplitude at pH 3. At pH 3, E_d' was 15-17 mN/m for PPI and PPM dispersions while E_d'' was around 2 mN/m for both systems, indicating a visco-elastic protein network. The E_d'

curves for both samples did not change with increasing amplitude. Therefore, at pH 3, both systems form an interfacial layer with similar stiffness (E_d') values as a function of amplitude.

When comparing the pH values, E_d' values of PPI dispersion at pH 3 were similar to E_d' at pH 7, pointing to similar strength at both pH values. In PPM dispersion at pH 3, E_d' was lower than at pH 7, pointing to a weaker interface at pH 3. The difference in PPM between the two pH values is likely caused due to insoluble protein particles present at pH 3. Due to low solubility, fewer proteins adsorb and interact at the droplet interface leading to a weak interfacial layer [158]. To further understand the rheological properties of the interfacial layers, Lissajous plots were plotted.

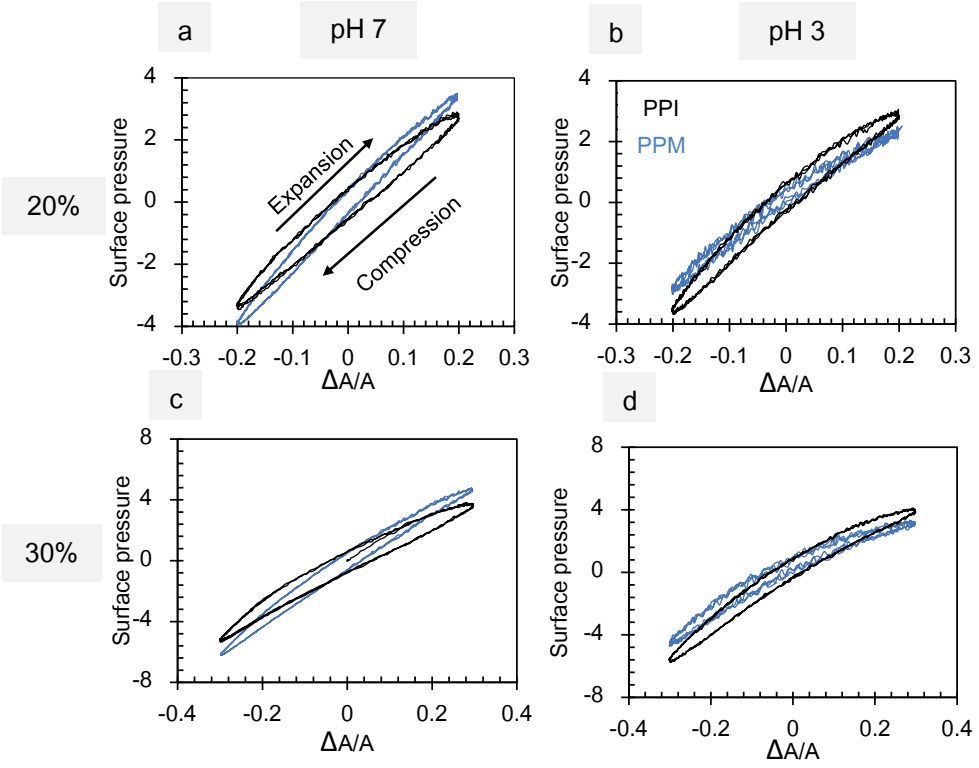

Figure 5.4: Interfacial Lissajous plots of 0.002 wt% protein in PPM dispersion (blue) and PPI dispersion (black) at 20 % dilatational amplitude (a) at pH 7, (b) at pH 3; at 30% dilatational amplitude (c) at pH 7 and, (d) at pH3.

Figure 5.4 shows the Lissajous plots of PPM and PPI at 20% and 30% dilatation amplitude. Lissajous curves were plotted as surface pressure as a function of change in relative area of deformation.

Figure 5.4.a and **Figure 5.4.c** show the Lissajous plots at pH 7 at 20% and 30% amplitude, respectively, for PPI and PPM. The Lissajous curves are ellipsoidal-shaped loops at both strain amplitudes for both systems, indicating a predominantly visco-elastic interface with a larger elastic response [159,160]. The loops show slight differences between PPI and PPM. The PPI stabilized interface plots show a wider loop in the expansion phase than PPM, indicating a more fluid-like response. Upon compression, PPI and PPM interfaces show a slight narrowing of the loop, indicating a hardening of the interface. Upon compression, the proteins are squeezed into smaller areas, creating a packed interface that becomes rigid as it is compressed. Such ability to be compressed indicates that pea proteins at pH 7 do not seem to form a strong interacting protein-protein network [161].

Figure 5.4.b and **Figure 5.4.d** show the Lissajous plots at pH 3 at 20% and 30% strain amplitude, respectively. Also, at pH 3, both PPM and PPI stabilized interfaces show a visco-elastic response upon dilatation. However, at pH 3, the loops show a noticeable bending upon expansion, indicating a slight softening behavior of the interface. Such a strain-softening behavior indicates that the interface could be deformed easily caused due to weak interactions. Proteins at pH 3 are present as aggregates, and therefore fewer proteins are adhered to the droplet interface, causing a weak interfacial layer [158]. Besides, the loops of the PPI interface are slightly wider than the PPM, indicating a slightly more viscous response, in line with the elastic moduli plot (**Figure 5.3.b**). Upon compression, both PPM and PPI loops show a slight hardening effect similar to pH 7. This behavior also indicates that proteins at the interface could be pushed closer to each other by compression, forming a jammed interface [160]. Therefore, at pH 3, the protein network is also weak and soft-solid, similar to pH 7.

The interfacial properties of PPI and PPM show slight differences. At pH 7, PPM forms a slightly stronger interface, whereas, at pH 3, PPI forms a stronger interface. PPI forms an interface that is equally stiff at both pH 7 and pH 3. In PPM, the interface is less stiff at pH 3, which might be due to the lack of sufficient soluble proteins in this system (protein solubility-20%). Nevertheless, the unpurified PPM reduces IFT and forms a protein interface around the oil droplet at pH 3. To study the emulsion properties of pea proteins,

50 wt% oil-in-water emulsions were prepared using 2 wt% protein dispersion (1wt% final protein concentration in emulsions) in PPM and PPI at pH 7 and pH 3. The protein to oil ratio was chosen based on our previous study on emulsifying properties of pea flour [96].

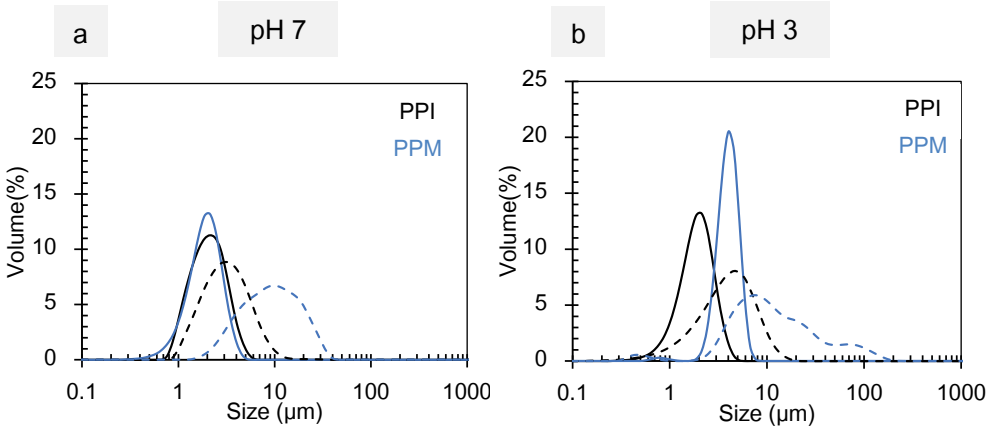

Figure 5.5: Size distribution of PPM stabilized emulsions (Blue) and PPI stabilized emulsions (Black) of individual droplets (solid line) and droplet aggregates (dashed lines) at (a) pH 7 and (c) at pH 3.

Figure 5.5.a & b shows the droplet and droplet aggregate size distribution for PPM and PPI stabilized emulsions at pH 7 and 3. At pH 7 (**Figure 5.5.a**), both PPM stabilized (blue) and PPI stabilized (black) emulsions show a monomodal droplet size distribution. The individual oil droplets are primarily between 1-10 μm with a peak around 2-3 μm. No difference in the droplet size between PPI and PPM is noticeable, and they overlap. The oil droplets in both systems were aggregated and were measured without the addition of SDS. Droplet aggregates also had a size distribution of about 20 μm for PPI emulsion and 30 μm for PPM emulsion.

At pH 3 (**Figure 5.5.b**), the emulsions show monomodal individual droplet size distribution, with the majority of oil droplets between 1-10 μm in size. PPM had larger size distribution than PPI. The peak for PPI was around 2 μm, while for PPM, it was around 5 μm. The larger droplet size in PPM indicates that the proteins in PPM may not be able to form small oil droplets, most likely due to their lower solubility.

In PPM at pH 3, most of the proteins are present as aggregates, leading to a lower amount of proteins taking part in forming the weak visco-elastic interfacial layer (**Figure 5.3.b**).

Moreover, the initial reduction of IFT in these mixtures is slow in these mixtures. Therefore, we hypothesize that the oil droplets may re-coalesce during homogenization due to a lack of strong interfacial layer formation and long adsorption of the proteins. The recoalescence results in larger oil droplets in PPM emulsion compared to PPI emulsions. Nevertheless, the larger oil droplets in PPM emulsions are still monomodal and are smaller than 10 µm.

At pH 3, the oil droplets in both systems were aggregated, and their size was measured without adding SDS. The aggregate size for PPI stabilized emulsions is between 500 nm to 20 µm. While for PPM stabilized emulsions, it is between 1-200 µm. Therefore, PPM emulsion also had a much larger aggregate size than PPI emulsion. The result indicates that droplets in PPM associate with each other more than in PPI emulsions.

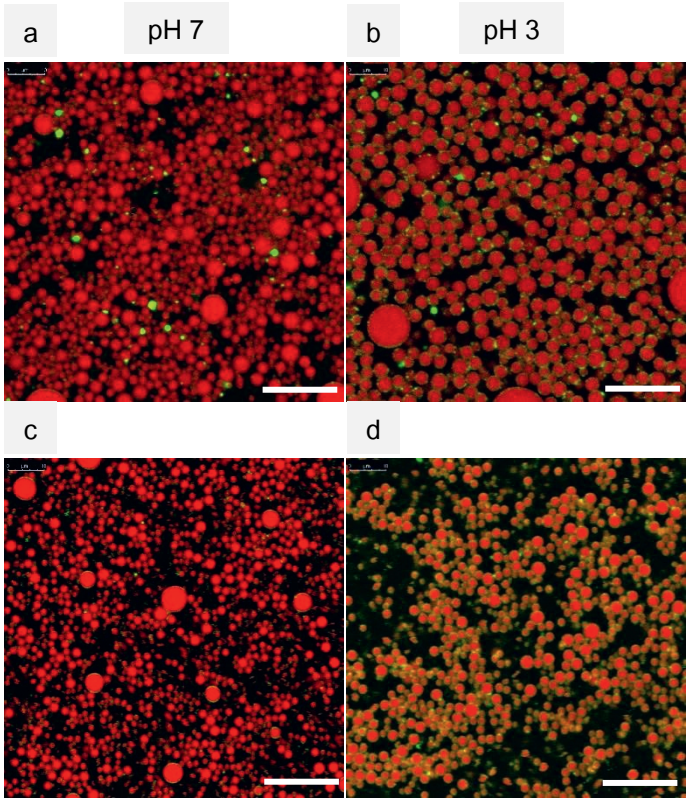

Figure 5.6: Confocal micrographs of 50 wt% oil emulsions stabilized with (a) PPM at pH 7, (b) PPM at pH 3, (C) PPI at pH 7 and, (d) PPI at pH 3; Oil droplets colored in red and proteins colored in green and scale bar: 20 µm

Confocal microscopy was employed to visualize the emulsion microstructure, and the images are shown in **Figure 5.6**. The micrographs show oil droplets stained in red and proteins stained in green. At pH 7, both PPM stabilized emulsions (**Figure 5.6.a**), and PPI stabilized emulsions (**Figure 5.6.c**) show similar microstructure. The droplet sizes visualized with the microscopy correspond well with the droplet size measured (**Figure 5.5**). The oil droplets are spherical and are also found partly in the aggregated state.

At pH 3, in both emulsions, more protein particles (green) are visible between the oil droplets than at pH 7. The PPM emulsions show larger oil droplets than PPI emulsions, which corresponds well with the size measurements. Moreover, protein particles can be seen in the droplet interstitial spaces for both emulsions. In PPM emulsion, the oil droplets seem to be connected and are arrested from moving.

The interfacial and emulsion properties showed that PPM behaves comparably to PPI. The protein mixtures can stabilize oil droplets to produce monomodal droplets, and their interfacial rheology is similar. Previous work has shown that protein purification processes affect the bulk properties of protein dispersions, such as viscosity and gelation [162]. To understand the effect of protein purification on the emulsion rheology, oscillatory strain and viscosity of a 50 wt% oil-in-water emulsion were studied.

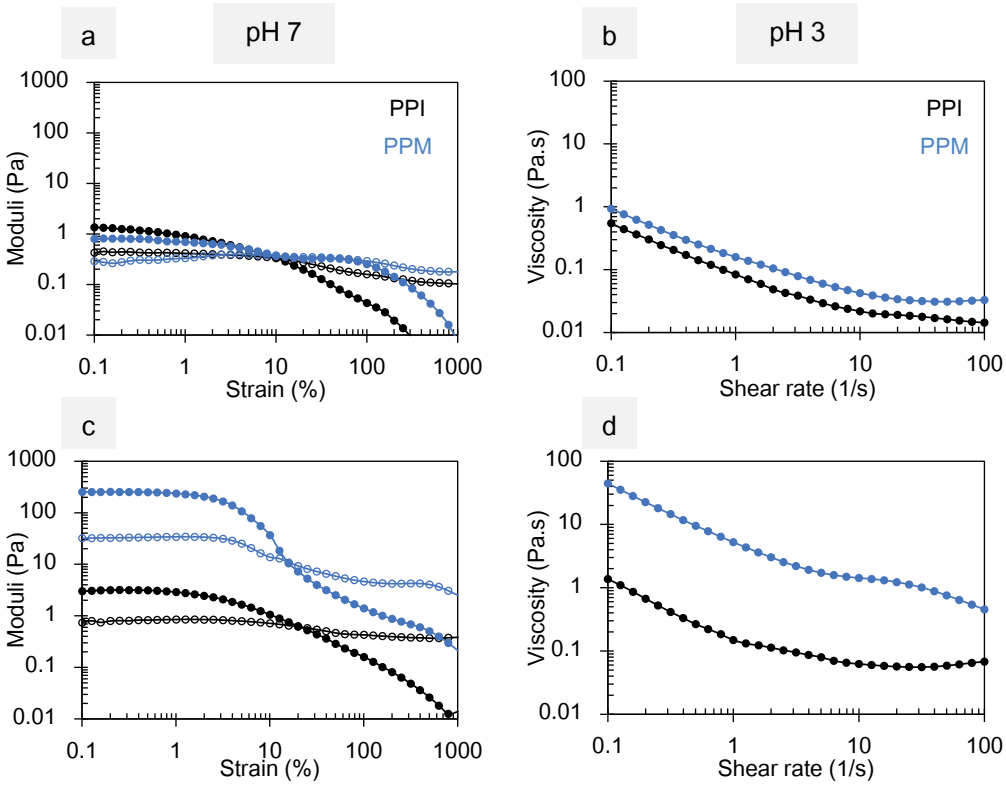

Figure 5.7: Rheological properties of PPM stabilized emulsions (blue) and PPI stabilized emulsions (black). Elastic (G') and loss moduli (G'') of emulsions as a function of strain amplitude (a) at pH 7 and (c) at pH 3; Apparent viscosity of emulsions as a function of shear rate (b) at pH 7 and (d) at pH 3.

Figure 5.7 shows the rheological behavior of 50 wt% oil-in-water emulsions stabilized by PPM and PPI at pH 7 and 3. **Figure 5.7.a & c** shows the strain-dependent elastic (G') and loss (G'') moduli at pH 7 and 3, respectively. **Figures 5.7.b & d** show the steady-state viscosity as a function of shear rate at pH 7 and 3, respectively.

At pH 7, both emulsions show a relatively higher G' than G'' at low strains. The G' values are around 1 Pa at low strain, and the G'' are below 0.8 Pa. A slightly higher G' points to an elastic material response from the emulsions. As the strain value increases, the G' value gradually decreases up to 20% strain. Above 20% strain, G'' gets larger than G'. Therefore, at large enough strains, the emulsions lose their elastic interaction and start to flow, characteristic of viscoelastic emulsions [132].

Similarly, the shear-rate-dependent viscosity (**Figure 5.7.b**) shows similar behavior for PPI and PPM stabilized emulsions. The viscosity at 0.1/s shear rate is similar for the 3 emulsions around 1 Pa. As the shear rate increases, the viscosity decreases. Such behavior points to a shear-thinning response from all the emulsions. It is known that the oil droplets in the emulsions are aggregated. These aggregates align and break down upon application of shear, which causes a shear-thinning response [79].

At pH 7, both PPI and PPM emulsions have similar behavior, indicating that protein purification does not influence their bulk behavior. Moreover, the presence of non-protein molecules also does not modify the visco-elastic and shear thinning properties.

Figure 5.7.b shows that elastic and loss modulus as a function of strain for the emulsions at pH 3. Both the emulsions exhibit higher G' than G'' at low strains, also pointing to an elastic gel at this condition. However, G' and G'' values are lower for PPI stabilized emulsions than PPM stabilized emulsions. The difference in moduli means that PPI emulsion is a weaker gel than the PPM stabilized emulsions. The PPM stabilized emulsion showed a higher initial G' value compared with PPI stabilized emulsion. For both emulsions, the G' decreases at large strains before G'' became dominant. The large difference between PPI and PPM could be attributed to the lower solubility of the proteins in PPM compared with PPI at this pH. Our previous work showed that the presence of protein particles creates increased droplet-droplet interaction [163]. The protein particles reside between the droplets and, through non-covalent attraction, create increased droplet-droplet interaction.

Similarly, it could be expected that in PPI emulsion at pH 3, the presence of insoluble material contributed to increased droplet-droplet interaction leading to the formation of a stronger emulsion gel in the PPM emulsions. The protein aggregates could create closer droplet-droplet contact through interaction with neighboring oil droplets or through a bridging mechanism. Such an interaction would lead to increased droplet-droplet interaction and stronger emulsion-gel [164,165]. The presence of stronger droplet-droplet interaction is also evident in the droplet aggregate sizes shown in Figure 5.

Figure 5.7.d shows the shear-rate-dependent viscosity of the emulsions at pH 3. The figure also shows that PPM emulsion had higher viscosity at low strains than PPI stabilized emulsions. However, in both PPM and PPI emulsions, the viscosity values decrease as a

function of shear, pointing to a shear-thinning fluid response. This is likely caused due to the alignment and flow of droplet aggregates present in both systems [166].

Comparison between pH 7 and pH 3 also shows the difference in the rheological properties of the emulsions. Both PPI stabilized and PPM stabilized emulsions at pH 3 were more viscous and formed stronger compared gels (higher G') with the corresponding emulsions at pH 7. In PPI emulsions, at pH 3, the initial G' was around 3 Pa, whereas, at pH 7, it was around 0.8 Pa. Similarly, PPM emulsion at pH 3 had a viscosity of 50 Pa at 0.1/s compared with 1 Pa at pH 7. Therefore, the bulk properties of pea proteins are affected by the formation of protein particles at pH 3 both in the extracted and unpurified protein mixtures.

In our previous research, we proved that PF could be used to stabilize oil-in-water emulsions. By comparing PF with PPM, we showed that starch does not play a role in the emulsion properties of the resulting emulsions at neutral pH at a 10 wt% oil emulsion [96]. By extension, in this work, we show that pea protein mixture (PPM) can stabilize emulsions with similar droplet size and rheological properties compared to alkaline extracted PPI at neutral pH. At acidic pH, PPM stabilizes emulsions with larger droplets (5 μm) than PPI (2 μm) due to lower solubility in PPM. Moreover, in acidic pH, PPM emulsions are stronger gels with higher viscosity compared with PPI emulsions. Producing stronger gels using PPM may be an added advantage when making concentrated emulsion-based food formulations since it opens up avenues to use less oil to achieve the desired viscosity compared to the extracted protein system.

5.4 Conclusions

In this work, we investigated the interfacial and emulsifying properties of pea protein mixtures (PPM) and compared them with alkaline extracted pea protein isolate (PPI). We found that unpurified PPM performed comparably well with purified PPI at pH 7 and 3 when tested for 50 wt% oil emulsion systems. At pH 7, both systems showed a similar interfacial rheological property. They stabilized emulsion droplets with monomodal size distribution and showed a similar rheological response. At pH 3, PPM had lower solubility than pea protein isolate. Their interfacial rheological properties were visco-elastic soft solid interfaces. In emulsions, PPM stabilized larger droplets (~ 5 μm) than PPI emulsions (~ 2 μm). This difference was likely caused by the presence of insoluble pea protein aggregates in PPM. The rheological response of PPI and PPM stabilized emulsions was also different

at pH 3. PPM emulsions formed a stronger visco-elastic gel with a higher viscosity compared with PPI emulsions. This was also likely caused by the presence of insoluble protein aggregates in PPM. These insoluble aggregates created a stronger droplet-droplet interaction, leading to a strong emulsion gel. Therefore, PPM can function as emulsifiers at acidic and neutral pH values and comparable to PPI. At pH 7, the functionality of PPM is similar to PPI, while at pH 3, the emulsifying ability is slightly lower than PPI. Our results show that unpurified pea protein mixture works comparably well with alkaline extracted pea protein isolates. The use of unpurified mixtures could be beneficial in acidic conditions because they can form more viscous emulsions than alkaline extracted PPI.

Chapter-6: Heat-set gelation of emulsions stabilized by pea flour

Submitted as:

Sridharan, S., Sagis, L. M., Meinders, M. B., Bitter, J. H., & Nikiforidis, C. V. (2021). Heat-set gelation of emulsions stabilized with pea flour

Abstract

Pea proteins are widely studied as emulsifying and gelling agents in soft food materials. The protein extraction process consumes energy and focuses merely on protein purity. To avoid extraction-related energy consumption, unpurified pea protein-starch mixtures could be used directly as functional ingredients. Such mixtures provide additional advantages due to their binary role, such as using proteins as emulsifiers and starch as a gelling agent. We investigated the heat-induced gelation and properties of emulsions stabilized by pea flour (PF) containing 20 wt% protein and 50 wt% starch, as well as with the starch removed by filtration (PPM). Both the PF stabilized and PPM stabilized emulsions gelled when the temperature increased above about 45°C. Gelation was followed by oscillatory rheology. At pH 7, starch (in PF) contributed to a higher elastic modulus (G'≈2000 Pa) compared with the emulsions without starch (G'≈1000 Pa). At pH 3, the presence of starch did not contribute to a higher G' in the emulsions. The presence of starch at both pH values affected the microstructure of the emulsion gels. The PF emulsions after heating were more brittle upon applied strain compared with the PPM emulsions. This brittle nature of the emulsions containing starch is attributed to the disruption of the protein oil-droplet network by the starch. Our results provide insight into emulsion gelation when using a native pea protein-starch mixture. Our study demonstrates that native protein blends with starch may increase gel strength depending on the system pH.

6.1 Introduction

Plant-based proteins are widely investigated as emulsifying and gelling agents in foods [22,167]. Cultivating plant protein sources such as peas produces about 0.3-0.4 kg CO_2 /100 g proteins compared with 10 kgCO_2 / 100-gram proteins for milk [7]. Therefore, there has been an increased interest in the transition from animal to plant proteins as part of efforts to fulfill climate change regulations [168].

Before being used in foods, plant proteins need to be extracted from their matrix. Protein extraction processes negatively impact the environmental benefits associated with plant proteins. Previous work has shown that wet extraction of pea seed proteins can consume about 30 MJ/ kg raw material instead of 15 MJ/kg in the dry separation process [26]. Also, the conventional extraction steps can lead to the loss of functional molecules such as carbohydrates [27]. Therefore, lowering the environmental impact of plant protein extraction processes remains a challenge. While optimization of protein extraction processes by using less energy-intensive steps is an important research focus, minimizing or avoiding purification steps might also be helpful to mitigate the negative impacts associated with plant protein extraction [27,169].

It has been shown that native plant protein mixtures containing non-protein molecules can function as emulsifiers and gelling agents in model food systems [36,64,84,169]. For example, native pea protein/starch mixtures contained in the unpurified pea flour were able to stabilize oil-in-water emulsions as such without the need for any purification steps [96]. Since this mixture contains both proteins and starch, it can create emulsion gels by heating. However, the influence of starch gelatinization on the gel microstructure has not been extensively investigated. Understanding the effect of starch on gel properties is necessary to use native pea flour as a structuring agent in emulsion gels.

Therefore, in this work, we investigate the potential simultaneous exploitation of proteins and starch in the native pea flour to form emulsion gels that resemble foods such as cheese and mayonnaise. The emulsifying properties of pea proteins would stabilize oil droplets, while the gelling properties of pea proteins and starch upon heating may aid in forming emulsion-gels [49,170]. We investigated the gelation behavior of pea flour (PF) and pea flour with the starch removed (pea protein mixture (PPM)) at two pH values within the range of pH used in foods. (pH 7 and pH 3). Starch was removed from PF by filtration, while

proteins are retained. The gelation dynamics as a function of temperature were followed by rheological analysis. The gel microstructure was studied using oscillatory rheology and confocal microscopy. The results provide mechanistic insight into the contribution of starch to the gelation and microstructure formation of pea protein stabilized emulsions.

6.2. Materials and Methods

6.2.1 Materials

Yellow peas were purchased from Alimex® B.V (Sint Kruis, The Netherlands). Rapeseed oil was obtained from Danone Nutricia Research (Utrecht, the Netherlands). Sodium hydroxide (NaOH), hydrochloric acid (HCl), Nile blue dye, and Rhodamine B® and Whatmann® qualitative filter paper 595 1/2 were all purchased from Sigma-Aldrich (Zwijndrecht, The Netherlands).

6.2.2 Methods

6.2.2.1 Pea Flour and Pea protein mixture preparation

Pea flour was obtained by milling and sieving yellow peas. Peas were milled using a Retsch® (Retsch GmbH, Haan, Germany) rotor mill fitted with a sieve cut-off of 80 µm. The peas were stored in the freezer at -20°C before milling. During milling, the temperature was kept below 40°C using cold water flow. The milled flour was then sieved to obtain flour particles below 45 µm using a Retsch® horizontal mechanical sieve shaker. The size of 45 µm was the smallest available sieve size, so it was used to keep particle size as small as possible. A known amount of PF was then dispersed in water, and the pH was adjusted to pH 7 or pH 3 using 0.5 M NaOH or 0.5 M HCl, respectively. The dispersion was allowed to stir for 3 hours at 300 rpm under magnetic stirring. This dispersion was further used for emulsification, known as PF dispersion.

To remove starch granules, filtration was used. A Whatman® 595 1/2 filter paper with a cut-off of 4-7 µm was used to filter under vacuum using vacuum filtration. In brief, a known amount of pea flour was dispersed in ultra-pure water and adjusted to pH 7. The dispersion was subjected to vacuum filtration in a custom-made vacuum filtration setup. The filtrate was collected and used further, known here as pea protein mixture (PPM) dispersion. Due to the removal of starch, the dry matter content in PPM dispersion was lower than the initial

PF used. However, very little protein was lost during filtration. For this study, the protein content was standardized to the same values in PF and PPM dispersions by adjusting the initial pea flour used.

6.2.2.2 Oil-in-water emulsion preparation

Pea flour dispersion and pea protein dispersion of varying concentrations were used as an aqueous phase to make emulsions. For 30 wt% oil emulsions, a dispersion containing 0.86 wt% proteins was prepared in ultra-pure water (4.3 wt% PF without filtration as PF dispersion or with filtration as PPM dispersion). Similarly, for 50wt% oil emulsion, a dispersion containing 2.0 wt% protein was prepared in ultra-pure water (10.0 wt% PF without filtration as PF dispersion or after filtration as PPM dispersion). The final protein concentrations for PF and PPM emulsions containing 10 wt%, 30 wt%, and 50 wt% oil were 0.2 wt%, 0.6 wt%, and 1.0 wt%, respectively. Previous work showed that for a 10 wt% oil-in-water emulsion, a 0.2 wt% protein concentration is sufficient to produce stable emulsions [96]. Therefore, we used this ratio to produce these emulsions in this study.

First, the protein dispersions were sheared under a high-speed rotor-stator homogenizer (IKA®) at 6000 rpm for 30 secs. Afterward, 30 wt% or 50 wt% canola oil was slowly added to the dispersion and homogenized for 1 minute at 10000 rpm. This resulted in a coarse emulsion. The coarse emulsion was further homogenized by passing through a GEA® (Niro Soavi NS 1001 L, Parma Italy) high-pressure homogenizer five times with the homogenization pressure set of 350 bars or 450 bars for 30 wt% and 50 wt% emulsions, respectively. All emulsions were made in duplicates following the same procedure and were allowed 3 hrs before further analysis.

6.2.2.3 Particles size

Droplet diameter distributions were measured using a Bettersizer S3 Plus (3P INSTRUMENTS GmbH & Co. KG, Odelzhausen, Germany) equipped with a hydro dispenser. The droplet diameter was presented as volume mean diameter $D_{4,3=}(\frac{\sum_1^n nD_i^4}{\sum_1^n nD_i^3})$.

6.2.2.4 Temperature-dependent gelation of emulsions

The temperature-induced gelation behavior of pea proteins was followed using a small amplitude oscillatory rheological test. An Anton-Paar 302 rheometer fitted with a cone-plate

geometry was used. A cone with 40 mm diameter and 4° angle was used, the cone truncation was 490 µm. The emulsions were loaded onto the bottom plate attached to a Peltier element. The top cone was lowered, and the samples were sealed with a solvent block to minimize evaporation.

After 5 minutes of idle time, a temperature sweep was applied. The temperature was raised from 20°C to 90°C at a heating rate of 3°C/min. The samples were held at 90°C for 10 minutes before cooling at 3°C/min back to 20°C. During the whole duration of the test, a constant strain of 0.5% and frequency of 6.28 rad/s was applied, and the elastic (G') and loss (G'') moduli were recorded.

6.2.2.5 Multiphoton Microscopy (MPM)

The microstructure of emulsions after heating was visualized using multiphoton microscopy. Multiphoton microscopy differs from a confocal setup in that it uses low energy near-infrared femtosecond laser. The fluorescent molecules are excited by multiple low-energy photons, enabling deeper penetration and reducing photobleaching in the samples (Larson, 2011). Therefore, MPM was used to image deeper into the dense gel samples in our study.

The emulsions (before heating) were stained with 7 µl Nile red (1mg/ml stock) for oil and 7 µl of Fast green FCF (1mg/ml stock) for protein. About 60 µL of the stained emulsions were transferred to a microscope glass slide fitted with a gene frame (Gene frame 65 µL adhesives, Thermo Fisher Scientific, United Kingdom). The gene frames were sealed with a 1.5H coverslip glass and placed in a water bath (100°C,15 min). The samples were then cooled and visualized using a multiphoton microscope.

The multiphoton microscope is a Leica confocal setup fitted with a Ti: Sapphire laser tunable from 700nm-1080 nm. The samples were imaged at a wavelength of 920 nm using a 40X water immersion objective. The emissions were captured between 480-600 nm for Nile red and 700-800 nm for Fast green. The images were processed using the accompanying Leica® confocal software.

6.2.2.6 Large amplitude oscillatory shear rheology

After measuring gel properties as a function of temperature, a 5-minute resting period at 20°C was allowed. Subsequently, the heat-set gels were analyzed using Large Amplitude Oscillatory Shear rheology (LAOS). The emulsions were analyzed in the same cone-plate geometry. An increasing strain amplitude from 0.1 % up to 1000% was applied at 6.28 rad/s frequency. The elastic and loss moduli were recorded as a function of time.

Also, the raw oscillatory strain data from each point of the strain sweep was recorded, and the waveform data was used to plot Lissajous plots. The Lissajous plots were plotted as stress vs. strain to obtain loops. These Lissajous plots provide further information about the microstructure of the emulsion-gels by recording their breakdown characteristics.

The area enclosed within the Lissajous curves represents the dissipated energy per unit volume during an oscillatory cycle. This area thus represents essential information from the Lissajous plots, as it reflects the loss of viscous energy at a given strain amplitude. When dividing this dissipated energy over the energy dissipated by ideal plastic material, the energy dissipation ratio (DR) is obtained [171]. The energy dissipation ratio can be calculated from the following equation:

$$\mathrm{DR} = \frac{\mathrm{E_d}}{(\mathrm{E_d})_{\mathrm{pp}}} = \frac{\pi \mathrm{G}^{"} \gamma_0}{4\sigma_{\max}} \qquad \text{Equation 6.1}$$

with G" is the loss modulus and $\sigma_{\max}$ is the maximum stress at an applied strain amplitude γ_0. E_d is the energy dissipated by the material, and $(E_d)_{pp}$ is the energy dissipated by a perfect plastic material. The energy dissipation ratio was plotted as a function of the strain amplitude. The energy dissipation curves provide compact information on the transition of the material from a predominantly elastic to predominantly viscous behavior.

6.3 Results and Discussion

Pea flour (PF) and pea protein mixture (PPM) were dispersed at an aqueous system at pH 7 and 3 and heated. A 3 wt% protein dispersion was chosen to study this behavior since this protein concentration (and pea flour concentration) gels sufficiently to be detected by the rheological measurement and is in the range used to stabilize emulsions. Lower protein concentrations did not provide sufficient gelling upon temperature to be studied, so they

are not shown in the figures. The results of the gelling behavior of the dispersions are shown below in **Figure 6.1**.

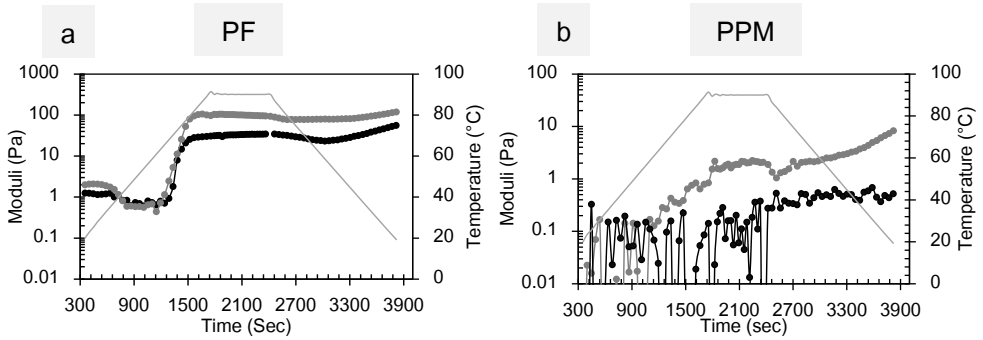

Figure 6.1: Elastic modulus (G') as a function of time measured during temperature ramp up from 20°C to 90°C holding for 10 min and ramp down to 20°C at a rate of 3°C/min for (a) Pea flour (PF: 3 wt% protein + 7.5 wt% starch) at pH 7 (—) and pH 3 (—) ; (b) Pea protein mixture (PPM: 3 wt% protein) at pH 7 (—) and pH 3 (—).

Figure. 6.1.a shows G' evolution for PF dispersions at pH 7 and pH 3 upon heating. At pH 7, before heating, the G' value was around below 0.1 Pa and was lower than G'' (not shown). Therefore, the dispersion at pH 7 was liquid-like before heating. Upon heating, the G' value increased and reached about 50 Pa at the end of the heating cycle. At pH 3, before heating, the G' was below 0.1 Pa and was below G'', indicating a liquid-like response. The G' value reached around 20 Pa at the end of the heating and cooling cycle. Before heating, both PF and PPM dispersions were liquid, and G' was lower than G'' (not shown). However, as the temperature reached about 60°C, G' values increased sharply, and the dispersions became gel-like with G' higher than G''. The steep increase around 60°C can be related to pea starch gelatinization [172]. Above this temperature, starch granules take up water and swell, leading to loss of crystallinity and eventually to leaching of amylose polymers [49]. Since starch is the major constituent in these systems, gelatinization plays a significant role in increasing G'.

Figure. 6.1.b shows the temperature sweep results for PPM dispersions at pH 7 and pH 3. Before heating, the PPM dispersions were liquid-like and did not have any measurable visco-elasticity (G' < G'' and noisy data). G' values gradually increased when the heat was applied, and the dispersions showed weak-gel-like behavior above 70°C (G' > G'').

However, the increase in G' was gradual for both samples and did not show a steep increase at 60 °C.

The final G' value for PPM dispersions at the end of the heat treatment was lower (0.6 Pa for pH 7 and 9 Pa for pH 3) than that of PF (20 and 50 Pa). In PF, starch gelatinization had a large impact on the G'. In PPM, the small increase in G' can be mainly attributed to protein denaturation and protein network formation [162]. In PPM gels, only ~ 3 wt% proteins were present, and to form strong protein gels, higher protein concentrations (> 7 wt%) are required to form self-supporting protein gels [170]. Overall, the gelation of the dispersions shows that starch gelatinization contributes to increasing G' in the dispersions.

To assess the emulsion-gelation behavior, oil-in-water emulsions were stabilized using both PF and PPM dispersions. Two oil concentrations of 30 wt% in the low-oil regime stabilized with 0.6 wt% protein (final) and 50 wt% in the mixed regime stabilized with 1.0 wt% protein (final) were chosen. Due to similar protein content in both PF and PPM stabilized emulsions, the effect of protein on gelation is expected to be similar for both samples. Therefore, any possible differences in the gelation behavior could be attributed to starch present in pea flour.

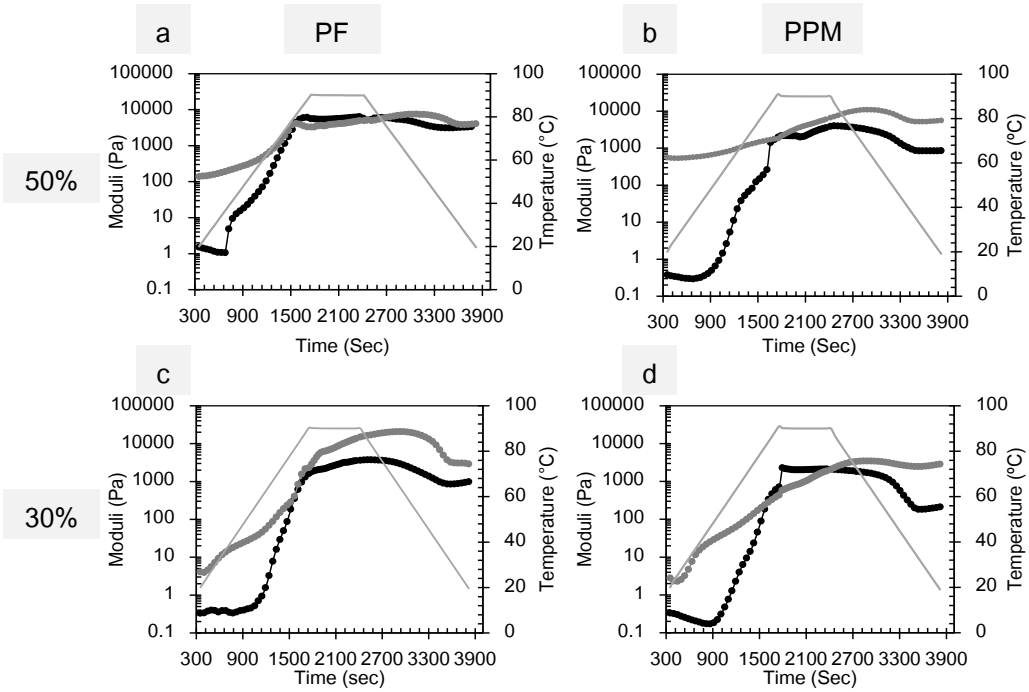

Figure 6.2: Elastic modulus (G') as a function of time measured during temperature ramp up from 20°C to 90°C holding for 10 min and ramp down to 20°C at a rate of 3°C/min for (a) Pea flour stabilized 30 wt% emulsion (c) Pea flour stabilized 50 wt% emulsions (b) PPM stabilized 30 wt% oil emulsion and (d) PPM stabilized 50 wt% oil emulsion. Emulsions at pH 7 (black) and pH 3 (gray).

Figure 6.2 shows the G' value as a function of time during temperature sweep for 30 wt% (bottom panels) and 50 wt% (top panels) emulsions stabilized by PF (left panels) and PPM (right panels). The plain grey line in the plots represents the temperature evolution also as a function of time.

Figure 6.2.a shows gelation behavior of 50 wt% oil emulsion stabilized with PF. At pH 7 (black curve), before heating, the G' value was around 2 Pa and was higher than G''(data not shown). A higher G' than G'' before heating showed that the emulsion was already a gel. Upon heating, the G' value increased from about 2 Pa to about 2000 Pa, with a sharp increase starting around 35-45°C. At pH 3 (gray curve), before heating, the G' value was about 200 Pa and was higher than G'' (data not shown). G' > G'' indicates that the emulsions at pH 3 were also a gel before heating. The G' value increased from 200 Pa to

about 3000 Pa after heating with a gradual increase in G' starting at about 30°C. Above 80°C, G' remained stable until cooled back down to 20°C.

Figure 6.2.c shows the gelation behavior for 30 wt% oil emulsion stabilized with PF. At pH 7 (black curve), the emulsions had a G' of 0.5 Pa, while emulsions at pH 3 had a higher G' of 5 Pa. At both pH values, G' increased sharply starting around 30-45°C. Overall the 30 wt% PF emulsion follows the same pattern as the 50 wt% oil PF emulsion.

Before heating, G' value of PF emulsion at pH 3 was higher than at pH 7. Upon heating, at both pH values, the G' increase started at a much lower temperature (30-45°C) than the starch gelatinization temperature seen in the PF dispersion (> 60°C). Therefore, the G' increase is not related to starch granule gelatinization. An increase in G' at lower temperatures has been reported for protein stabilized emulsion gels [173], attributed to aggregation and rearrangement of oil droplets at 40-50°C [174,175].

Figure 6.2.b shows the emulsion gelation for 50 wt% oil PPM emulsions at pH 7 (black) and pH 3 (gray) as a function of time. At pH 7, the G' value before heating for emulsions was about 0.5 Pa. Upon heating, a sharp increase in G' is seen at about 40°C and reaches about 800 Pa after heating. For emulsions at pH 3, before heating, the G' is about 800 Pa and G' is higher than G''. Therefore, before heating, emulsions at pH 3 form stronger gel compared with pH 7. Upon heating, a gradual increase in G' values occurs at a temperature of about 35°C and continues throughout the heating cycle. During this period, the G' increases from about 800 Pa to about 2000 Pa after heating. The final G' of emulsions at pH 3 is higher than that of emulsions at pH 7.

Figure 6.2.d shows the gelation behavior of 30 wt% oil PPM emulsions. The G' value for pH 7 was lower (0.4 Pa) than for pH 3 emulsion (10 Pa). Moreover, both emulsions increased in G' upon heating starting around 30°C. Overall, the final G' for 30 wt% emulsions was lower than 50 wt% PPM emulsions at their respective pH. Higher G' with higher oil content indicates the active role played by the droplets in forming emulsion gels [173]. However, no differences in gelation dynamics are seen for 30 wt% emulsions compared with 50wt% emulsions.

Overall, both PF and PPM emulsions show different rheological properties for pH 3 and 7. Before heating, both PF and PPM emulsions at pH 7 were weaker gel (lower G') compared to emulsions at pH 3. This could be attributed to the behavior of proteins in these pH values.

Previous research has shown that the higher viscosity and gel strength are due to the formation of protein particles at pH 3 due to non-covalent interactions [163].

The PF emulsion and PPM emulsion show similar gelation behavior with an increase in G' at around 40°C. This temperature at which G' increases is much lower than starch gelatinization (60°C) and protein denaturation in aqueous phases (75°C). Moreover, the similar gelation dynamics of PF and PPM emulsion show that the gelation is most likely initiated at lower temperatures by droplet aggregation in both cases. The aggregation is most likely caused by interactions between proteins at the oil droplet interface and proteins in the bulk and proteins in other oil droplets. Similar observations have also been made for soy protein stabilized emulsions [174]. After heating, differences in gel strength between PF and PPM emulsion were observed at pH 7. The 50 wt% PF emulsion showed a higher G' (2000 Pa) than the PPM emulsion at pH 7 (800 Pa). However, the same effect was not seen in the emulsions at pH 3. So, starch gelatinization increases gel strength only at pH 7 and not at pH 3.

The gelation dynamics for the emulsions were also affected by pH. The emulsions at pH 7 showed a sharp increase in G' upon heating between 35-50°C, while emulsions at pH 3 showed a relatively gradual increase in G'. The difference could be attributed to the difference in the gel strength before heating. Emulsions at pH 7 form a weaker gel prior to heating than pH 3, caused by protein aggregation at pH 3 [163]. Therefore, oil droplets at pH 3 form a stronger gel that shows a relatively smaller increase resulting in slow rearrangement of droplet aggregates upon heating.

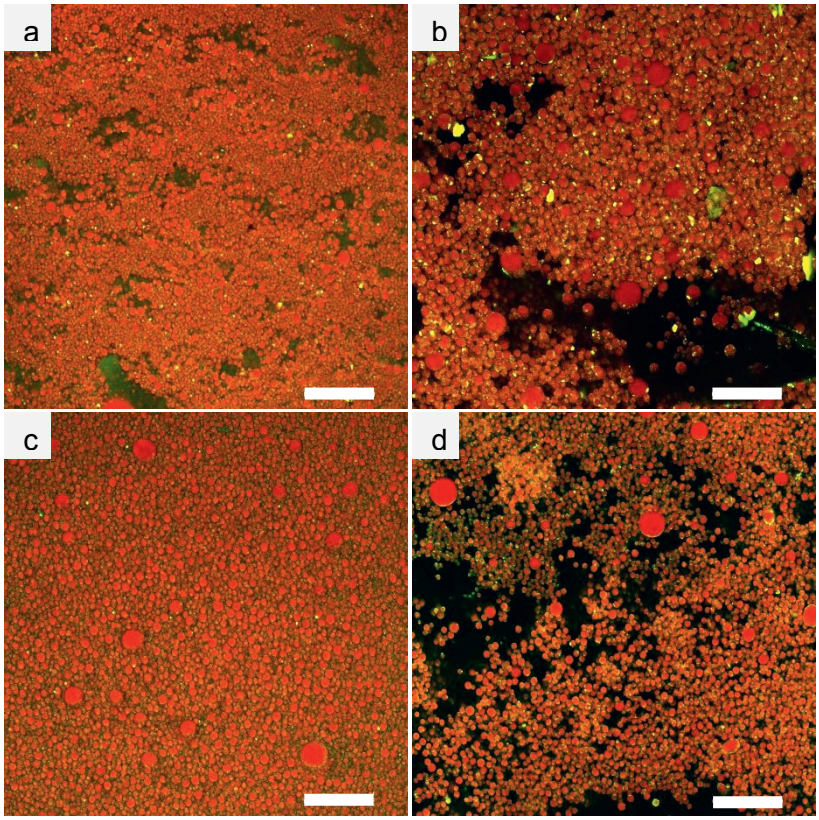

Figure 6.3: Confocal micrographs of 50 wt% oil emulsions after heating and subsequent cooling, stabilized with (a) Pea flour (PF) at pH 7, (b) PF at pH 3, (c) Pea protein mixture (PPM) at pH 7, (d) Pea protein mixture (PPM) at pH 3. Oil stained in red and protein in green. Scale bar: 50 µm.

The confocal micrograph was used to visualize the emulsion microstructure after heating the emulsions. **Figure 6.3** shows representative confocal images of 50 wt% oil emulsions stabilized with PF and PPM at pH 7 and 3. Oil droplets are shown in red, and proteins are shown as green fluorescence. In all the four emulsions after heating, the oil is still present as intact oil droplets, indicating the emulsions were stable upon heating.

Figure 6.3.a and **Figure 6.3.b** show the emulsion-gels of pea flour emulsions at pH 7 and pH 3, respectively. At pH 7, the oil droplets are evenly spread across the space and are closely packed with small gaps in between. At pH 3, the oil droplets seem to be densely aggregated with a lot of free space in between. The microstructure indicates that at pH 7, a more homogeneous gel is formed compared with emulsions at pH 3. **Figure 6.3.b** and **Figure 6.3.d** show the emulsion-gels after heating PPM emulsions at pH 7 and 3,

respectively. At pH 7, the oil droplets in the PPM emulsions are also evenly spread throughout the space. The oil droplets are in close contact with one another. At pH 3, the PPM emulsions also show that the oil droplets form patches on dense aggregates with empty spaces in between.

The gelation dynamics and microstructure analysis indicate that G' increases due to oil droplets rearrangement in all the emulsions, and starch plays a minor role. However, the microstructure of the material might still be affected by the presence of starch in the emulsions. Therefore, to further assess starch's effect on the microstructure, oscillatory shear rheology was applied to 50 wt% oil emulsions stabilized with PF and PPM.

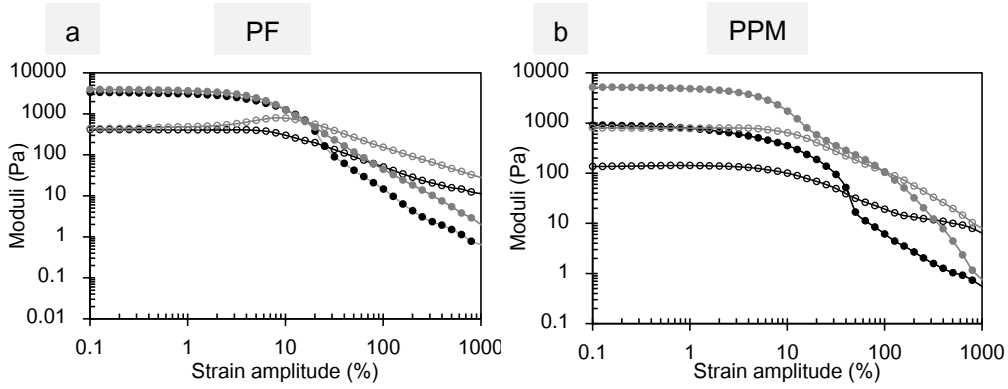

Figure 6.4: Strain sweep showing G' (filled symbols) and G'' (unfilled symbols) measured at 20°C after temperature sweep test for (a) 50 wt% oil PF stabilized emulsions at pH 7 (black) and pH 3 (gray), respectively and, (b) 50 wt% oil PPM stabilized emulsions at pH 7 (black) and pH 3 (gray).

To investigate the gel microstructure after heating, an oscillatory strain sweep was employed. **Figure 6.4** shows the G' (filled symbols) and G'' (unfilled symbols) values as a function of strain amplitude for 50 wt% oil PF and PPM emulsions at pH 7 and pH 3.

Figure 6.4.a shows the strain sweeps of emulsion gels 50 wt% oil PF emulsions at pH 7 (black) and pH 3 (gray). At pH 7, the G' values for the emulsion at low strain is around 3000 Pa and G'' is about 600 Pa. Higher G' than G'' up to 10% strain, indicates the formation of a solid viscoelastic emulsion-gel. Above 10% strain, the G' of the emulsions starts to decrease, and around 25% strain, the G' value drops below the G'' value, indicating a more liquid-like response. At pH 3, the G' value of emulsions is also 3000 Pa at low strains, and

with increasing strain, the G' decreases gradually. At about 20% strain, the emulsion at pH 3 becomes viscous as G'' becomes higher than G'.

The gel strength is similar for both emulsions at pH 7 and 3, which shows that both emulsions form equally strong emulsion-gels upon heating. However, for emulsions at pH 3, the G'' shows a slight local increase at about 15% strain. Such an increase is termed a weak strain overshoot (or type III behavior; [176]) and implies that the rate of network bond creation and breakage both increase with strain amplitude, but the latter increases faster. The initial overshoot results from the reformation of clusters, and the subsequent decrease at higher amplitude results from larger-scale rearrangements. No such increase in G'' is observed for emulsions at pH 7, which shows Type I behavior in which both G' and G" smoothly decrease [176].

Figure 6.4.b shows the strain sweeps of PPM emulsions at pH 7 (black) and pH 3 (gray). Also, in PPM emulsions, the G' (1000-5000 Pa) values were higher than the G'' (200-1000 Pa) at low strains (<10%). The higher G' value indicated a solid viscoelastic emulsion-gel was formed after heating. In PPM emulsions at pH 7, the G' value remained constant and higher than G'' up to about 1% strain. Above 1% strain G' gradually decreased and around 40% strain, G' decreased below G'' indicating a transition to a liquid-like response. At pH 3, G' was higher than G'' up to 5% strain. As strain increased above 5%, G' decreased and eventually above 100% strain, became lower than G''.

The emulsion-gels made with PF and PPM at pH 7 showed differences in their strain-dependent behavior. At low strains, PF emulsions had a higher G' value compared with PPM emulsion. Higher G' in the starch-containing emulsion-gel indicated that the starch might play a role in increasing gel strength. However, in emulsions at pH 3, there were no differences in G' value between PF emulsions and PPM emulsions. This difference based on pH could be attributed to the initial nature of the emulsions before heating. In emulsions at pH7, a weak emulsion-gel is present before heating. Therefore, upon heating, the gelatinization of starch contributes to increasing the overall gel strength. However, at pH 3, the emulsions are already stronger gels, possibly due to droplet-droplet interaction. Therefore, at pH 3, the gel strength is dominated by droplet-droplet interaction, and starch gelatinization plays no noticeable role in increasing gel strength (G').

Strain sweep plots do not show any possible effect of starch on the microstructure of the emulsions upon heating. Therefore, to further understand the effect of starch on the microstructure of the emulsion-gels, Lissajous plots were plotted from the strain sweep experiments. **Figure 6.5** shows the elastic Lissajous plots, plotted for 5 strain amplitudes as a stress v strain plot [143]. The stress and strain values are normalized to 1 by dividing them by the corresponding maximum value. The elastic stress contribution is also plotted as a grey dotted lines within the loops.

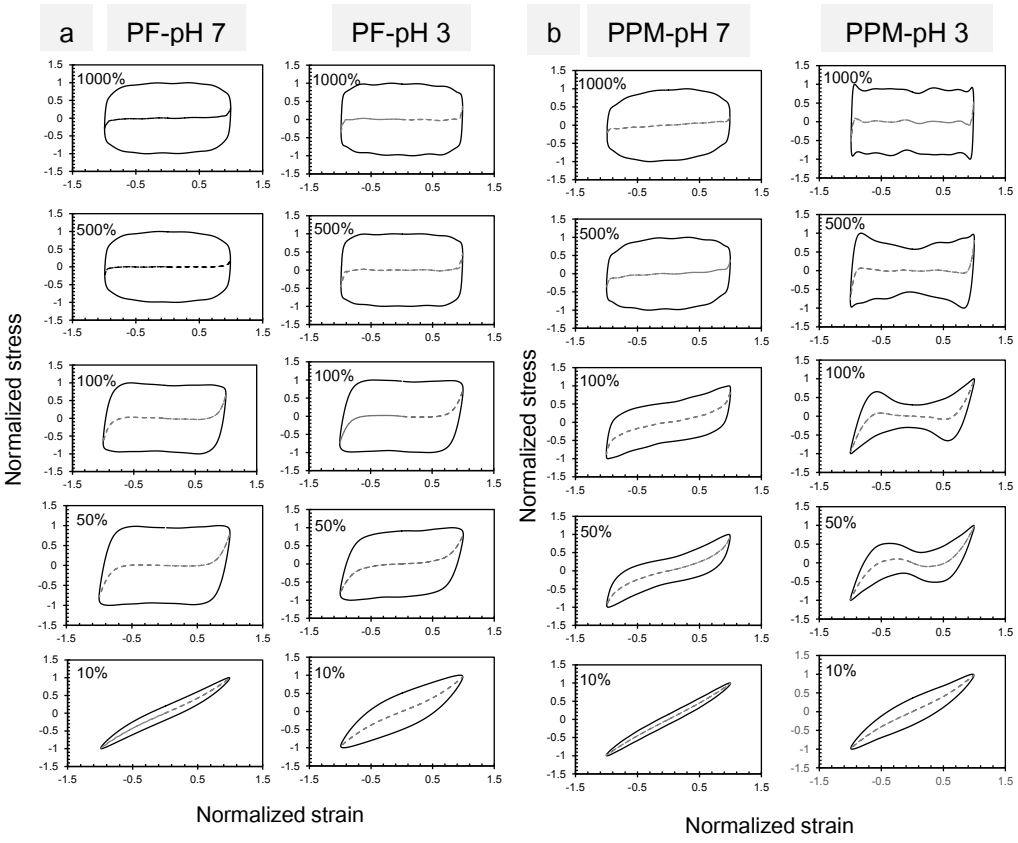

Figure 6.5: Lissajous plots obtained from waveform data of the strain sweeps of 50 wt% oil emulsion stabilized by (a) Pea flour (PF) at pH 7 and pH 3; and (b) Pea protein mixture (PPM) at pH 7 and pH 3; at 10%, 50%, 100%, 500% and, 1000% strains (with arrows pointing to stress overshoots).

Figure 6.5.a shows the Lissajous plots of 50 wt% PF at pH 7 and pH 3 for strains of 10%,50%,100%, 500% and 1000%. At pH7, at 10% strain, the PF emulsion gel shows

narrow plots, with a small deviation from an elliptical shape. The elastic contribution to the stress (the dashed line) shows a very mild upswing near maximum strain. Such a shape indicates a near-linear visco-elastic response from the material [144]. As the strain increases to 50% and 100%, the response of the emulsion gels abruptly changes to a rectangular shape with rounded corners. Such a shape indicates a plastic material response with a higher viscous contribution [177]. Above 100% strain, the emulsion gels show a rounded loop, with a near-zero elastic contribution for almost the entire loop, indicating a predominantly viscous behavior.

For emulsions at pH 3, at 10% strain, the loops of the emulsions are significantly wider and have a more deformed elliptical shape than PF at pH 7. The relatively higher viscous contribution coincides with the weak strain overshoot in G" we see in **Figure 6.4**. As the strain increases to about 50 and 100% strains, rounded rectangular loops are seen. Overall, the breakdown of PF emulsion gels at pH 7 and pH 3 are similar with a transition from near-linear behavior at 10% strain to plastic behavior at 50%, and above 100% strain, their response becomes predominantly viscous.

Figure 6.5.b shows the Lissajous plots of 50 wt% emulsion gels stabilized with PPM at pH 7 and 3. The evolution of the loops from 10% to 1000% strains for both systems can be seen. For PPM emulsions at pH 7, at 10% strain, a narrow-elongated loop can be seen. The loops are significantly narrower than those of emulsion gels prepared with PF. Such a shape points to a linear visco-elastic material response, dominated by the elastic contribution. As the strain increases to 50% and 100% strain, the response gradually changes to a more rhomboidal shape, with a larger enclosed area than 10% strain. In this strain range, the PF emulsion gels already showed plastic behavior. The PPM emulsion gels retain more elasticity, which is also evident from the nonzero slope of the elastic contribution around zero intracycle strain. Above 100% strain, a rounded rectangular plot is seen, and the response becomes predominantly viscous.

PPM emulsion gels at pH 3 behave similarly to those prepared at pH 7 at 10% strain but with a relatively larger viscous contribution. However, at 50% and 100% strain, the shape of the loop becomes increasingly distorted. The widening of the loop indicates a relative increase in the viscous contribution to the response of the material. At 50% and 100% strain, the loops show overshoots in the total stress (see arrows) and in the elastic contribution to the stress (dashed lines). At the lower-left and upper-right corners, the

direction of strain reverses, and the strain rate is zero, leading to a stress build-up in the material. As the strain proceeds, the material possesses elastic contacts, which increases both the total stress and the elastic stress contributions (see arrows). The increase in stress proceeds until a yielding is observed, indicated by the gradual change in slope of the total stress (curved corners). Upon a further change in stress, the material stress decreases. The drop in total stress as the strain sweep proceeds signals a shear-thinning behavior under the applied frequency.

Moreover, the overshoot in the total stress is significantly higher than the overshoot in the elastic stress, indicating a significant shear thinning in the predominantly viscous phase of the response. A similar overshoot in elastic stress at 50% and 100% strain was also observed for non-heated pea protein stabilized emulsions at pH 3 [163]. At this pH, about 50-60% of the proteins are present in the form of particles. These protein particles are formed through attractive protein-protein interactions, which creates adhesive interaction between oil droplets resulting in increased elastic bonds between the oil droplets. In such a case, the emulsion shows a stress-overshoot behavior, indicative of the breakage of the additional interactions [163]. Above 100% strain, the material becomes viscous dominated, showing rectangular loops with sharp corners.

Overall, the breakdown of PPM emulsions at pH 7 and 3, with a gradual transition from the elastic response at 10% to viscous response at 500%. Emulsions at pH 3 also showed the presence of stronger interactions between droplets in the medium amplitude regime, while at pH 7 no such interactions were present.

The Lissajous analysis shows clearly emulsion-gels with starch and without starch form different microstructures. At both pH values, in the presence of starch, more brittle gels with an abrupt breakdown are formed, while in the absence of starch, more cohesive gels are formed. We hypothesize that starch gels are formed partially upon heating, which disrupts the formation of a continuous droplet network. Starch gels containing higher amylose content are known to break down abruptly upon strain [177]. Therefore, the breakdown mechanism in the PF emulsion gels is dictated by the breakdown of starch gels.

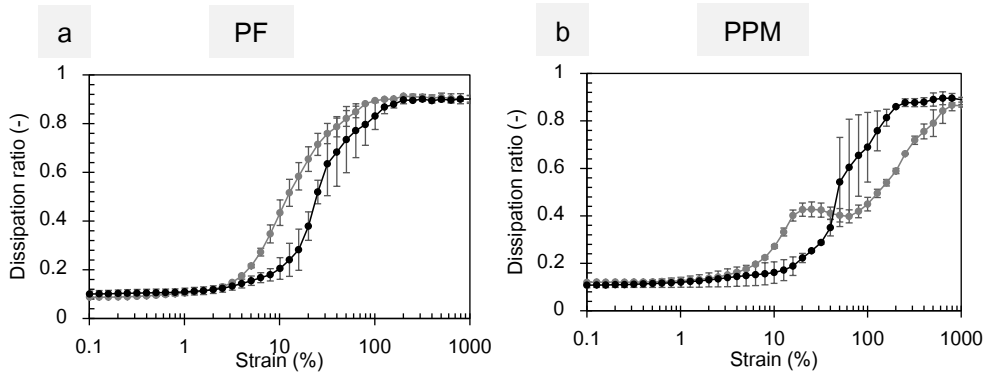

Figure 6.6: Dissipation ratio as a function of strain measured at a constant frequency of 6.2 rad/s of (a) 50 wt% oil emulsion stabilized by PF at pH 7 (—) and pH 3 (—); (b) 50 wt% oil emulsion stabilized by PPM at pH 7 (—) and pH 3 (—).

A more compact way of interpreting the non-linear breakdown mechanism of the emulsion-gels is to plot the dissipation ratio (DR) as a function of strain amplitude. DR represents the ratio of viscous to elastic response of the material upon the strain. The DR value lies between 0 and 1, with the lower values indicate an elastic response and the higher values indicate a viscous response [178]. DR as a function of strain can provide insights into the microstructural transition from elastic to viscous dominated material response [145]. **Figure 6.6** shows the DR plotted as a function of strain for 50 wt% oil emulsions stabilized by PF (**Figure 6.6.a**) and by PPM (**Figure 6.6.b**).

Figure.6.6.a shows the DR for PF as a function of strain at pH 7 (black) and pH 3 (gray). At pH 7, at strains below 2%, the emulsion-gels exhibit a plateau of about 0.1. The low DR value at low strains indicates a predominantly elastic material response. As the strain increases, DR increases gradually to about 0.2 at 10% strain. Upon further increase to medium strain, the DR value increases to about 0.9 at 200% strain, indicating a viscous response. At pH 3, the DR value of PF emulsion is about 0.1 at strains below 2%. As the strain increases, the DR value increases and reaches above 0.2 at 4% strain. Eventually, with increasing strain, the DR value increases, indicating the material becomes more viscous. Above 100% strain, the DR value reaches about 0.9, indicating a predominantly viscous behavior [145]. At pH 3, the increase in DR occurs at smaller strains than at pH 7. The faster breakdown shows that PF emulsions at pH 3 show a more brittle response than

at pH 7 at intermediate strains. The observation also aligns with the homogenous microstructure seen in confocal micrographs of the emulsions at pH 3 (**Figure 6.3.b**).

Figure 6.6.b shows the DR ratio as a function of strain for 50 wt% oil emulsion stabilized by PPM at pH 7 and 3. At pH 7, the DR curve is around 0.1 and does not change much to about 5% strain. Above 5% strain, the DR value increases and reaches about 0.9 at about 200% strain. At pH 3, at low strains below 5%, the DR value remains at 0.1 as the strain increases above 3%, the DR value increases. Upon further increase in strain, the DR value reaches 0.9 above 200% strain. In PPM emulsions, the DR value increases at lower strain for emulsions at pH 3 compared with pH 7. This indicates that the emulsions at pH 3 are more brittle than pH 7. This observation also aligns well with the microstructure images of the PPM emulsions (**Figure 6.3.c&d**). The PPM emulsions at pH 7 showed homogenous droplet distribution, while at pH 3, dense droplet regions and empty spaces co-existed.

Moreover, the DR of PPM emulsion at pH 3 has a two-mode breakdown. In the medium strain region (20%-100%), a local peak in DR is noticeable. The PPM emulsion at pH 3 consists of protein particles, which create additional droplet-droplet interactions. Therefore, the bump in DR could indicate a two-mode breakdown of the emulsion. The first mode is the breakage of attractive droplet-droplet interactions, and the second is the macroscopic yielding and flow of the emulsion-gel [138]. In the DR of the emulsion-gel (gray line), the DR value increases from 6% strain to about 20% strain, indicating an increasing plastic contribution due to strain. During this period, the material is strained and does not break down or yield, and the elasticity is retained possibly by droplet-droplet contact. As medium strains between 20%-100% are applied, the interaction between oil droplets is broken, indicated by a stable DR value (change in slope). Even though the droplet interactions are broken, the oil droplets are surrounded by neighboring oil droplets known as a cage, and the emulsion does not yield. A relatively stable DR value indicates this caged stage between 50-100% strain. Upon further increase in strain, the second breakdown mode is initiated, indicated by the increase in DR value. The DR value increase corresponds to the breaking of the oil droplet cage and subsequent yielding or flow of the emulsion gel. A similar two-mode yielding behavior has been observed for weakly attractive emulsion-gels [138].

When comparing PF and PPM emulsions, the increase in DR occurs at lower strains for PF emulsions compared with PPM emulsions. This faster increase in DR in PF emulsions

indicates that PF emulsions show an abrupt increase in viscous contribution compared with PPM emulsions. Moreover, the PF emulsions at both pH values are brittle compared with PPM emulsions at each pH. Therefore, it is clear that starch creates a brittle gel network at both pH values in the emulsions upon heating.

Overall, our results from the temperature-dependent gelation dynamics show that the emulsion gelation is dominated by oil droplet interactions and rearrangements for all the emulsions, whether they contain starch or not. Starch contributed to the gel strength (higher G') at pH 7, while at pH 3, no effect of starch was seen. The emulsion-gels formed in the presence of starch broke down at lower strains and more abruptly, possibly due to the formation of inhomogeneous matrix containing patches of starch-gels between droplet-network. It is worth noting that, in our study, native protein-starch mixtures were used, so the starch to protein ratio was fixed (2.5:1). However, adding more starch to the system could further increase gel strength at pH 7 or modify the microstructure further and be explored in future research.

6.4 Conclusions

In this study, we investigated the heat-driven gelation and microstructural properties of emulsions stabilized by pea proteins in the presence of starch and without. The effect of starch was studied by preparing emulsions stabilized with pea protein mixture, which was obtained after removing starch by filtration. In all the emulsions, G' increased at 40°C, which is below the starch gelatinization (60°C) and protein denaturation temperatures (> 70°C). The increase in G' at 40°C occurred due to droplet-droplet aggregation and rearrangement due to heating. The influence of starch depends on the pH of the emulsions. At pH 7, starch increased gel strength and led to a gel matrix that broke down more abruptly and at lower strains than PPM emulsions. At pH 3, starch did not increase gel strength but led to a gel that broke down more abruptly at lower strains than PPM emulsion. Our results clearly show that starch plays a limited role in increasing gel strength, while they play an important role in modifying microstructure into one which breaks down abruptly at low strains. Our results provide insight into the microstructural and rheological properties of pea protein-starch mixtures in emulsion gels. The results

could provide a design guide for producing food materials with desired mechanical properties based on pea protein-stabilized emulsions.

Chapter-7: General discussion

7.1 Main findings

7.1.1 Overview

Peas are starch-rich seeds containing about 50 wt% starch along with about 20 wt% protein. Pea proteins are used as emulsifiers and gelling agents in food products. Before their use, in general, the proteins are extracted through an alkaline aqueous extraction process aiming to produce purified protein extracts with 70-90 wt% protein purity. The extraction process involves multiple steps and consumes about 30 MJ/kg material processed. Therefore, a more straightforward extraction process with fewer steps or no protein purification (i.e. using pea flour as such) could improve the protein purification process, from an energy consumption perspective. For instance, using pea flour would reduce the process related energy consumption from 30 MJ/kg pea processed to 10-12 MJ/kg pea processed [26]. However, when less purification or no purification is used, proteins are obtained in mixtures with 20-60 wt% protein purity, together with non-protein components such as starch, fibers and oil. Consequently, to use simpler protein purification processes, the interfacial properties of pea protein mixtures and rheological properties of emulsions stabilized with protein mixtures need to be investigated. The primary aim of this thesis was to create a mechanistic understanding of the interfacial properties of pea protein mixtures and the mechanical (rheological) properties of emulsions stabilized with pea protein mixtures.

In pea protein mixtures, the primary component of interest in terms of emulsifying and gelling functionality are proteins, so most of this thesis focused on these functionalities of pea proteins. In these protein mixtures, also significant amounts of non-protein molecules such as starch could be present. The effect of starch on the emulsion rheological properties and the emulsifying functionality of proteins were investigated. This thesis is divided into two major research lines based on the research focus on purified proteins and protein mixtures.

The first research line of the thesis focuses on understanding the interfacial and emulsifying properties of purified pea proteins extracted by the alkaline extraction process. **Chapter-3** and **Chapter-4** deal with the understanding of purified pea proteins. In these two chapters, the emulsifying mechanism of pea proteins at acidic pH and the emulsion rheological properties at acidic and neutral pH values were mechanistically understood. The second

research line uses the knowledge generated in the first research line to understand the functionality of protein mixtures as emulsifiers. **Chapter-2, Chapter-5,** and **Chapter-6** deal with pea protein mixtures as functional emulsifying and gelling agents. In this research line, we investigated the emulsifying behavior and emulsion rheological properties (structuring behavior) of pea protein mixtures containing large amounts of starch at neutral and acidic pH values.

To obtain fundamental insights into the behavior of purified proteins and protein mixtures, we investigated molecular properties such as solubility, surface charge, and composition and linked them to the interfacial activity and interfacial rheological properties. The protein-protein interaction in the aqueous and oil-water interface driven by pH was also investigated. From the fundamental understanding, the link between molecular properties and emulsion rheological and microstructural properties were mechanistically understood. Using this approach, we deliver design principles to produce food products using pea protein mixtures.

7.1.2 Conclusions

Conventionally, purified plant proteins are used as functional ingredients. In this thesis, we challenge the status quo of using purified plant proteins as emulsifying and structuring agents. So we started with investigating the emulsifying properties of native unpurified pea flour (**Chapter-2).** To obtain pea flour, peas with 50 wt% starch and 20 wt% protein were milled into a fine powder (pea flour - PF) and were tested for their interfacial and emulsifying properties. To understand the effect of protein purity, pea flour (PF) was compared with pea protein mixture, obtained by filtration of PF to remove starch granules while retaining the proteins. The pea protein mixture (PPM) contained 55 wt% proteins and about 5 wt% starch. Both PF and PPM were able to reduce interfacial tension similarly compared with what has been reported for purified proteins. The interface was stabilized by a visco-elastic protein network in both PF and PPM.

Additionally, model oil-in-water emulsions were prepared with 10 wt% oil at pH 7, and the emulsifying ability of pea flour was assessed. The emulsions showed decreased droplet size with increased protein concentration, and both PF and PPM stabilized emulsions showed similar viscosities at similar average droplet size. The results clearly showed that proteins mainly drove the interfacial activity in this native mixture. The non-protein

molecules, including starch, did not negatively hinder the emulsifying property of pea proteins. The findings from this chapter, show that for the investigated systems protein purification is not necessary for using pea proteins as emulsifying agents.

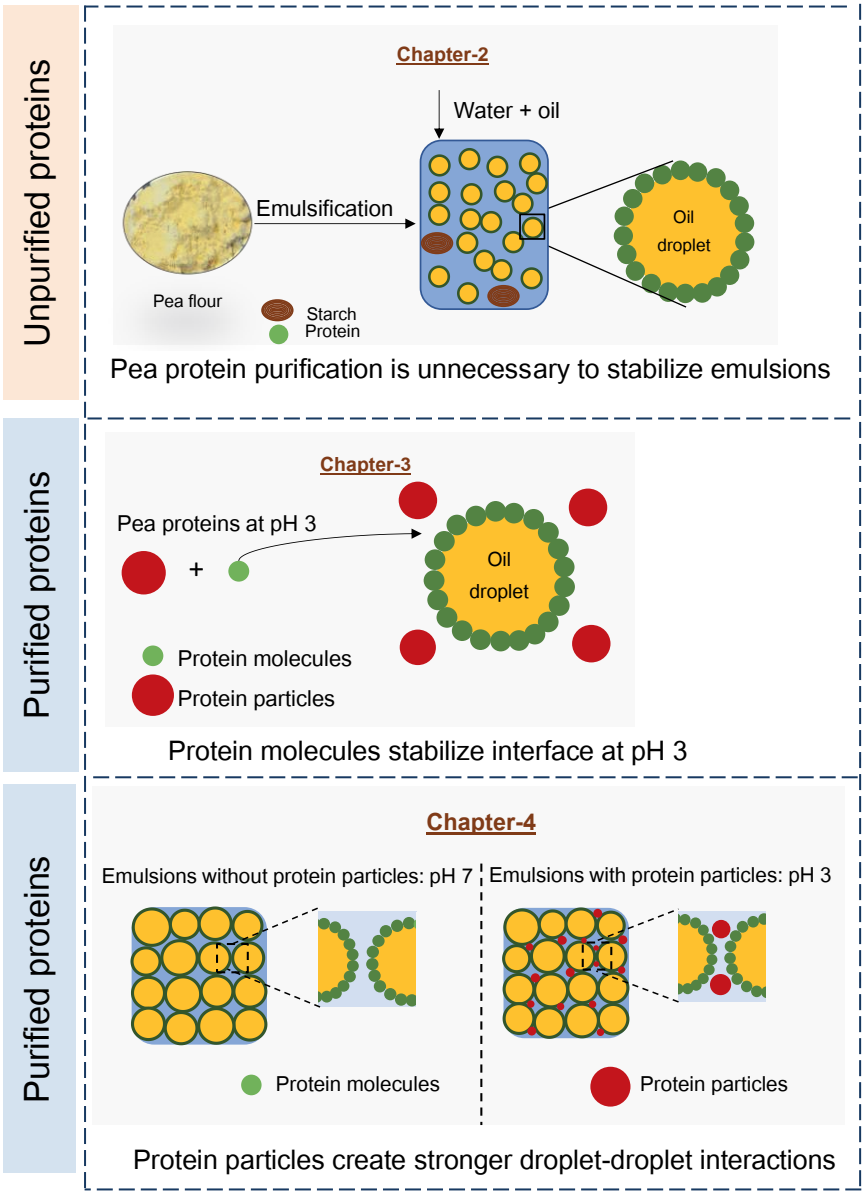

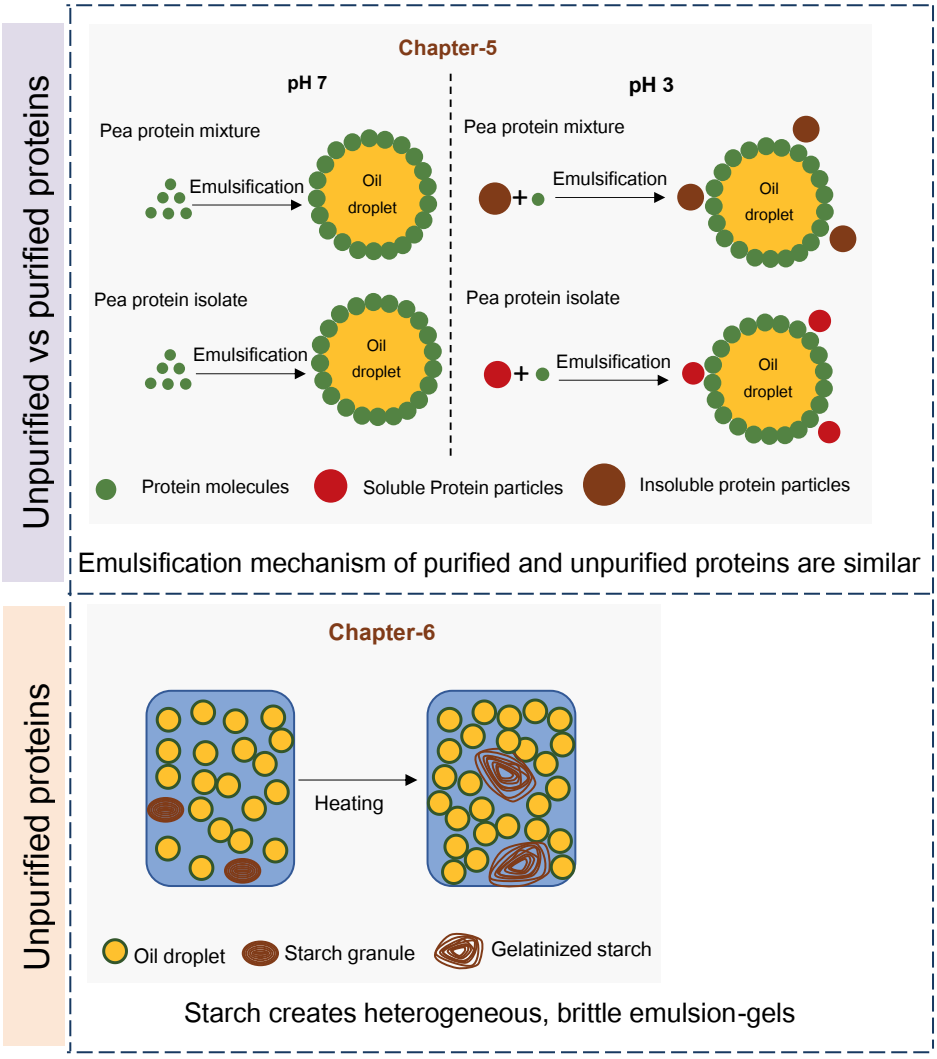

Figure 7.1: Thesis chapters and main findings.

For food applications, it is essential to assess the emulsifying and interfacial properties of proteins at both neutral and acidic pH. Emulsifying behavior of pea proteins at acidic pH is not well understood. Thus, before investigating the properties of unpurified protein mixtures, a fundamental understanding of purified pea proteins was necessary. Therefore, in **Chapter-3,** we investigated the interfacial and emulsifying properties of alkaline extracted pea protein isolates (85 wt% protein purity). First, the behavior of pea proteins at pH 3 was investigated. The proteins formed self-assembled particles at acidic pH and co-existed with protein molecules. When such a mixture is used to stabilize emulsions, the

protein molecules stabilize the oil droplet interface while the protein particles do not take part in this stabilization. This result is important since, it fills an essential knowledge gap, by revealing the mechanism of emulsification by pea proteins at pH 3. Further the role of the non-adsorbed protein particles on the bulk emulsion properties were investigated (**Chapter-4)**. We investigated the bulk properties of emulsions when self-assembled particles were present (pH 3) compared to when self-assembled particles were absent (pH 7). To do this, jammed oil-in-water emulsions containing 70 wt% oil were prepared, and their rheological properties were assessed. The emulsions behaved like an elastic gel system with a jammed microstructure in the absence of protein particles. Whereas when protein particles were present, the emulsions acted as a firmer gel with elastoplastic material properties.

Further rheological analysis revealed that protein particles were able to stick the oil droplets together. This behavior created strong droplet-droplet interaction, making the material behave like a plastic system. The drastic change in behavior due to protein particles was demonstrated by 3D printing the emulsions. When emulsions without protein particles were 3D printed, the material could not self-stand, whereas the emulsions with protein particles were able to retain the printed structure. We showed using mechanistic insights, how pea (plant) protein behavior can be tuned to create 3D printable emulsions. This is a simple approach, as it involves a pH trigger followed by emulsification. The results show for the first time, that using pea proteins, 3D printable edible materials can be designed using a simple pH trigger.

With the mechanistic insight created from chapter-1 showing that protein purification was unnecessary and chapter-3 & 4, which provided fundamental insights of pea proteins behavior at acidic pH, we aimed to combine these findings to understand the behavior of protein mixtures as emulsifying agents (**Chapter-5)**. In this chapter, the emulsifying functionality of unpurified pea protein mixtures (PPM) and alkaline aqueous extracted pea protein isolates (PPI) were compared. This comparison is important to understand and apply pea protein mixtures, since protein isolate is the widely used standard in food systems. The comparison extended beyond model oil-in-water emulsions to include higher oil content (50 wt% oil) and assess functionality at both neutral (pH 7) and acidic (pH 3) conditions. The results clearly showed that both the unpurified PPM and purified PPI behaved similarly in reducing interfacial tension and forming stable oil droplets at neutral

pH. However, at pH 3, the proteins in the unpurified PPM were only 20% soluble compared with 60% solubility in PPI. Due to this difference in solubility, PPM formed a weaker visco-elastic interface compared with PPI. PPM also formed larger oil droplets (5 um) compared with PPI (2 µm).

Nevertheless, in both cases, the emulsions were stable against coalescence. The resulting emulsion properties were also investigated for 50 wt% oil-in-water emulsions. The results showed that at pH 7, both PPM and PPI formed weak visco-elastic emulsion materials with G' slightly higher than G''. At pH 3, PPM emulsions formed much stronger emulsion gels compared with PPI emulsions. As shown in Chapter-4, the higher G' is also related to insoluble protein particles in PPM, leading to increased droplet-droplet interaction. Overall, this chapter further proves that the purification of proteins is unnecessary. At pH 3, the unpurified (PPM) protein mixture would be beneficial in producing stronger emulsion gels (higher G'). By directly comparing PPI and PPM, we provided a clear understanding of the functionality of pea protein mixtures against the more standard pea protein isolate. The results provide an essential guideline for using pea protein mixtures as emulsifier in place of PPI.

In **Chapter-6,** heating was investigated as a means to structure emulsion-gels when using pea protein mixtures. Especially when considering the use of pea flour, the presence of starch could enhance the gelling behavior upon heating compared with only proteins. Accordingly, in this chapter, we investigated the heat-set gelation properties of pea flour in emulsion systems. To examine the effect of starch, PF (50 wt% starch, 20 wt% protein) stabilized emulsion and PPM (55 wt% protein) stabilized emulsions were studied at both acidic and neutral pH values. Our results showed that starch only contributed to a small extent to increasing gel strength at pH 7, while at pH 3, it did not contribute at all. Gelation was initiated primarily by droplet-droplet rearrangement and interactions. However, starch influenced the microstructure of the emulsions at both pHs. When starch was present, the emulsion-gels showed breakdown at lower strains than when no starch was present. Therefore, starch created brittle emulsion-gels, possibly due to disruption of the droplet-droplet attractive interaction and thus droplet-network formation.

From the experimental work in this thesis, we have successfully shown that it is possible to use pea protein mixtures without extensive processing and purification. Our results show that protein mixtures work equally well in stabilizing oil-water emulsions. We show that, the

use of mixtures also has added advantage that it produces emulsions with higher viscosity and gel strength. Overall, using peas as a model legume source, The findings of this thesis show that native legume protein mixtures containing non-protein molecules should be considered seriously as functional structuring agents in food materials. The findings also clearly highlight the versatile and added functionality of protein mixtures against isolated proteins.

7.2 Pea Proteins as structuring agents in foods: Design guidelines for the future

Proteins are mostly used in their isolated form in many food products. Traditionally, when dairy proteins are employed, they are naturally obtained from the characteristic processing steps in the dairy industry, such as whey proteins from the side stream of cheese making [11]. Once separated, the proteins are mixed with fats and sugars to create the food product desired. However, when looking use plant-based ingredients, they are stored in specific organelles within a solid seed matrix. Consequently, additional processing steps are necessary to obtain purified proteins from within the solid matrix. However, foods are constructed from multiple components such as proteins, fats, and starch, which interact to create textures [14–16]. Plant sources are rich in more than one of these components, such as peas – 20 wt% protein and 50 wt% starch. So, a shift in focus from protein purity towards protein mixtures is a better alternative for obtaining plant-based protein ingredients. Such protein mixtures containing large amounts of non-protein molecules are obtained by simple processing steps such as filtration instead of aqueous alkaline extraction and centrifugation. They are known as mildly purified or unpurified mixtures [27,179].

The idea of using unpurified or less purified plant protein mixtures is not novel [63,64]. Previous studies have already explored the possibility of using unpurified protein mixtures as emulsifying agents [28,169]. However, many of these studies mainly focus on creating a more straightforward process to obtain functional protein mixtures and do not solely focus on the functionality [50,179]. In this thesis, we focused exclusively on the emulsifying and gelling functionality of the protein mixtures. Specifically, we created a fundamental understanding of how physico-chemical properties such as protein solubility are affected when proteins are present in mixtures and how the properties affect their functionality. Overall, in this thesis, some key design guidelines are provided for using purified proteins and mildly purified or unpurified protein mixtures. The main insights gained in this thesis

are: (1) Protein purification is not necessary for producing function pea proteins. (2) In the unheated state, protein behavior dictates emulsion properties, and starch does not contribute to emulsion properties. (3) Proteins can behave as both emulsifying and structuring agents in oil-in-water emulsions (4) Starch creates brittle emulsion gels upon heating.

7.2.1 Pea protein purification unnecessary

The first insight obtained is that protein purification is not necessary for emulsifying functionality of pea proteins. This finding was systematically proven in **Chapter-2** and **Chapter-5**. In chapter-2 the results clearly show that native PF can be considered a protein system suitable for emulsification. The result is promising to use PF as a native emulsifying mixture in many food systems to produce emulsions with comparable manner to isolated pea proteins. The research was further expanded in Chapter-5, by linking molecular protein properties such as charge, aggregation state and, solubility, we showed that when present together with starch, pea proteins could still function as emulsifier. The findings in chapter-5 were a result of direct comparison between pea proteins in isolated form and in mixtures. The result showed that protein purification is not a pre-requisite to stabilize emulsions using pea proteins. Pea proteins in mixture and in purified form can both stabilize and produce emulsions. The future vision is that such design guidelines would also be extended to more plant proteins apart from peas. It is likely that for legume plant sources, such as lentils, chickpeas protein extraction may not be necessary to use the proteins as emulsifiers. The finding paves the way to eliminate the protein extraction process based on the needs of the final product.

7.2.2 Emulsion properties are dictated by protein behavior

The second insight obtained in this thesis is that 'In the unheated state, emulsion properties are dictated by protein behavior, and starch does not contribute to emulsion properties. The finding was also proven in **Chapter-2**, the results revealed that the viscosity of emulsions and aggregation state of oil droplets were not affected by the presence of starch. We showed that, even in mixtures of proteins and other components, proteins largely influence the emulsification and emulsion rheological behavior from this mixture (10 wt% oil emulsion at pH 7). Therefore, the findings demonstrate that by understanding protein behavior in mixtures, emulsions with similar physical properties may be produced,

compared with when using purified pea proteins. The results have shown that, protein mixtures can replace purified proteins. The reduction in energy intensive processing steps such as centrifugation and reduced use of water, would reduce the resource use associated with pea protein extraction.

7.2.3 Proteins can behave as both emulsifying and structuring agent

The third insight obtained in this thesis is that 'Protein particles can behave both as emulsifying and structuring agents in oil-in-water emulsions. In **Chapter-3,** we investigated the fundamental protein behavior at pH 3. The findings showed that at pH 3, about 60% of pea proteins self-associate into protein particles due to attractive non-covalent interactions, and 40% remain as dissolved individual protein molecules. The protein aggregation behavior was linked to emulsifying mechanism. The research revealed that when pea proteins are used at pH 3 to stabilize emulsions, the protein molecules stabilize the interface while protein particles remain in bulk. Using this fundamental understanding, the results showed (**Chapter-4)** that the free protein particles could increase viscosity and gel strength to form 3D printable material. By combining fundamental protein research and linking it to final material property, mechanistic insight was created on the ability to build 3D printable material. This finding is important, since it shows that plant proteins could be used in a simple manner to make 3D printable foods, expanding its use into specialized foods.

3D printing as a technique has the potential to be applied in foods and bio-materials [122,150]. 3D printing has been explored as a way to produce specialized foods in a hospital setting or for people with special medical needs and even as a domestic kitchen tool to create foods [121,149,150]. However, the adoption of food 3D printing has been held back due to the lack of biopolymers that can be used to construct foods with printable properties (elastoplasticity). Therefore, our findings open the possibility to use pea proteins and other plant proteins to construct printable foods. We expect that more plant protein sources could be explored as bio-polymers to construct 3D printable foods. However, to be able to successfully utilize plant proteins to create printable materials, a multi-disciplinary approach is necessary. 3D printing has long been investigated in tissue engineering, human organ construction, space exploration by material physicists, engineers, and rheologists. Therefore, food scientists need to work with scientists from these disciplines to understand and construct 3D printable foods: Specific research is

necessary to study the material properties when using different protein sources using rheological and scattering tools. Moreover, investigating the sensory and flavor profile of printed foods by collaborating with sensory scientists and flavor chemists is necessary.

Our approach to create 3D printable materials using plant proteins could also be an essential step when considering upcoming areas of food research. One such area is the research on cultured meat. Cultured meat or lab-grown meat is growing meat cells in a controlled environment without the need to kill an animal. Currently, unstructured, ground meat-type structures could be produced successfully using this method and can replace animal farming in the future. However, the cells need to grow in specific patterns along defined directions to create more structured meats. To achieve the specific structure, the cells need a guiding scaffold. Besides guiding, the scaffolds also need to be porous in structure to allow permeation of nutrients. Currently, scaffolding is one of the bottlenecks for cultured structured meat research. One issue is that scaffolding by 3D printing is performed using materials made out of non-edible synthetic polymers, which need to be removed after growing the piece of meat and are unpractical on large scales. Therefore, using plant protein stabilized emulsions as 3D printable scaffolds could be an excellent option to make structured cultured meat. Emulsion-based scaffolds have been investigated to grow tissues by tissue engineers [125,180,181]. We envision a similar approach could be explored using plant proteins for cultured meat production.

The use of emulsion-based 3D printed scaffolds could work as follows: First, 3D printable emulsions need to be prepared with dispersed phase that can be easily removed, for instance, by solvent evaporation. When such an emulsion is 3D printed as desired, the dispersed phase (droplet phase) could be removed, and the remaining material forms an edible, porous scaffold. The porosity of the scaffold could be controlled by changing the droplet size and volume fraction of the droplets [181]. The meat cells may then grow and differentiate along the plant protein based scaffolds. The porosity would aid in delivery of growth nutrients and act as permeable chamber. Therefore, this approach could potentially tackle two important issues in structured cultivated meat production. First, we could create tune able porous scaffolds, which can deliver nutrients. Secondly we can use a relatively simple approach and produce edible scaffolds that do not need to be removed before consumption.

To realize this, food scientists need to work on fundamental understanding on how to manipulate plant proteins to form adhesive particles which can further be used to form 3D printable particles. Moreover, food scientists need to work in tandem with tissue engineers, since tissue engineers have investigated emulsion-based scaffolds for a long time. Therefore, in cultured meat research the co-working of tissue engineers, material scientists and food scientists would be necessary to realize this vision. Specifically, questions such as how to optimally produce printable scaffolds need to be investigated. Then, from a material science perspective, the scaffold's stretchability, load-bearing ability and porosity need to be investigated. Lastly, how well the meat cells adhere to and grow on the printed scaffold must be analyzed from a biological perspective. Since 3D printing is able to produce intricate structures, it could be possible to design porous scaffolds which could deliver nutrients for growth to cells on thick meat pieces. We envision that in the long term our research could lay foundation for 3D printing edible scaffolds for precision structured cell-based meat production.

The ability to 3D print plant-based proteins can also enable them to be used in medicinal food applications. For instance, plant protein-based materials could be used to produce matrix that can deliver bio-active molecules and drugs as necessary. The approach could enable at-home printing of matrices mixed with the desired amount of drug or bio-active molecules. Personalized health and care can be realized using this approach. Such a prospect can be realized if edible plant proteins are investigated further as 3D printable polymer constructs. We hope our research sheds light on the possibility to use plant proteins for 3D printing edible materials and will eventually lead to mainstream use of 3D printing using plant proteins.

So far, the application of protein particles was discussed in the context of purified pea proteins. Similar to purified pea proteins, unpurified pea proteins mixtures also form protein particles at pH 3. These protein particles are insoluble, as opposed to soluble aggregates in purified pea proteins. The insoluble nature of pea proteins in mixtures can increase viscosity in emulsions by droplet-droplet interaction, as shown in **Chapter-4** for purified pea proteins. The effect of protein particles was drastic in the mixtures that the viscosity and gel strength were about a 100 times higher when using mixtures. Therefore, the proteins can act as a viscosity enhancer apart from being just an emulsifier. The dual role of proteins in oil-water systems is a crucial finding from this thesis. The findings showed

that by using protein mixtures at acidic pH, protein aggregates are formed, which could function as an emulsifier and as a structuring (viscosity enhancing) agent simultaneously. The results have important practical implications for high viscosity oil-based foods such as mayonnaise. The ability to use protein particles, to produce 100 times more viscous emulsions with compared to using purified pea proteins is useful design knowledge. Firstly, the finding will lead to a reduction in cost and improve the health outlook by reducing the amount of oil used. Moreover, by reducing the amount of oil, the sustainability of the product can be greatly enhanced, since oil extraction is a cumbersome process. In this chapter, we show that by linking protein behavior to the final material property, food products can be designed to meet modern day demands while making it cheaper and more sustainable.

7.2.4 Starch creates brittle emulsion gels upon heating

The fourth insight obtained in this thesis is that 'Starch creates brittle emulsion gels upon heating. The findings, described in **Chapter-6**, show that upon heating emulsion-gels containing starch become brittle (that they fracture at lower strain). Therefore, when brittle food material is envisioned, such as in a plant-based cheese alternative, using a native protein-starch mixture will be beneficial. The results show that protein processing could be avoided and simply milled peas (pea flour) could be used as an emulsifying mixture. The mixture serves a dual purpose where the proteins emulsify the oil while the starch gels upon heating. In such a microstructure, starch gels disrupt the formation of oil droplet gel. Therefore, a heterogeneous microstructure is creates, leading to a brittle emulsion-gel.

In this thesis, we successfully delivered design guidelines for using plant protein mixtures as functional proteins using peas as a model source. The approach used in this thesis links protein behavior, tuned by pH to emulsifying behavior. We also report, pH and heat as means to structure emulsions to tune the rheological properties of oil-in-water emulsions. Our approach has played an important part in creating a mechanistic understanding of pea protein mixtures and will hopefully lead to expand the use of pea protein mixtures beyond traditional emulsifying role. We hope that future research will build on this approach for pea proteins and other plant protein sources for structuring research.

7.3 Future challenges and opportunities

The use of less purified, native protein mixtures also has other challenges that are not dealt with in this thesis. These include the feasibility to use protein mixtures in specific foods and the negative impact on taste due to unprocessed protein mixtures.

Regarding the feasibility to use protein mixtures as functional agents in food products, the biggest constraint is that the protein mixtures contain proteins, starch, etc., in specific ratios. Therefore, when certain food formulations require higher amounts of one of the components, this component needs to be added in pure form. Therefore, there is still a need for extensive purification of plant ingredients, which offsets the energetic advantage of less pure ingredients. Moreover, specific food formulations may be negatively impacted by non-protein constituents; for instance, a milk-like structure may be negatively affected by the presence of insoluble proteins, which precipitate and render the milk low-quality. Similarly, when healthy food products such as high protein drinks (20 wt% protein, 5-10 wt% fat and no starch) are envisioned, purification of the proteins is necessary. When envisioning such high protein products, unpurified proteins (50 wt% protein purity) may need about 40 wt% of solids instead of 25 wt% solids for purified proteins, leading to a drastic change in the final product property. Therefore, protein mixtures are not always the better choice in terms of application. A more suitable approach is to keep in mind the final food product's application and required textural properties. Then using the requirements, the right protein choice, such as mixture vs. purified, needs to be evaluated. To do this, design guidelines such as those formulated in this thesis are essential. Moreover, these design guidelines need to be formulated based on fundamental understanding of the protein mixtures and purified proteins.

Apart from suitability, getting a ‘good tasting’ product is another crucial challenge [182]. Unprocessed protein mixtures from plants may still retain raw or cooked taste profiles [183,184]. These sensory profiles may overpower the taste and smell of the product that is envisioned. The challenges mentioned above in minimally processed plant protein mixtures need to be addressed to apply them in foods. Therefore, when investigating the use of plant protein mixtures as functional ingredients, future research should also specifically look at possible off-flavors in the unprocessed or mildly processed protein mixture and their interaction with the food matrix. This approach could identify and eliminate or suppress negative sensory attributes. The sensory studies need to be

conducted in tandem with the functionality studies to give a holistic design view that considers taste and techno-functionality.

As seen above, when using plant proteins, there are multiple means to produce food products and several challenges to be tackled. So far, generic processing to obtain pure protein ingredients has been the standard approach. However, a reverse design approach could be used as an effective means to valorize plant ingredients and minimize processing. In the reverse design approach, the physicochemical properties of the product envisioned need to be formulated first. The product properties such as rheological properties, physicochemical system conditions, the composition need to be determined by food scientists together with product technologists and sensory scientists. Subsequently, the correct type of mixtures or purified ingredients must be tested to attain such a product. Fundamental research is necessary for this area from food chemists, physical chemists, physicists, and engineers to understand how the molecular properties of different components can be controlled and how the change affects the material property. The knowledge generated in this step needs to link molecular properties to final material properties.

Further, the links need to be translated into design guidelines with both quantitative and qualitative guiding principles. The knowledge generation needs to look at many different plant protein sources and study the most common food product conditions such as pH, ionic strength, heat. The wealth of knowledge generated and desired product properties could then be matched using the design guidelines. The ultimate end goal to this should be to build a design tool-based on mechanistic understanding. The desired product parameters are given as input in such a tool, and the different plant protein sources and processing conditions are provided as output. The modeling work needs fundamental physicists, mathematicians, engineers, physical chemists to work in tandem. Continued work to improve and expand the model to also include sensory and nutritional qualities would also be necessary for the future. If such a model tool is designed effectively, that will open up great possibilities to diversify and use different plant protein sources effectively in food products. Ultimately, using this tool, a food product developer should be able to input the desired product property and find different combinations of plant-based ingredients that could be processed in specific manners to attain such properties. Naturally, a great deal of time, effort, and human resources is needed to achieve such a goal. In this regard, our

thesis has started with a small step in this direction, and future research will hopefully continue to realize this expansive goal.

References

[1] L. Aleksandrowicz, R. Green, E.J.M. Joy, P. Smith, A. Haines, The impacts of dietary change on greenhouse gas emissions, land use, water use, and health: A systematic review, PLoS One. 11 (2016) 1–16. doi:10.1371/journal.pone.0165797.

[2] S. Whitmee, A. Haines, C. Beyrer, F. Boltz, A.G. Capon, B.F. De Souza Dias, A. Ezeh, H. Frumkin, P. Gong, P. Head, R. Horton, G.M. Mace, R. Marten, S.S. Myers, S. Nishtar, S.A. Osofsky, S.K. Pattanayak, M.J. Pongsiri, C. Romanelli, A. Soucat, J. Vega, D. Yach, Safeguarding human health in the Anthropocene epoch: Report of the Rockefeller Foundation-Lancet Commission on planetary health, Lancet. 386 (2015) 1973–2028. doi:10.1016/S0140-6736(15)60901-1.

[3] N. Ramankutty, A.T. Evan, C. Monfreda, J.A. Foley, Farming the planet: 1. Geographic distribution of global agricultural lands in the year 2000, Global Biogeochem. Cycles. 22 (2008) 1–19. doi:10.1029/2007GB002952.

[4] S.J. Vermeulen, B.M. Campbell, J.S.I. Ingram, Climate change and food systems, Annu. Rev. Environ. Resour. 37 (2012) 195–222. doi:10.1146/annurev-environ-020411-130608.

[5] M. Springmann, K. Wiebe, D. Mason-D'Croz, T.B. Sulser, M. Rayner, P. Scarborough, Health and nutritional aspects of sustainable diet strategies and their association with environmental impacts: a global modelling analysis with country-level detail, Lancet Planet. Heal. 2 (2018) e451–e461. doi:10.1016/S2542-5196(18)30206-7.

[6] M.E. Nelson, M.W. Hamm, F.B. Hu, S.A. Abrams, T.S. Griffin, Alignment of healthy dietary patterns and environmental sustainability: A systematic review, Adv. Nutr. 7 (2016) 1005–1025. doi:10.3945/an.116.012567.

[7] J. Poore, T. Nemecek, Reducing food ' s environmental impacts through producers and consumers, Science (80-.). 360 (2018) 987–992. doi:10.1126/science.aaq0216.

[8] R.S.H. Lam, M.T. Nickerson, Food proteins: A review on their emulsifying properties using a structure-function approach, Food Chem. 141 (2013) 975–984. doi:10.1016/j.foodchem.2013.04.038.

[9] C.H. Tang, Globular proteins as soft particles for stabilizing emulsions: Concepts

and strategies, Food Hydrocoll. 103 (2020) 105664. doi:10.1016/j.foodhyd.2020.105664.

[10] D.J. McClements, Biopolymers in Food Emulsions, First Edit, Elsevier Inc., 2009. doi:10.1016/B978-0-12-374195-0.00004-5.

[11] A. Kilara, M.N. Vaghela, Whey proteins, Second Edi, Elsevier Ltd., 2018. doi:10.1016/B978-0-08-100722-8.00005-X.

[12] M.R. Patel, R.J. Baer, M.R. Acharya, Increasing the protein content of ice cream, J. Dairy Sci. 89 (2006) 1400–1406. doi:10.3168/jds.S0022-0302(06)72208-1.

[13] T. Krahl, H. Fuhrmann, S. Dimassi, Ice Cream, 2016. doi:10.1016/B978-0-08-100371-8.00009-9.

[14] J. Ubbink, A. Burbidge, R. Mezzenga, Food structure and functionality: a soft matter perspective, Soft Matter. 4 (2008) 1147–1150. doi:10.1039/b800106e.

[15] A.R. Patel, Functional and Engineered Colloids from Edible Materials for Emerging Applications in Designing the Food of the Future, Adv. Funct. Mater. 30 (2020) 1–34. doi:10.1002/adfm.201806809.

[16] R.G.M. van der Sman, A.J. Van Der Goot, The science of food structuring, Soft Matter. 4 (2008) 1147–1150. doi:10.1039/b800106e.

[17] C. Brennan, U. Tiwari, Functional And Physicochemical Properties of Non-Starch Polysaccharides, 1st ed., Elsevier Ltd, 2011. doi:10.1016/B978-0-12-382018-1.00006-X.

[18] A.G. Marangoni, J.P.M. Van Duynhoven, N.C. Acevedo, R.A. Nicholson, A.R. Patel, Advances in our understanding of the structure and functionality of edible fats and fat mimetics, Soft Matter. 16 (2020) 289–306. doi:10.1039/c9sm01704f.

[19] S.L. Turgeon, S.I. Laneuville, Protein + Polysaccharide Coacervates and Complexes. From Scientific Background to their Application as Functional Ingredients in Food Products, First Edit, Elsevier Inc., 2009. doi:10.1016/B978-0-12-374195-0.00011-2.

[20] W. Kim, Y. Wang, C. Selomulya, Dairy and plant proteins as natural food emulsifiers, Trends Food Sci. Technol. 105 (2020) 261–272. doi:10.1016/j.tifs.2020.09.012.

[21] K. Kuwata, S. Era, M. Hoshino, V. Forge, Y. Goto, C.A. Batt, Solution structure and dynamics of bovine β-lactoglobulin A, Protein Sci. 8 (2008) 2541–2545. doi:10.1110/ps.8.11.2541.

[22] A.K. Stone, A. Karalash, R.T. Tyler, T.D. Warkentin, M.T. Nickerson, Functional attributes of pea protein isolates prepared using different extraction methods and cultivars, Food Res. Int. 76 (2015) 31–38. doi:10.1016/j.foodres.2014.11.017.

[23] B.G. Swanson, Pea and lentil protein extraction and functionality, J. Am. Oil Chem. Soc. 67 (1990) 276–280. doi:10.1007/BF02539676.

[24] A.C.Y. Lam, A. Can Karaca, R.T. Tyler, M.T. Nickerson, Pea protein isolates: Structure, extraction, and functionality, Food Rev. Int. 34 (2018) 126–147. doi:10.1080/87559129.2016.1242135.

[25] C. Kornet, P. Venema, J. Nijsse, E. van der Linden, A.J. van der Goot, M. Meinders, Yellow pea aqueous fractionation increases the specific volume fraction and viscosity of its dispersions, Food Hydrocoll. 99 (2020) 105332. doi:10.1016/j.foodhyd.2019.105332.

[26] M. Geerts, A. van Veghel, F.K. Zisopoulos, A. van der Padt, A. Jan van der Goot, Exergetic comparison of three different processing routes for yellow pea (Pisum sativum): Functionality as a driver in sustainable process design, J. Clean. Prod. 183 (2018) 979–987. doi:10.1016/j.jclepro.2018.02.158.

[27] A.J. Van Der Goot, P.J.M. Pelgrom, J.A.M. Berghout, M.E.J. Geerts, L. Jankowiak, N.A. Hardt, J. Keijer, M.A.I. Schutyser, C. V. Nikiforidis, R.M. Boom, Concepts for further sustainable production of foods, J. Food Eng. 168 (2016) 42–51. doi:10.1016/j.jfoodeng.2015.07.010.

[28] M.E.J. Geerts, E. Mienis, C. V. Nikiforidis, A. van der Padt, A.J. van der Goot, Mildly refined fractions of yellow peas show rich behaviour in thickened oil-in-water emulsions, Innov. Food Sci. Emerg. Technol. 41 (2017) 251–258. doi:10.1016/j.ifset.2017.03.009.

[29] M.E.J. Geerts, C. V Nikiforidis, J. Van Der Goot, A. Van Der Padt, Protein nativity explains emulsifying properties of aqueous extracted protein components from yellow pea, (2017). doi:10.1016/j.foostr.2017.09.001.

[30] M.E.J. Geerts, M. Strijbos, A. van der Padt, A.J. van der Goot, Understanding functional properties of mildly refined starch fractions of yellow pea, J. Cereal Sci.

(2017). doi:10.1016/j.jcs.2017.03.025.

[31] D. Karefyllakis, S. Altunkaya, C.C. Berton-Carabin, A.J. van der Goot, C. V. Nikiforidis, Physical bonding between sunflower proteins and phenols: Impact on interfacial properties, Food Hydrocoll. 73 (2017) 326–334. doi:10.1016/j.foodhyd.2017.07.018.

[32] J.P. Janzen, G.W. Brester, V.H. Smith, L. Hall, P.O. Box, Dry Peas: Trends in Production, Trade, and Price, Agric. Mark. Policy Cent. (2014).

[33] A. Tassoni, T. Tedeschi, C. Zurlini, I.M. Cigognini, J. Petrusan, Ó. Rodr, S. Neri, A. Celli, L. Sisti, P. Cinelli, F. Signori, G. Tsatsos, M. Bondi, S. Verstringe, G. Bruggerman, P.F.X. Corvini, and Chickpeas — Valorization of Agro-Industrial Residues and Applications of Derived Extracts, Molecules. (2020). doi:10.3390/molecules25061383.

[34] D. Nikolopoulou, K. Grigorakis, M. Stasini, M.N. Alexis, K. Iliadis, Differences in chemical composition of field pea (Pisum sativum) cultivars: Effects of cultivation area and year, Food Chem. 103 (2007) 847–852. doi:10.1016/j.foodchem.2006.09.035.

[35] T.G. Burger, Y. Zhang, Recent progress in the utilization of pea protein as an emulsifier for food applications, Trends Food Sci. Technol. 86 (2019) 25–33. doi:10.1016/j.tifs.2019.02.007.

[36] P.J.M. Pelgrom, A.M. Vissers, R.M. Boom, M.A.I. Schutyser, Dry fractionation for production of functional pea protein concentrates, Food Res. Int. 53 (2013) 232–239. doi:10.1016/j.foodres.2013.05.004.

[37] P.S. John Gatehouse, Ronald Croy, Donald Boulter, The synthesis and structure of pea storage proteins- critical reviews in plant sciences, Crit. Rev. Plant Sceinces. 1 (1984) 287–314.

[38] R.R. Croy, M.S. Hoque, J. a Gatehouse, D. Boulter, The major albumin proteins from pea (Pisum sativum L). Purification and some properties., Biochem. J. 218 (1984) 795–803. doi:10.1042/bj2180795.

[39] B.Y. Lu, L. Quillien, Y. Popineau, Foaming and emulsifying properties of pea albumin fractions and partial characterisation of surface-active components, J. Sci. Food Agric. 80 (2000) 1964–1972. doi:10.1002/1097-0010(200010)80:13<1964::AID-JSFA737>3.0.CO;2-J.

[40] A. Reinkensmeier, S. Bußler, O. Schlüter, S. Rohn, H.M. Rawel, Characterization of individual proteins in pea protein isolates and air classified samples, Food Res. Int. 76 (2015) 160–167. doi:10.1016/j.foodres.2015.05.009.

[41] Uniprot, (n.d.). https://www.uniprot.org/.

[42] V. Ducel, J. Richard, Y. Popineau, F. Boury, Adsorption kinetics and rheological interfacial properties of plant proteins at the oil-water interface, Biomacromolecules. 5 (2004) 2088–2093. doi:10.1021/bm049739h.

[43] K. Shevkani, N. Singh, A. Kaur, J.C. Rana, Structural and functional characterization of kidney bean and field pea protein isolates: A comparative study, Food Hydrocoll. 43 (2015) 679–689. doi:10.1016/j.foodhyd.2014.07.024.

[44] H.N. Liang, C.H. Tang, PH-dependent emulsifying properties of pea [Pisum sativum (L.)] proteins, Food Hydrocoll. 33 (2013) 309–319. doi:10.1016/j.foodhyd.2013.04.005.

[45] J. Gueguen, M. Chevalier, J.B. And, F. Schaeffer, Dissociation and aggregation of pea legumin induced by pH and ionic strength, J. Sci. Food Agric. 44 (1988) 167–182. doi:10.1002/jsfa.2740440208.

[46] H. Liang, C. Tang, Pea protein exhibits a novel Pickering stabilization for oil-in-water emulsions at pH 3.0, LWT - Food Sci. Technol. 58 (2014) 463–469. doi:10.1016/j.lwt.2014.03.023.

[47] C. Dagorn-Scavanier, J. Gueguen, J. Lefebvre, Emulsifying Properties of Pea Globulins as Related to Their Adsorption Behaviors, J. Food Sci. 52 (1987) 335–341. doi:10.1111/j.1365-2621.1987.tb06607.x.

[48] S. Simsek, M.C. Tulbek, Y. Yao, B. Schatz, Starch characteristics of dry peas (Pisum sativum L.) grown in the USA, Food Chem. 115 (2009) 832–838. doi:10.1016/j.foodchem.2008.12.093.

[49] W.S. Ratnayake, R. Hoover, T. Warkentin, Pea starch: Composition, structure and properties - A review, Starch/Staerke. 54 (2002) 217–234. doi:10.1002/1521-379X(200206)54:6<217::AID-STAR217>3.0.CO;2-R.

[50] P.J.M. Pelgrom, R.M. Boom, M.A.I. Schutyser, Functional analysis of mildly refined fractions from yellow pea, Food Hydrocoll. 44 (2015) 12–22. doi:10.1016/j.foodhyd.2014.09.001.

[51] T.Y. Bogracheva, V.J. Morris, S.G. Ring, C.L. Hedley, The Granular Structure of C-Type Pea Starch and Its Role in Gelatinization, Biopoly. 45 (1998) 323–332.

[52] H.R. Sharif, P.A. Williams, M.K. Sharif, S. Abbas, H. Majeed, K.G. Masamba, W. Safdar, F. Zhong, Current progress in the utilization of native and modified legume proteins as emulsifiers and encapsulants – A review, Food Hydrocoll. 76 (2018) 2–16. doi:10.1016/j.foodhyd.2017.01.002.

[53] N. Krog, Functions of emulsifiers in food systems, J. Am. Oil Chem. Soc. 54 (1977) 124–131. doi:10.1007/BF02894388.

[54] M. Yerramilli, N. Longmore, S. Ghosh, Improved stabilization of nanoemulsions by partial replacement of sodium caseinate with pea protein isolate, Food Hydrocoll. 64 (2017) 99–111. doi:10.1016/j.foodhyd.2016.10.027.

[55] J.I. Boye, S. Aksay, S. Roufik, S. Ribéreau, M. Mondor, E. Farnworth, S.H. Rajamohamed, Comparison of the functional properties of pea, chickpea and lentil protein concentrates processed using ultrafiltration and isoelectric precipitation techniques, Food Res. Int. (2010). doi:10.1016/j.foodres.2009.07.021.

[56] X. Wang, T.D. Warkentin, C.J. Briggs, B.D. Oomah, C.G. Campbell, S. Woods, Total phenolics and condensed tannins in field pea (*Pisum sativum* L.) and grass pea (*Lathyrus sativus* L .), Euphytica. 101 (1998) 97–102.

[57] M. Fredrikson, P. Biot, M.L. Alminger, N.G. Carlsson, A.S. Sandberg, Production process for high-quality pea-protein isolate with low content of Oligosaccharides and phytate, J. Agric. Food Chem. 49 (2001) 1208–1212. doi:10.1021/jf000708x.

[58] A.R. Taherian, M. Mondor, J. Labranche, H. Drolet, D. Ippersiel, F. Lamarche, Comparative study of functional properties of commercial and membrane processed yellow pea protein isolates, Food Res. Int. 44 (2011) 2505–2514. doi:10.1016/j.foodres.2011.01.030.

[59] M. Cheryan, J.J. Rackis, Phytic acid interactions in food systems, 1980. doi:10.1080/10408398009527293.

[60] L.A. Pfaltzgraff, M. De Bruyn, E.C. Cooper, V. Budarin, J.H. Clark, Food waste biomass: A resource for high-value chemicals, Green Chem. 15 (2013) 307–314. doi:10.1039/c2gc36978h.

[61] Q. Jin, L. Yang, N. Poe, H. Huang, Integrated processing of plant-derived waste

to produce value-added products based on the biorefinery concept, Trends Food Sci. Technol. 74 (2018) 119–131. doi:10.1016/j.tifs.2018.02.014.

[62] J.A.M. Berghout, P.J.M. Pelgrom, M.A.I. Schutyser, R.M. Boom, A.J. Van Der Goot, Sustainability assessment of oilseed fractionation processes: A case study on lupin seeds, J. Food Eng. 150 (2015) 117–124. doi:10.1016/j.jfoodeng.2014.11.005.

[63] S.O. Agboola, O.A. Mofolasayo, B.M. Watts, R.E. Aluko, Functional properties of yellow field pea (Pisum sativum L.) seed flours and the in vitro bioactive properties of their polyphenols, Food Res. Int. 43 (2010) 582–588. doi:10.1016/j.foodres.2009.07.013.

[64] K.H. Mcwatters, J.P. Cherry, Emulsification, Foaming and Protein Solubility Properties of Defatted Soybean, Peanut, Field Pea and Pecan Flours, J. Food Sci. 42 (1977) 1444–1447. doi:10.1111/j.1365-2621.1977.tb08395.x.

[65] A. Tsoukala, E. Papalamprou, E. Makri, G. Doxastakis, E.E. Braudo, Adsorption at the air-water interface and emulsification properties of grain legume protein derivatives from pea and broad bean, Colloids Surfaces B Biointerfaces. 53 (2006) 203–208. doi:10.1016/j.colsurfb.2006.08.019.

[66] P. Cunniff, Official methods of analysis of AOAC Internationl. Volume II, Food composition;additives;natural contaminants, 16th ed., AOAC INTERNATIONAL, Arlington, 1995.

[67] G. Loglio, P. Pandolfini, R. Miller, A. V Makievski, F. Ravera, M. Ferrari, Novel Methods to Study Interfacial Layers, in: D. Möbius, R. Miller (Eds.), Nov. Methods to Study Interfacial Layers, Elsevier, 2001: pp. 439–483. doi:https://doi.org/10.1016/S1383-7303(01)80038-7.

[68] N. Diftis, V. Kiosseoglou, Competitive adsorption between a dry-heated soy protein-dextran mixture and surface-active materials in oil-in-water emulsions, Food Hydrocoll. 18 (2004) 639–646. doi:10.1016/j.foodhyd.2003.11.007.

[69] S. Naguleswaran, T. Vasanthan, Dry milling of field pea (Pisum sativum L.) groats prior to wet fractionation influences the starch yield and purity, Food Chem. 118 (2010) 627–633. doi:10.1016/j.foodchem.2009.05.045.

[70] M. Karbaschi, M. Lotfi, J. Krägel, A. Javadi, D. Bastani, R. Miller, Rheology of interfacial layers, Curr. Opin. Colloid Interface Sci. 19 (2014) 514–519.

doi:10.1016/j.cocis.2014.08.003.

[71] E.H. Lucassen-Reynders, J. Benjamins, V.B. Fainerman, Dilational rheology of protein films adsorbed at fluid interfaces, Curr. Opin. Colloid Interface Sci. 15 (2010) 264–270. doi:10.1016/j.cocis.2010.05.002.

[72] J. Krägel, M. O'Neill, A. V. Makievski, M. Michel, M.E. Leser, R. Miller, Dynamics of mixed protein-surfactant layers adsorbed at the water/air and water/oil interface, Colloids Surfaces B Biointerfaces. 31 (2003) 107–114. doi:10.1016/S0927-7765(03)00047-X.

[73] A. Dan, G. Gochev, J. Krägel, E. V. Aksenenko, V.B. Fainerman, R. Miller, Interfacial rheology of mixed layers of food proteins and surfactants, Curr. Opin. Colloid Interface Sci. 18 (2013) 302–310. doi:10.1016/j.cocis.2013.04.002.

[74] W. Peng, X. Kong, Y. Chen, C. Zhang, Y. Yang, Y. Hua, Effects of heat treatment on the emulsifying properties of pea proteins, Food Hydrocoll. 52 (2016) 301–310. doi:10.1016/j.foodhyd.2015.06.025.

[75] C. Freitas, R.H. Müller, Effect of light and temperature on zeta potential and physical stability in solid lipid nanoparticle (SLN®) dispersions, Int. J. Pharm. 168 (1998) 221–229. doi:10.1016/S0378-5173(98)00092-1.

[76] E. Dickinson, Hydrocolloids as emulsifiers and emulsion stabilizers, Food Hydrocoll. 23 (2009) 1473–1482. doi:10.1016/j.foodhyd.2008.08.005.

[77] R.J.B.M. Delahaije, H. Gruppen, M.L.F. Giuseppin, P.A. Wierenga, Towards predicting the stability of protein-stabilized emulsions, Adv. Colloid Interface Sci. 219 (2015) 1–9. doi:10.1016/j.cis.2015.01.008.

[78] M. Chen, J. Lu, F. Liu, J. Nsor-Atindana, F. Xu, H.D. Goff, J. Ma, F. Zhong, Study on the emulsifying stability and interfacial adsorption of pea proteins, Food Hydrocoll. 88 (2019) 247–255. doi:10.1016/j.foodhyd.2018.09.003.

[79] J. Floury, A. Desrumaux, J. Lardières, Effect of high-pressure homogenization on droplet size distributions and rheological properties of model oil-in-water emulsions, Innov. Food Sci. Emerg. Technol. 1 (2000) 127–134. doi:10.1016/S1466-8564(00)00012-6.

[80] C. Sun, S. Gunasekaran, M.P. Richards, Effect of xanthan gum on physicochemical properties of whey protein isolate stabilized oil-in-water emulsions, Food Hydrocoll. 21 (2007) 555–564.

doi:10.1016/j.foodhyd.2006.06.003.

[81] B. Ozturk, D.J. McClements, Progress in natural emulsifiers for utilization in food emulsions, Curr. Opin. Food Sci. 7 (2016) 1–6. doi:10.1016/j.cofs.2015.07.008.

[82] D. Pimentel, M. Pimentel, Sustainability of meat-based and plant-based diets and the environment, Am. J. Clin. Nutr. 78 (2003) 660–663. doi:10.1093/ajcn/78.3.660S.

[83] P.J.M. Pelgrom, R.M. Boom, M.A.I. Schutyser, Functional analysis of mildly refined fractions from yellow pea, Food Hydrocoll. 44 (2015) 12–22. doi:10.1016/j.foodhyd.2014.09.001.

[84] E. Ntone, J.H. Bitter, C. V. Nikiforidis, Not sequentially but simultaneously: Facile extraction of proteins and oleosomes from oilseeds, Food Hydrocoll. 102 (2020) 105598. doi:10.1016/j.foodhyd.2019.105598.

[85] M. Nikbakht Nasrabadi, S.A.H. Goli, A. Sedaghat Doost, B. Roman, K. Dewettinck, C. V. Stevens, P. Van der Meeren, Plant based Pickering stabilization of emulsions using soluble flaxseed protein and mucilage nano-assemblies, Colloids Surfaces A Physicochem. Eng. Asp. 563 (2019) 170–182. doi:10.1016/j.colsurfa.2018.12.004.

[86] M. Nikbakht Nasrabadi, S.A.H. Goli, A. Sedaghat Doost, K. Dewettinck, P. Van der Meeren, Bioparticles of flaxseed protein and mucilage enhance the physical and oxidative stability of flaxseed oil emulsions as a potential natural alternative for synthetic surfactants, Colloids Surfaces B Biointerfaces. 184 (2019). doi:10.1016/j.colsurfb.2019.110489.

[87] S.E. Molina Ortiz, J.R. Wagner, Hydrolysates of native and modified soy protein isolates: Structural characteristics, solubility and foaming properties, Food Res. Int. 35 (2002) 511–518. doi:10.1016/S0963-9969(01)00149-1.

[88] A.C. Karaca, N. Low, M. Nickerson, Emulsifying properties of chickpea, faba bean, lentil and pea proteins produced by isoelectric precipitation and salt extraction, Food Res. Int. 44 (2011) 2742–2750. doi:10.1016/j.foodres.2011.06.012.

[89] C. Chang, S. Tu, S. Ghosh, M.T. Nickerson, Effect of pH on the inter-relationships between the physicochemical, interfacial and emulsifying properties for pea, soy, lentil and canola protein isolates, Food Res. Int. 77 (2015) 360–367.

doi:10.1016/j.foodres.2015.08.012.

[90] M. Jarpa-Parra, F. Bamdad, Z. Tian, H. Zeng, F. Temelli, L. Chen, Impact of pH on molecular structure and surface properties of lentil legumin-like protein and its application as foam stabilizer, Colloids Surfaces B Biointerfaces. 132 (2015) 45–53. doi:10.1016/j.colsurfb.2015.04.065.

[91] C.M. Roth, B.L. Neal, A.M. Lenhoff, Van der Waals interactions involving proteins, Biophys. J. 70 (1996) 977–987. doi:10.1016/S0006-3495(96)79641-8.

[92] A. Sarkar, E. Dickinson, Sustainable food grade Pickering emulsions stabilized by plant-based particles, Curr. Opin. Colloid Interface Sci. 49 (2020) 69–81.

[93] S. Zhang, M. Holmes, R. Ettelaie, A. Sarkar, Pea protein microgel particles as Pickering stabilisers of oil-in-water emulsions: Responsiveness to pH and ionic strength, Food Hydrocoll. 102 (2020). doi:10.1016/j.foodhyd.2019.105583.

[94] S. Amin, G. V. Barnett, J.A. Pathak, C.J. Roberts, P.S. Sarangapani, Protein aggregation, particle formation, characterization & rheology, Curr. Opin. Colloid Interface Sci. 19 (2014) 438–449. doi:10.1016/j.cocis.2014.10.002.

[95] N. Tangsuphoom, J.N. Coupland, Effect of surface-active stabilizers on the microstructure and stability of coconut milk emulsions, Food Hydrocoll. 22 (2008) 1233–1242. doi:10.1016/j.foodhyd.2007.08.002.

[96] S. Sridharan, M.B.J. Meinders, J.H. Bitter, C. V. Nikiforidis, Native pea flour as stabilizer of oil-in-water emulsions: No protein purification necessary, Food Hydrocoll. 101 (2019) 105533. doi:10.1016/j.foodhyd.2019.105533.

[97] M. Rayner, D. Marku, M. Eriksson, M. Sjöö, P. Dejmek, M. Wahlgren, Biomass-based particles for the formulation of Pickering type emulsions in food and topical applications, Colloids Surfaces A Physicochem. Eng. Asp. 458 (2014) 48–62. doi:10.1016/j.colsurfa.2014.03.053.

[98] H.P. Erickson, Size and shape of protein molecules at the nanometer level determined by sedimentation, gel filtration, and electron microscopy, Biol. Proced. Online. 11 (2009) 32–51. doi:10.1007/s12575-009-9008-x.

[99] C. V. Nikiforidis, C. Ampatzidis, S. Lalou, E. Scholten, T.D. Karapantsios, V. Kiosseoglou, Purified oleosins at air–water interfaces Constantinos, Soft Matter. (2013) 1354–1363. doi:10.1039/c2sm27118d.

[100] J. Boye, F. Zare, A. Pletch, Pulse proteins: Processing, characterization, functional properties and applications in food and feed, Food Res. Int. 43 (2010) 414–431. doi:10.1016/j.foodres.2009.09.003.

[101] J. Xiao, Y. Li, Q. Huang, Recent advances on food-grade particles stabilized Pickering emulsions: Fabrication, characterization and research trends, Trends Food Sci. Technol. 55 (2016) 48–60. doi:10.1016/j.tifs.2016.05.010.

[102] B.. Midmore, Low surface coverage-colloids and surfaces -synthetic particles.pdf, Colloids Surfaces A Physicochem. Eng. Asp. 132 (1997) 257–265.

[103] M. Destribats, M. Rouvet, C. Gehin-Delval, C. Schmitt, B.P. Binks, Emulsions stabilised by whey protein microgel particles: Towards food-grade Pickering emulsions, Soft Matter. 10 (2014) 6941–6954. doi:10.1039/c4sm00179f.

[104] A. Araiza-Calahorra, A. Sarkar, Pickering emulsion stabilized by protein nanogel particles for delivery of curcumin: Effects of pH and ionic strength on curcumin retention, Food Struct. 21 (2019). doi:10.1016/j.foostr.2019.100113.

[105] M. Destribats, V. Lapeyre, M. Wolfs, E. Sellier, F. Leal-Calderon, V. Ravaine, V. Schmitt, Soft microgels as Pickering emulsion stabilisers: Role of particle deformability, Soft Matter. 7 (2011) 7689–7698. doi:10.1039/c1sm05240c.

[106] E. Dickinson, Biopolymer-based particles as stabilizing agents for emulsions and foams, Food Hydrocoll. 68 (2017) 219–231. doi:10.1016/j.foodhyd.2016.06.024.

[107] K.J. l'Anson, M.J. Miles, J.R. Bacon, H.J. Carr, N. Lambert, V.J. Morris, D.J. Wright, Structure of the 7S globulin (vicilin) from pea (Pisum sativum), Int. J. Biol. Macromol. 10 (1988) 311–317. doi:10.1016/0141-8130(88)90010-4.

[108] P. Plietz, D. Zirwer, B. Schlesier, K. Gast, G. Damaschun, Shape, symmetry, hydration and secondary structure of the legumin from Vicia faba in solution, Biochim. Biophys. Acta (BBA)/Protein Struct. Mol. 784 (1984) 140–146. doi:10.1016/0167-4838(84)90120-1.

[109] E. Adal, A. Sadeghpour, S. Connell, M. Rappolt, E. Ibanoglu, A. Sarkar, Heteroprotein Complex Formation of Bovine Lactoferrin and Pea Protein Isolate: A Multiscale Structural Analysis, Biomacromolecules. 18 (2017) 625–635. doi:10.1021/acs.biomac.6b01857.

[110] A. Gharsallaoui, E. Cases, O. Chambin, R. Saurel, Interfacial and emulsifying characteristics of acid-treated pea protein, Food Biophys. 4 (2009) 273–280.

doi:10.1007/s11483-009-9125-8.

[111] A.T. Tenorio, E.W.M. De Jong, C. V. Nikiforidis, R.M. Boom, A.J. Van Der Goot, Interfacial properties and emulsification performance of thylakoid membrane fragments, Soft Matter. 13 (2017) 608–618. doi:10.1039/c6sm02195f.

[112] M.R. Sommer, L. Alison, C. Minas, E. Tervoort, P.A. Rühs, A.R. Studart, 3D printing of concentrated emulsions into multiphase biocompatible soft materials, Soft Matter. 13 (2017) 1794–1803. doi:10.1039/C6SM02682F.

[113] C.B. Highley, K.H. Song, A.C. Daly, J.A. Burdick, Jammed Microgel Inks for 3D Printing Applications, Adv. Sci. 6 (2019) 1–6. doi:10.1002/advs.201801076.

[114] K. Vithani, A. Goyanes, V. Jannin, A.W. Basit, S. Gaisford, B.J. Boyd, An Overview of 3D Printing Technologies for Soft Materials and Potential Opportunities for Lipid-based Drug Delivery Systems, Pharm. Res. 36 (2019). doi:10.1007/s11095-018-2531-1.

[115] X. Li, X. Xu, L. Song, A. Bi, C. Wu, Y. Ma, M. Du, B. Zhu, High Internal Phase Emulsion for Food-grade 3D Printing Materials, ACS Appl. Mater. Interfas. (2020). doi:10.1021/acsami.0c11434.

[116] C. He, M. Zhang, Z. Fang, 3D printing of food: pretreatment and post-treatment of materials, Crit. Rev. Food Sci. Nutr. 60 (2020) 2379–2392. doi:10.1080/10408398.2019.1641065.

[117] S. Moon, J.Q. Kim, B.Q. Kim, J. Chae, S.Q. Choi, Processable Composites with Extreme Material Capacities: Toward Designer High Internal Phase Emulsions and Foams †, Chem. Mater. 32 (2020) 4838–4854. doi:10.1021/acs.chemmater.9b04952.

[118] S. Huan, R. Ajdary, L. Bai, V. Klar, O.J. Rojas, Low Solids Emulsion Gels Based on Nanocellulose for 3D-Printing, Biomacromolecules. 20 (2019) 635–644. doi:10.1021/acs.biomac.8b01224.

[119] F. Yang, M. Zhang, B. Bhandari, Recent development in 3D food printing, Crit. Rev. Food Sci. Nutr. 57 (2017) 3145–3153. doi:10.1080/10408398.2015.1094732.

[120] H. Jiang, L. Zheng, Y. Zou, Z. Tong, S. Han, S. Wang, 3D food printing: main components selection by considering rheological properties, Crit. Rev. Food Sci. Nutr. 59 (2019) 2335–2347. doi:10.1080/10408398.2018.1514363.

[121] J.I. Lipton, M. Cutler, F. Nigl, D. Cohen, H. Lipson, Additive manufacturing for the food industry, Trends Food Sci. Technol. 43 (2015) 114–123. doi:10.1016/j.tifs.2015.02.004.

[122] J.Y. Zhang, J.K. Pandya, D.J. McClements, J. Lu, A.J. Kinchla, Advancements in 3D food printing: a comprehensive overview of properties and opportunities, Crit. Rev. Food Sci. Nutr. 0 (2021) 1–18. doi:10.1080/10408398.2021.1878103.

[123] J. Sun, W. Zhou, L. Yan, D. Huang, L. ya Lin, Extrusion-based food printing for digitalized food design and nutrition control, J. Food Eng. 220 (2018) 1–11. doi:10.1016/j.jfoodeng.2017.02.028.

[124] A. Derossi, R. Caporizzi, D. Azzollini, C. Severini, Application of 3D printing for customized food. A case on the development of a fruit-based snack for children, J. Food Eng. 220 (2018) 65–75. doi:10.1016/j.jfoodeng.2017.05.015.

[125] T. Yang, Y. Hu, C. Wang, B.P. Binks, Fabrication of Hierarchical Macroporous Biocompatible Scaffolds by Combining Pickering High Internal Phase Emulsion Templates with Three-Dimensional Printing, ACS Appl. Mater. Interfaces. 9 (2017) 22950–22958. doi:10.1021/acsami.7b05012.

[126] Y. Liu, W. Zhang, K. Wang, Y. Bao, J. Mac Regenstein, P. Zhou, Fabrication of Gel-like Emulsions with Whey Protein Isolate Using Microfluidization: Rheological Properties and 3D Printing Performance (Food and Bioprocess Technology, (2019), 12, 12, (1967-1979), 10.1007/s11947-019-02344-5), Food Bioprocess Technol. 12 (2019) 1980–1981. doi:10.1007/s11947-019-02356-1.

[127] S. Sridharan, M.B.J. Meinders, J.H. Bitter, C. V. Nikiforidis, On the emulsifying properties of self-assembled pea protein particles, Langmuir. 36 (2020) 12221–12229. doi:10.1021/acs.langmuir.0c01955.

[128] K.J. Klemmer, L. Waldner, A. Stone, N.H. Low, M.T. Nickerson, Complex coacervation of pea protein isolate and alginate polysaccharides, Food Chem. 130 (2012) 710–715. doi:10.1016/j.foodchem.2011.07.114.

[129] K.W. Desmond, E.R. Weeks, Influence of particle size distribution on random close packing of spheres, Phys. Rev. E - Stat. Nonlinear, Soft Matter Phys. 90 (2014) 1–6. doi:10.1103/PhysRevE.90.022204.

[130] H.S. Kim, T.G. Mason, Advances and challenges in the rheology of concentrated emulsions and nanoemulsions, Adv. Colloid Interface Sci. 247 (2017) 397–412.

doi:10.1016/j.cis.2017.07.002.

[131] D. Bonn, M.M. Denn, L. Berthier, T. Divoux, S. Manneville, Yield stress materials in soft condensed matter, Rev. Mod. Phys. 89 (2017) 1–44. doi:10.1103/RevModPhys.89.035005.

[132] Y. Hemar, D.S. Horne, Dynamic rheological properties of highly concentrated protein-stabilized emulsions, Langmuir. 16 (2000) 3050–3057. doi:10.1021/la9908440.

[133] M. Hermes, P.S. Clegg, Yielding and flow of concentrated Pickering emulsions, Soft Matter. 9 (2013) 7568–7575. doi:10.1039/c3sm50889g.

[134] M.C. Rogers, K. Chen, M.J. Pagenkopp, T.G. Mason, S. Narayanan, J.L. Harden, R.L. Leheny, Microscopic signatures of yielding in concentrated nanoemulsions under large-amplitude oscillatory shear, Phys. Rev. Mater. 2 (2018). doi:10.1103/PhysRevMaterials.2.095601.

[135] H.G. Sim, K.H. Ahn, S.J. Lee, Large amplitude oscillatory shear behavior of complex fluids investigated by a network model: A guideline for classification, J. Nonnewton. Fluid Mech. 112 (2003) 237–250. doi:10.1016/S0377-0257(03)00102-2.

[136] K.N. Pham, G. Petekidis, D. Vlassopoulos, S.U. Egelhaaf, W.C.K. Poon, P.N. Pusey, Yielding behavior of repulsion- and attraction-dominated colloidal glasses, J. Rheol. (N. Y. N. Y). 52 (2008) 649–676. doi:10.1122/1.2838255.

[137] G.L. Hunter, E.R. Weeks, The physics of the colloidal glass transition, Reports Prog. Phys. 75 (2012). doi:10.1088/0034-4885/75/6/066501.

[138] S.S. Datta, D.D. Gerrard, T.S. Rhodes, T.G. Mason, D.A. Weitz, Rheology of attractive emulsions, Phys. Rev. E - Stat. Nonlinear, Soft Matter Phys. 84 (2011) 3–8. doi:10.1103/PhysRevE.84.041404.

[139] C. Pellet, M. Cloitre, The glass and jamming transitions of soft polyelectrolyte microgel suspensions, Soft Matter. 12 (2016) 3710–3720. doi:10.1039/c5sm03001c.

[140] V. Trappe, V. Prasad, L. Cipelletti, P.N. Segre, D.A. Weitz, Jamming phase diagram for attractive particles, Nature. 411 (2001) 772–775. doi:10.1038/35081021.

[141] T.G. Mason, J. Bibette, D.A. Weitz, Elasticity of Compressed Emulsions, Phys. Rev. Lett. 75 (1995) 2051–2054. doi:10.1097/BRS.0000000000000152.

[142] E.D. Knowlton, D.J. Pine, L. Cipelletti, A microscopic view of the yielding transition in concentrated emulsions, Soft Matter. 10 (2014) 6931–6940. doi:10.1039/c4sm00531g.

[143] R.H. Ewoldt, G.H. McKinley, A.E. Hosoi, Fingerprinting Soft Materials: A Framework for Characterizing Nonlinear Viscoelasticity, 52 (2007) 1427–1458. doi:10.1122/1.2970095.

[144] K. Hyun, J.G. Nam, M. Wilhellm, K.H. Ahn, S.J. Lee, Large amplitude oscillatory shear behavior of PEO-PPO-PEO triblock copolymer solutions, Rheol. Acta. 45 (2006) 239–249. doi:10.1007/s00397-005-0014-x.

[145] F.K.G. Schreuders, L.M.C. Sagis, I. Bodnár, P. Erni, R.M. Boom, A.J. van der Goot, Small and large oscillatory shear properties of concentrated proteins, Food Hydrocoll. 110 (2021). doi:10.1016/j.foodhyd.2020.106172.

[146] K. Hyun, J.G. Nam, M. Wilhelm, K.H. Ahn, S.J. Lee, Nonlinear response of viscoelastic fluids under LAOS (large amplitude shear flow), Korea-Australia Rheol. J. 15 (2003) 97–105.

[147] K. Hyun, S. H Kim, K. H Ahn, S. J Lee, Large amplitude oscillatory shear as a way to classify the complex fluids, J. Nonnewton. Fluid Mech. 107 (2002) 51–65. doi:10.4103/2319-4170.165000.

[148] A. Nesterenko, A. Drelich, H. Lu, D. Clausse, I. Pezron, Influence of a mixed particle/surfactant emulsifier system on water-in-oil emulsion stability, Colloids Surfaces A Physicochem. Eng. Asp. 457 (2014) 49–57. doi:10.1016/j.colsurfa.2014.05.044.

[149] Y.K. Suppiramaniam, A. Thangarasu, A. Wilson, J.A. Moses, A. Chinnaswamy, 3D printing of encapsulated probiotics: Effect of different post-processing methods on the stability of Lactiplantibacillus plantarum (NCIM 2083) under static in vitro digestion conditions and during storage, Lwt. 146 (2021) 111461. doi:10.1016/j.lwt.2021.111461.

[150] L. Zhao, M. Zhang, B. Chitrakar, B. Adhikari, Recent advances in functional 3D printing of foods: a review of functions of ingredients and internal structures, Crit. Rev. Food Sci. Nutr. 0 (2020) 1–15. doi:10.1080/10408398.2020.1799327.

[151] E. Dickinson, J. Chen, Heat-set whey protein emulsion gels: Role of active and inactive filler particles, J. Dispers. Sci. Technol. 20 (1999) 197–213. doi:10.1080/01932699908943787.

[152] E. Dickinson, Emulsion gels: The structuring of soft solids with protein-stabilized oil droplets, Food Hydrocoll. 28 (2012) 224–241. doi:10.1016/j.foodhyd.2011.12.017.

[153] S. Qamar, Y.J. Manrique, H. Parekh, J.R. Falconer, Nuts, cereals, seeds and legumes proteins derived emulsifiers as a source of plant protein beverages: A review, Crit. Rev. Food Sci. Nutr. 0 (2019) 1–21. doi:10.1080/10408398.2019.1657062.

[154] M. Thrane, P. V. Paulsen, M.W. Orcutt, T.M. Krieger, Soy Protein: Impacts, Production, and Applications, Elsevier Inc., 2016. doi:10.1016/B978-0-12-802778-3.00002-0.

[155] M.B. Bara, M.B. Peši, P. Stanojevi, A.Ž. Kosti, Techno-functional properties of pea (Pisum sativum) protein isolates-a review, 269 (2015) 1–18. doi:10.2298/APT1546001B.

[156] J. Yang, G. Liu, H. Zeng, L. Chen, Effects of high pressure homogenization on faba bean protein aggregation in relation to solubility and interfacial properties, Food Hydrocoll. 83 (2018) 275–286. doi:10.1016/j.foodhyd.2018.05.020.

[157] J.M.R. Patino, M.R.R. Niño, C.C. Sánchez, S.E.M. Ortiz, M.C. Añón, Dilatational properties of soy globulin adsorbed films at the air-water interface from acidic solutions, J. Food Eng. 68 (2005) 429–437. doi:10.1016/j.jfoodeng.2004.06.020.

[158] J. Yang, I. Thielen, C.C. Berton-Carabin, E. van der Linden, L.M.C. Sagis, Nonlinear interfacial rheology and atomic force microscopy of air-water interfaces stabilized by whey protein beads and their constituents, Food Hydrocoll. 101 (2020) 105466. doi:10.1016/j.foodhyd.2019.105466.

[159] L.M.C. Sagis, P. Fischer, Nonlinear rheology of complex fluid-fluid interfaces, Curr. Opin. Colloid Interface Sci. 19 (2014) 520–529. doi:10.1016/j.cocis.2014.09.003.

[160] E.B.A. Hinderink, L. Sagis, K. Schroën, C.C. Berton-Carabin, Behavior of plant-dairy protein blends at air-water and oil-water interfaces, Colloids Surfaces B Biointerfaces. 192 (2020) 111015. doi:10.1016/j.colsurfb.2020.111015.

[161] E. Ntone, T. van Wesel, L.M.C. Sagis, M. Meinders, J.H. Bitter, Nikifori, Adsorption of rapeseed proteins at oil_water interfaces. Janus-like napins dominate the interface, J. Colloid Interface Sci. 583 (2021) 459–469.

[162] R. Kornet, J. Veenemans, P. Venema, A.J. van der Goot, M. Meinders, L. Sagis, E. van der Linden, Less is more: Limited fractionation yields stronger gels for pea proteins, Food Hydrocoll. 112 (2021) 106285. doi:10.1016/j.foodhyd.2020.106285.

[163] S. Sridharan, M.B.J. Meinders, L.M. Sagis, J.H. Bitter, C.V. Nikiforidis, Sticking jammed oil droplets with adhesive pea protein particles for elastoplastic edible 3D printed materials, Wiley-VCH. 2101749 (2021) 1–11. doi:10.1002/adfm.202101749.

[164] M. Kaganyuk, A. Mohraz, Role of particles in the rheology of solid-stabilized high internal phase emulsions, J. Colloid Interface Sci. 540 (2019) 197–206. doi:10.1016/j.jcis.2018.12.098.

[165] A. Pandey, M. Derakhshandeh, S.A. Kedzior, B. Pilapil, N. Shomrat, T. Segal-Peretz, S.L. Bryant, M. Trifkovic, Role of interparticle interactions on microstructural and rheological properties of cellulose nanocrystal stabilized emulsions, J. Colloid Interface Sci. 532 (2018) 808–818. doi:10.1016/j.jcis.2018.08.044.

[166] T.F. Tadros, Fundamental principles of emulsion rheology and their applications, Colloids Surfaces A Physicochem. Eng. Asp. 91 (1994) 39–55. doi:10.1016/0927-7757(93)02709-N.

[167] S. Ben-Harb, M. Panouillé, D. Huc-Mathis, G. Moulin, A. Saint-Eve, F. Irlinger, P. Bonnarme, C. Michon, I. Souchon, The rheological and microstructural properties of pea, milk, mixed pea/milk gels and gelled emulsions designed by thermal, acid, and enzyme treatments, Food Hydrocoll. 77 (2018) 75–84. doi:10.1016/j.foodhyd.2017.09.022.

[168] H. Aiking, J. de Boer, The next protein transition, Trends Food Sci. Technol. 105 (2020) 515–522. doi:10.1016/j.tifs.2018.07.008.

[169] D. Karefyllakis, H. Octaviana, A.J. van der Goot, C. V. Nikiforidis, The emulsifying performance of mildly derived mixtures from sunflower seeds, Food Hydrocoll. 88 (2019) 75–85. doi:10.1016/j.foodhyd.2018.09.037.

[170] P.J. Shand, H. Ya, Z. Pietrasik, P.K.J.P.D. Wanasundara, Physicochemical and textural properties of heat-induced pea protein isolate gels, Food Chem. 102 (2007) 1119–1130. doi:10.1016/j.foodchem.2006.06.060.

[171] R.H. Ewoldt, P. Winter, J. Maxey, G.H. McKinley, Large amplitude oscillatory shear of pseudoplastic and elastoviscoplastic materials, Rheol. Acta. 49 (2010) 191–212. doi:10.1007/s00397-009-0403-7.

[172] T.S. Leite, A.L.T. de Jesus, M. Schmiele, A.A.L. Tribst, M. Cristianini, High pressure processing (HPP) of pea starch: Effect on the gelatinization properties, LWT - Food Sci. Technol. 76 (2017) 361–369. doi:10.1016/j.lwt.2016.07.036.

[173] J.V.C. Silva, B. Jacquette, L. Amagliani, C. Schmitt, T. Nicolai, C. Chassenieux, Heat-induced gelation of micellar casein/plant protein oil-in-water emulsions, Colloids Surfaces A Physicochem. Eng. Asp. 569 (2019) 85–92. doi:10.1016/j.colsurfa.2019.01.065.

[174] K.H. Kim, J.M.S. Renkema, T. Van Vliet, Rheological properties of soybean protein isolate gels containing emulsion droplets, Food Hydrocoll. 15 (2001) 295–302. doi:10.1016/S0268-005X(01)00028-5.

[175] E. Dickinson, Colloid science of mixed ingredients, Soft Matter. 2 (2006) 642–652. doi:10.1039/b605670a.

[176] K. Hyun, M. Wilhelm, C.O. Klein, K.S. Cho, J.G. Nam, K.H. Ahn, S.J. Lee, R.H. Ewoldt, G.H. McKinley, A review of nonlinear oscillatory shear tests: Analysis and application of large amplitude oscillatory shear (LAOS), Prog. Polym. Sci. 36 (2011) 1697–1753. doi:10.1016/j.progpolymsci.2011.02.002.

[177] S. Precha-Atsawanan, D. Uttapap, L.M.C. Sagis, Linear and nonlinear rheological behavior of native and debranched waxy rice starch gels, Food Hydrocoll. 85 (2018) 1–9. doi:10.1016/j.foodhyd.2018.06.050.

[178] P. Ptaszek, Large amplitudes oscillatory shear (LAOS) behavior of egg white foams with apple pectins and xanthan gum, Food Res. Int. 62 (2014) 299–307. doi:10.1016/j.foodres.2014.03.002.

[179] P.J.M. Pelgrom, J.A.M. Berghout, A.J. van der Goot, R.M. Boom, M.A.I. Schutyser, Preparation of functional lupine protein fractions by dry separation, LWT - Food Sci. Technol. 59 (2014) 680–688. doi:10.1016/j.lwt.2014.06.007.

[180] Y. Hu, J. Wang, X. Li, X. Hu, W. Zhou, X. Dong, C. Wang, Z. Yang, B.P. Binks,

Facile preparation of bioactive nanoparticle/poly(ε-caprolactone) hierarchical porous scaffolds via 3D printing of high internal phase Pickering emulsions, J. Colloid Interface Sci. 545 (2019) 104–115. doi:10.1016/j.jcis.2019.03.024.

[181] B. Aldemir Dikici, F. Claeyssens, Basic Principles of Emulsion Templating and Its Use as an Emerging Manufacturing Method of Tissue Engineering Scaffolds, Front. Bioeng. Biotechnol. 8 (2020). doi:10.3389/fbioe.2020.00875.

[182] M. Cheryan, J.J. Rackis, Critical Reviews in Food Science & Nutrition Phytic acid interactions in food systems, 2009. doi:10.1080/10408398009527293.

[183] D.J. McClements, E. Newman, I.F. McClements, Plant-based Milks: A Review of the Science Underpinning Their Design, Fabrication, and Performance, Compr. Rev. Food Sci. Food Saf. 18 (2019) 2047–2067. doi:10.1111/1541-4337.12505.

[184] S. Sethi, S.K. Tyagi, R.K. Anurag, Plant-based milk alternatives an emerging segment of functional beverages: a review, J. Food Sci. Technol. 53 (2016) 3408–3423. doi:10.1007/s13197-016-2328-3.

Summary

Chapter-1 provides the general introduction and outline for this thesis. In this chapter, we explain the impact of global food production. Food production occupies about one-third of the land and produces about a quarter of global greenhouse gases. Specifically, animal-based foods produce more greenhouse gases than plant-based foods. For instance, animal-based foods such as cow meat generate about 20-50 kgCO_2 equivalent to produce 100 grams of proteins, whereas plants require about 0.2-0.3 kgCO_2 equivalent to produce 100 grams of proteins. Therefore, due to environmental concerns, there is global interest in transitioning to a more plant-based food system. We also make the case that, in this transition, proteins have been given a lot of attention. The emphasis on proteins is because proteins are an essential macro-nutrient necessary for human sustenance.

Moreover, proteins are used as emulsifying and gelling agents in many food products such as cheese. Therefore, replacing animal-sourced proteins with plant-based proteins as functional agents has been widely investigated. However, plant protein use is held back due to a lack of thorough understanding of their Physico-chemical and functional properties, such as emulsifying and gelling properties. Therefore, there is a need to understand the functional and physicochemical properties of plant proteins. We explain that this thesis aims to add new understandings of plant-based proteins' physicochemical and functional properties.

Another drawback of using plant proteins is the need for an extensive purification process to extract proteins from the plant matrix. Large amounts of water and mechanical forces are necessary to extract plant proteins from the seed matrix. Such a resource-intensive process increases the environmental footprint of plant proteins and leads to process-related losses of carbohydrates and proteins. So, avoiding extensive purification and using an extraction process with fewer processing steps may be a suitable alternative to reduce resource use in plant proteins. Such milder processing would produce protein extracts with more non-protein molecules such as starch. A thorough understanding of the structuring ability of protein mixtures containing non-protein molecules is necessary to apply them successfully in foods. The understanding of plant-based mixtures as functional ingredients is also an important research focus of this thesis. To investigate the functional properties of plant-based mixtures, peas were chosen as the plant protein source to be investigated in this thesis. In the next section, we lay out the reasons to investigate peas as a potential plant protein source. Peas are a leguminous crop, which is widely grown around the world.

This makes them an easily accessible source of plant proteins. Moreover, peas contain 50 wt% starch and 20 wt% protein, making them good proteins and carbohydrates. The proteins in peas are also known to be suitable emulsifiers of food-grade oil-in-water emulsions. Finally, we provide the aim and the outline of this thesis: To create mechanistic insights into the structuring ability of pea protein mixtures in emulsion-based model food materials. In the last section of this chapter, we provide the outline of this thesis, which contains 7 chapters, including the introduction, 5 experimental chapters, and a general discussion.

Chapter-2 established the proof of concept for this thesis. In this chapter, we provide experimental evidence for using unpurified pea flour as emulsifier in oil-water systems. Pea seeds were milled to obtain pea flour (PF), which contained 50 wt% starch and 20 wt% protein. The PF was investigated as an emulsifier in a 10% oil-water emulsion system at pH 7. We found that the proteins in this mixture were the interfacial stabilizing agent, and the non-protein components did not hinder the interfacial stabilization by the proteins. The results showed that a protein to oil ratio of 1:50 (wt:wt) was sufficient to produce stable emulsions at neutral pH when a 10% oil emulsion was prepared. The effect of starch on the emulsion rheological properties was also tested. To investigate the effect of starch, it was removed from PF by an aqueous filtration process, and the resulting mixture was termed pea protein mixture (PPM). The effect of starch on viscosity was investigated by comparing emulsions stabilized with PF and with PPM. The comparison showed that the presence of starch did not influence the emulsifying property and emulsion viscosity. Overall, the chapter shows that pea protein purification is unnecessary to use as an emulsifying agent in oil-water systems.

Many food products are designed to be in acidic pH values. Therefore, we also investigated the emulsifying behavior of pea proteins at pH 3. However, due to the lack of extensive studies of pea proteins at pH 3, we first decided to study extensively purified pea proteins to gain fundamental insights. In **Chapter-3**, we studied the interfacial and emulsifying properties of purified pea protein isolates (PPI) at pH 3. Pea proteins were found to partly self-associate into protein particles of 100-500 nm size at pH 3. About 60% of the proteins were self-assembled into particles, while the remaining 40% were present as individual protein molecules. A 10% oil-in-water emulsions were prepared, and the droplet size and surface coverage were experimentally measured. Theoretical surface coverages of the

emulsions were also calculated based on the protein size, protein particle size, and droplet size. The theoretical and the experimental surface coverage were compared to understand the role of protein molecules and protein particles on interfacial stabilization. The results showed that in this mixture at pH 3, the protein molecules stabilized the oil droplets while the protein particles remained in bulk.

To understand the effect of protein particles on the emulsion rheological behavior, we investigated the rheological properties of emulsions with and without protein particles in **Chapter-4**. Emulsions were prepared with 70 wt% oil at pH 7, where no protein particles were present, and at pH 3, where protein particles were present. We tested the rheological properties and attempted to 3D print both the emulsions. The emulsions without protein particles (pH 7) were visco-elastic emulsion gels. Upon 3D printing, the emulsions were not able to self-stand. The emulsions with protein particles (pH 3) formed elastoplastic material. The emulsion was able to self-stand upon extrusion from the 3D printer and retained the printed structure for up to 48 hours. Our results showed that the protein particles formed at pH 3 created adhesive droplet-droplet interaction, resulting in an elastoplastic emulsion.

In chapter-3, we thoroughly investigated the properties of pea proteins and their emulsifying mechanism. In chapter-2, we proved that at pH 7, protein purification was unnecessary for using pea protein mixtures as emulsifiers. In **Chapter-5**, we further expanded on the findings of Chapter-2 and Chapter-3 to understand the emulsifying ability. In Chapter-5, we investigate the interfacial and emulsifying properties of pea proteins in pea protein isolate (PPI) and pea flour (PF) at both acidic and neutral pH. The interfacial and emulsifying abilities of both PF and PPI were similar at neutral pH. However, at acidic pH, the emulsifying ability of PF was slightly lower. Slightly larger oil droplets were formed when using PF (5 μm) than PPI (2 μm).

The difference in droplet size was caused due to lower protein solubility in PF (20%) compared to PPI (60%) at pH 3. Lower solubility leads to fewer proteins available to cover the interface and to the stabilization of larger droplets. Besides, pea proteins aggregate (low solubility) and form protein particles. The presence of insoluble protein particles increases the viscosity of the PF stabilized emulsions compared to PPI stabilized emulsions at pH 3. The finding shows that PF can be used as an emulsifier in place of PPI at pH 7 and 3. At pH 7, emulsions with similar size and viscosity can be formed. So, a direct

replacement of PPI by PF is possible. At pH 3, PF stabilizes larger oil droplets compared with PPI, indicating slightly less functionality of PF compared with PPI. Nevertheless, an increase in viscosity and gel strength for PF stabilized emulsions at pH 3 may produce more viscous food products.

Starch is the main component (50 wt%) in pea flour (PF). Starch can be gelatinized using heat and can form starch gels. In chapter-1, we showed that starch in PF did not influence the viscosity of 10 wt% oil-in-water emulsions at pH 7 when they were present in the granular form without gelatinization. In **Chapter-6**, we extend the finding and investigate the heat-set gelation and gel properties of emulsions stabilized with PF at pH 7 and 3. Specifically, the effect of starch was investigated upon heating the emulsion gels. To investigate the effect of starch, two protein systems were used. First, milled peas, called pea flour (PF), contain 50 wt% starch and 20 wt% protein. Second, starch was removed from PF by filtration, and the starch-free protein mixture known as pea protein mixture (PPM) was used. 50 wt% oil-in-water emulsions with both PF and PPM as stabilizers were prepared at both pH 7 and 3. Gelation as a function of heating was investigated by heating from 20°C to 90°C and then cooling back to 20°C. The heat set gelation showed that a specific increase in gel strength around the starch gelatinization temperature was not observed. The final gel strength was slightly higher at pH 7 for emulsions containing starch (PF emulsions) than emulsions without starch (PPM emulsions). Whereas at pH 3, starch did not increase the final gel strength. However, Lissajous plots at pH 7 and 3 revealed that starch played a prominent role in creating more brittle emulsion gels, which broke down at lower strains than emulsions without starch. Starch formed patchy starch gel that disrupted continuous emulsion droplet gel formation, leading to a brittle response. Overall, it was concluded that the presence of starch is beneficial to create brittle emulsion-gel structures.

In **Chapter-7,** we summarized the results obtained in detail. We also discussed how our results could be translated into broader protein transition studies. We make a case for avoiding plant protein purification from a technical standpoint. More specifically, we show that using less purified pea protein sources can function equally well than a more purified protein system in terms of emulsifying functionality at pH 7 and 3 when tested at an oil-to-protein ratio of 50:1. We also make a case that, purely from a structuring standpoint, the presence of native mixtures of starch and protein may be beneficial. However, a careful

design choice, based on what the final product properties are, is necessary. In the final section, we lay out our vision for the future of plant-based protein research and use. We hope that future research of plant proteins would look into a broader context than simply as a replacer of traditional animal-based proteins. For instance, plant proteins may be used in the future to create entirely new food structures and be part of specialized food products such as 3D printed convenience foods. A more in-depth understanding of plant protein functional properties would lead to better use and push the boundaries of the future of our food systems.

Acknowledgments

The last four years and the time leading up to those four years have been quite a journey. I have been lucky that I had some fantastic people around me who helped shape my life both within and outside of my PhD. Although I call it my PhD, it was a significant collaboration with many different people; without whom I would not have been able to finish this PhD. In this long list of people I would like to acknowledge, firstly, I would like to thank my supervisors, **Costas**, **Marcel**, and **Harry**, for their continued support and guidance through my PhD. **Costas**, you have been a fantastic mentor who helped me develop my academic and personal skills. I will cherish our friendly, honest conversations about my thesis, science, and society in general. **Marcel**, thank you for your positive attitude and for always being ready for discussion. I have learned a great deal from your honest feedback and critical thinking. **Harry**, I am thankful to have you involved in my PhD. You always took up the vital task of looking at my research overview and made me put my research in perspective. Your ability to see the big picture and your emphasis on clear science communication is something I will always strive to emulate as much as I can throughout my career. Besides my official supervisors, I would like to thank **Leonard Sagis** for helping me with most of my rheology methods and explanations. Leonard, your explanations and on-point feedback have helped me immensely. You have had a significant impact on my technical skills and understanding. Your balanced attitude is something I will never forget.

Besides the big official names, I would like to thank the 2 little people who have had an immense impact on my PhD thesis. Their names may not be on the official name list, but these people have been pivotal during the last four years. **Elena** and **Carlos**. I am forever grateful to both of you for tolerating my craziness and being always there for me. **Elena**, our scientific and unscientific discussions were one of the nicest parts of my thesis. I cannot imagine the last years without these discussions. Thanks for always calming me down and making my life a little easier. I never felt alone and through happy times but especially in the tough times. I always felt it was a two-person journey thanks to being 2 PhDs in the same group under the same supervisor. **Carlos**, the poor outsider (not a PhD), I am so happy to have you listening to the complaints of my PhD situation and delays. I am so grateful that you always reminded me, I worry too much for no reason, and you were always right (no surprises). Thanks, Carlopedia, for your patience.

I would also like to thank colleagues and friends at **BCT**, particularly the PhDs and postdocs, for the fun discussions and the coffee breaks. These interactions were unique and special as they were my first social interaction in a job setting. I have enjoyed being part of BCT, and thanks to every one of you. I would also like to thank my MSc students (not students anymore) **Jesper**, **Achraf**, and **Jasper** for their scientific and social contributions to my thesis. It was a fun ride, and thanks to your personal touches, I learned and modified my working methods based on your feedback. I would also like to thank the **TiFN group** of PhD colleagues and academic staff for some rigorous scientific discussions. These interactions have helped me learn a lot from every single one of you. I am sure you will all have a great career and a fun time overall. I would also like to thank the technical staff who have been behind the scenes helping me with technical and experimental questions and facilitating my work in the lab. **Susan**, **Annemarie**, **Nadine**, **Harry Baptist**, **Roy, Irene**, and **Helene**, you have all helped me immensely and, without your kind support, I would not have been able to perform my experimental work. Your smiley and helpful attitude have made my day better on so many occasions.

Lastly, I would like to thank my friends in the Netherlands and back home in India. You guys know who you are; I am not going to mention all your names here. You have all been accommodating when I needed a break to get away from the stress and relax. My memory will remember those tough times, and I will always be thankful you were all there. My family has also been so supportive and understanding of the demands of my PhD. I always knew you guys had my back no matter what, which made my life easier and helped me focus on my work.

I have not mentioned many names in this acknowledgment, but so many people shaped this thesis and my PhD that it is hard to acknowledge every person. So many people have helped me understand myself and my work culture through long and short interactions, and I am happy and thankful for every one of those, however insignificant or small they may seem.

About the author

Lakshminarasimhan Sridharan, easily known as Simha, was born on 6th August 1993, in the southeast of India in the town of Puttur. As so many Indians did in the 2000s, he obtained a Bachelor's in Engineering (Chemical) from St. Joseph's College of Engineering, Anna University in Chennai.

In 2015, he decided to pursue a master's degree in Food Science and came to Wageningen for this reason. At Wageningen University, he pursued MSC in Food Technology with a specialization in sustainable food process Engineering. He conducted his master thesis at the Food Process Engineering group entitled: 'Flavour Encapsulation in Oil Body Emulsions Obtained From Rapeseeds.' He then conducted a research internship at Fonterra Research and Development Center at Palmerston North, New Zealand. His internship was entitled 'Pickering Emulsions Stabilized with Cellulose Nano Crystals.' Following this internship, he completed his MSc studies. Subsequently, he started as a PhD candidate at the Bio-based Chemistry and Technology in October 2017. His PhD work was primarily on understanding the structuring ability of pea protein mixtures in emulsion-based systems. The results of his thesis are presented in this book.

Simha can be contacted at: simha.sridharan@gmail.com

List of publications

This Thesis

Sridharan, S., Meinders, M. B., Bitter, J. H., & Nikiforidis, C. V. (2020). Pea flour as stabilizer of oil-in-water emulsions: Protein purification unnecessary. *Food Hydrocolloids*, *101*, 105533.

Sridharan, S., Meinders, M. B., Bitter, J. H., & Nikiforidis, C. V. (2020). On the emulsifying properties of self-assembled pea protein particles. *Langmuir*, *36*(41), 12221-12229.

Sridharan, S., Meinders, M. B., Sagis, L. M., Bitter, J. H., & Nikiforidis, C. V. (2021). Jammed Emulsions with Adhesive Pea Protein Particles for Elastoplastic Edible 3D Printed Materials. *Advanced Functional Materials*, 2101749.

Sridharan, S., Meinders, M. B., Sagis, L. M., Bitter, J. H., & Nikiforidis, C. V. "Brittle emulsion-gels via heating emulsions stabilized with native pea flour". Submitted.

Sridharan, S., Meinders, M. B., Sagis, L. M., Bitter, J. H., & Nikiforidis, C. V. "Effect of protein purification on the interfacial and bulk rheological properties of pea proteins in oil-water mixtures.". Submitted.

Others

Kornet, R., **Sridharan, S**., Venema, P., Sagis, LMC., Nikiforidis, CV., van der Goot, A.J., Meinders, M.B.J., van der Linden, E., "Fractionation methods affect the gelling properties of pea proteins in emulsion-filled gels". Submitted.

Ntone, E., Rosenbaum, B., **Sridharan, S**., Willems, S.B.J., Moultos, O.A., Vlugt, T.J.H., Meinders, M.B.J., Sagis, L.M.C., Bitter, J.H., "Smart Lipid Balloons: Stimuli-responsive natural lipid droplets for selective lipid trafficking". Submitted.

Overview of completed training activities

Discipline specific activities

Conferences and meetings

EFFoST Conference, Nantes, France (2018).

CHAINS conference, Vlaardingen, The Netherlands (2018).

1st Oil Body Conference, Wageningen, The Netherlands (2018).

15th International hydrocolloids conference, Melbourne, Australia (2020).

95th ACS colloid and surface science symposium, Online (2021).

Courses

Food proteins: Functionality, modifications and analysis, VLAG, Wageningen, The Netherlands (2018).

Summer school Glycosciences, VLAG, Wageningen, The Netherlands (2018).

Confocal Microscopy Course, University of York, York, England (2019).

General courses

PhD week, VLAG, Barlo, The Netherlands (2018).

Start to supervise BSc and MSc Thesis students, WGS, Wageningen, The Netherlands (2019).

Scientific publishing, WGS, Wageningen, The Netherlands (2019).

Scientific Writing, WGS, Wageningen, The Netherlands (2019).

Grant proposal writing, WGS, Wageningen, The Netherlands (2020).

Optional

Scientific PhD excursion to Denmark and Sweden, BCT, 2018.

Bio-based Soft materials group meetings (BIOSOM), BCT (WUR), 2018-2021.

BCT lunch meetings, BCT (WUR), 2017-2021.

TiFN PhD meetings, WUR, 2017-2021.

Abbreviations

VLAG: Graduate School for Nutrition, Food Technology, Agrobiotechnology and Health Science

WGS: Wageningen Graduate School

WUR: Wageningen University and Research centre

BCT: Bio-Based Chemistry and Technology

Colophon

This research formed part of a project that was organized by TiFN, a public-private partnership on pre-competitive research in food and nutrition. The public partners were responsible for the design of study, data collection and analysis, decision to publish and manuscript preparation. The private partners namely Danone, Fromageries Bel, PepsiCo and Unilever have contributed through regular discussions and knowledge sharing. Co-funding for the project was obtained from the Netherlands Organization for Scientific Research (NWO) and the Top-Consortium for Knowledge and Innovation Agri&Food (TKI)

Financial Support from Wageningen University and TiFN for performing the research and for printing this thesis is gratefully acknowledged.

Cover design: Ines Vilalva (Ines Vilalva design)

This thesis was printed by Proefschriftmaken (100 copies)